A NEW MECHANISM FOR GENOMIC NUCLEOSOME POSITIONING BY NATIVE ISWI AND ENGINEERED CHD CHROMATIN REMODELING PROTEINS IS DRIVEN BY SEQUENCE-SPECIFIC DNA BINDING.

by

DRAKE ANDREW DONOVAN

A DISSERTATION

Presented to the Department of Chemistry and Biochemistry
and the Division of Graduate Studies of the University of Oregon
in partial fulfillment of the requirements
for the degree of
Doctor of Philosophy

June 2021

DISSERTATION APPROVAL PAGE

Student: Drake Andrew Donovan

Title: A New Mechanism for Genomic Nucleosome Positioning by Native ISWI and Engineered CHD Chromatin Remodeling Proteins is Driven by Sequence-Specific DNA Binding.

This dissertation has been accepted and approved in partial fulfillment of the requirements for the Doctor of Philosophy degree in the Department of Chemistry and Biochemistry by:

Brad Nolen	Chairperson
Eric Selker	Advisor
Pete von Hippel	Core Member
Matt Barber	Institutional Representative

and

Andrew Karduna	Interim Vice Provost for Graduate Studies

Original approval signatures are on file with the University of Oregon Division of Graduate Studies.

Degree awarded June 2021

DISSERTATION ABSTRACT

Drake Andrew Donovan

Doctor of Philosophy

Department of Chemistry and Biochemistry

June 2021

Title: A New Mechanism for Genomic Nucleosome Positioning by Native ISWI and Engineered CHD Chromatin Remodeling Proteins is Driven by Sequence-Specific DNA Binding.

Encoded within DNA are all the instructions that a cell needs to survive, and these instructions must be regulated such that cells take the appropriate actions in response to environmental and developmental cues. One way that the DNA is regulated is that a portion of it is wrapped around proteins to form structures known as nucleosomes, which makes the wrapped DNA inaccessible to the machinery that reads the genetic code. Thus, the location of these nucleosome structures on the DNA plays a large role in which genes are active at what times.

The location of nucleosomes on the DNA is partially regulated by a family of enzymes called chromatin remodeling proteins. While the function of chromatin remodeling proteins to position nucleosomes is well understood, the mechanisms by which they do so have not been thoroughly tested and are thought to be non-specific. It is unknown, for example, how chromatin remodeling proteins know when and where to position a nucleosome on a given DNA sequence. Reconciling how these supposedly

non-specific molecular machines result in highly specific chromatin structures is the focus of this dissertation.

The first part of this work challenges the idea that a chromatin remodeling protein in yeast, Isw2, acts as a non-specific nucleosome spacer. Instead, the use of biochemical and genomic techniques shows us that Isw2 is directly targeted to particular nucleosomes in a sequence-specific manner through interactions with other proteins. Further, it suggests that this mechanism may potentially exist in humans.

In the second part of this work, we use the idea of sequence-specific targeting seen in Isw2 to engineer another chromatin remodeling protein, Chd1. This allows us to directly target particular nucleosomes in a synthetic manner both in test tubes and in living cells. Excitingly, we show that the use of these engineered proteins allows us to control DNA access and downstream biological outputs in yeast.

Overall, this dissertation contributes a completely new understanding of how chromatin remodeling proteins can be directed to act on specific target nucleosomes both natively in eukaryotes and synthetically by researchers.

This dissertation includes previously published co-authored material.

CURRICULUM VITAE

NAME OF AUTHOR: Drake Andrew Donovan

GRADUATE AND UNDERGRADUATE SCHOOLS ATTENDED:

University of Oregon, Eugene, Oregon
Eastern Washington University, Cheney, Washington
Spokane Community College, Spokane, Washington

DEGREES AWARDED:

Doctor of Philosophy, Chemistry and Biochemistry, 2021, University of Oregon
Bachelor of Science, 2016, Eastern Washington University
Associate of Arts, 2014, Spokane Community College

AREAS OF SPECIAL INTEREST:

Biochemistry
Molecular Biology
Protein Engineering

PROFESSIONAL EXPERIENCE:

Graduate Research Fellow, University of Oregon, 2017-2021
Graduate Teaching Fellow, University of Oregon, 2016-2017

GRANTS, AWARDS, AND HONORS:

General University Scholar, University of Oregon, 2018-2019

National Institute of Health Molecular Biology and Biophysics Training Grant, University of Oregon, 2018-2019

Epicypher Travel Award, University of Oregon, 2018

National Institute of Health Genetics Training Grant, University of Oregon, 2017-2018

Dean's First Year Merit Award, University of Oregon, 2016-2017

Washington State Opportunity Scholar, Eastern Washington University, 2014-2016

Transfer Honors Scholar, Eastern Washington University, 2014-2016

PUBLICATIONS:

McKnight, L.E., Crandall, J.G., Bailey, T.B., Banks, O.G.B., Orlandi, K., Truong, V.N., **Donovan, D.A.**, Waddell, G.L., Wiles, E.T., Hansen, S.D., Selker, E.U., McKnight, J.N. (2021). Rapid and Inexpensive Preparation of Genome-Wide Nucleosome Footprints from Model and Non-Model Organisms. STAR Protocols, in press.

Donovan, D.A., Crandall, J.G., Truong, V.N., Vaaler, A.L., Bailey, T.B., Dinwiddie, D., Banks, O.G.B., Mcknight, L.E., McKnight, J.N. (2021). Basis of Specificity for a Conserved and Promiscuous Chromatin Remodeling Protein. eLife 10:e64061

Donovan, D.A., Crandall, J.G., Banks, O.G.B., Jensvold, Z.D., Truong, V., Dinwiddie, D., McKnight, L.E., McKnight, J.N. (2019). Engineered chromatin remodeling proteins for precise nucleosome positioning. Cell Reports 29:2520–2535.

Bateman, C.M., Beal, H., Barker, J.E., Thompson, B.L., **Donovan, D.A.**, …Tinsley, C.W.K., Zakharov, L.N., Abbey, E.R. (2018). One-Step Conversion of Potassium Organotrifluoroborates to Metal Organoborohydrides. Organic Letters 20:3784-3787

ACKNOWLEDGMENTS

I would like to start off by acknowledging all the people that I have interacted with in my life that are not mentioned here by name. Every day the smile of a stranger can help contribute to a positive, productive tomorrow. I would like to thank Dr. Jeff McKnight and Dr. Laura McKnight for taking me into the fledgling McKnight Company and providing me the space that I needed to grow as a scientist and as a human. Jeff, thank you for demonstrating so clearly to me how to be a leader and for showing me the power of never-ending inquisition (and squinting). Laura, thank you for all of our over-the-desk conversations and your behind-the-scenes work to keep the lab running, as well as for teaching me how to do many of the advanced molecular biology techniques employed in this work (such as my first PCR). I am so fortunate to have worked with two of the most intelligent, compassionate, and benevolent people I have ever met for the last 5 years of my life. I would also like to acknowledge my committee members Dr. Brad Nolen, Dr. Pete von Hippel, Dr. Eric Selker and Dr. Matt Barber who always offered constructive advice and their support at every junction. Speaking of support, I want to thank my parents, Darren and Sheri, for helping me to pursue my own happiness and for always doing their best at keeping me alive as a child. I would very much like to thank the mountains and forests of Oregon for keeping me fulfilled throughout graduate school, as well as all my friends from IMB and beyond who have explored these wonderful places with me. Finally, I would like to thank my partner Emily, whose encouragement, love, and understanding is bottomless. She's the DNA to my histone octamer (or something like that). Thank you all!

This work is dedicated to Jeff McKnight, who is unequivocally one of the most phenomenal, extraordinary, and important humans I have ever encountered in my life. Thank you for being so abnormal and for helping me understand what that really means. I miss you.

TABLE OF CONTENTS

Chapter Page

LIST OF FIGURES

Figure Page

CHAPTER I

FUNCTIONS OF NATIVE CHROMATIN REMODELING PROTEINS IN GENETIC REGULATION

Chapter I contains previously published co-authored material.

Chapter II contains previously published co-authored material.

Chapter III contains previously published co-authored material.

*****This chapter contains previously published co-authored material.

Donovan, D.A., Crandall, J.G., Truong, V.N., Vaaler, A.L., Bailey, T.B., Dinwiddie, D., Banks, O.G.B., Mcknight, L.E., McKnight, J.N. (2021). Basis of Specificity for a Conserved and Promiscuous Chromatin Remodeling Protein. eLife 10:e64061

Author Contributions: Conceptualization, D.A.D. and J.N.M.; Methodology, D.A.D., J.G.C., V.N.T., A.L.V., T.B.B., L.E.M., and J.N.M.; Investigation, D.A.D., J.G.C., V.N.T., A.L.V., T.B.B., L.E.M., and J.N.M.; Writing – Original Draft, D.A.D. and J.N.M.; Writing – Review & Editing, D.A.D., J.G.C., A.L.V., O.G.B.B., L.E.M., and J.N.M.; Visualization, D.D., O.G.B.B, and J.N.M.; Supervision, L.E.M. and J.N.M.; Project Administration, J.N.M.; Funding Acquisition, J.N.M.

The Structure of Chromatin

Chromatin consists of the nucleic acids and proteins that make up the functional genome of all eukaryotic organisms. The most basic regulatory and structural unit of chromatin is the nucleosome. Each nucleosome is defined as an octamer of histone proteins, which is wrapped by approximately 147 base pairs of genomic DNA (Luger et al., 1999; Kornberg, 1974). The specific positioning of nucleosomes on the underlying DNA can have significant effects on downstream processes, such as promoter accessibility and molecular recruitment, which ultimately serve to alter gene expression. Although nucleosomes are dynamic structures that are constantly assembled, disassembled, and repositioned in the genome, their positions at gene-regulatory elements such as transcription start sites (TSSs) show characteristic organization (Lai and Pugh, 2017). Despite decades of research, the mechanisms leading to precise nucleosome locations in cells are still being defined.

What Are Chromatin Remodeling Proteins?

Nucleosome positioning is dynamically established by a group of enzymes known as ATP-dependent chromatin remodeling proteins (ChRPs) (Zhou et al., 2016). Extensive biochemical and structural characterization has been performed on this group of proteins from various families (Clapier et al., 2017). The chromodomain-helicase-DNA binding (CHD) and imitation switch (ISWI) families of ChRPs have been characterized as nonspecific nucleosome sliding and spacing factors *in vitro* (Stockdale et al., 2006; Hauk

et al., 2010; McKnight et al., 2011; Kagalwala et al., 2004; Lusser et al., 2005; Tsukiyama et al., 1999; Pointner et al., 2012).

In yeast, flies, and mammals, ChRPs generate evenly spaced nucleosome arrays at transcription start sites and organize genomic chromatin at other defined boundaries (Pointner et al., 2012; Lee et al., 2007; Mavrich et al., 2008a; Valouev et al., 2011; Krietenstein et al., 2016; Wiechens et al., 2016; Baldi et al., 2018; Gkikopoulos et al., 2011; Zhang et al., 2011). However, relatively little is known about the *in vivo* biological regulation of these spacing factors, and it is not understood how they can accurately and reproducibly position nucleosomes throughout the genome in different cellular contexts.

The Current Model of ISWI and CHD Chromatin Remodeling Protein Function

A widely accepted model is that ChRPs pack nucleosome arrays against a noninteracting barrier, such as an unrelated DNA binding protein or another nucleosome (Krietenstein et al., 2016; Zhang et al., 2011; Mavrich et al., 2008b). In this way, general regulatory factors (GRFs) could establish chromatin landscapes with differing nucleosome arrays in response to changes in the cellular environment. In support of this model, nucleosome arrays near GRFs and other DNA binding elements appear to be phased relative to the binding motifs of the sequence-specific DNA binding factors in cells and in biochemically reconstituted cell-free systems (Krietenstein et al., 2016; Baldi et al., 2018; Yan et al., 2018).

This model suggests that boundaries of nucleosome arrays are determined by the binding of barrier factors. Implicit in this barrier model are the assumptions that ChRPs

act as nonspecific nucleosome spacing machines throughout the genome and that specific ChRP and GRF interactions are not required to establish nucleosome positions. While this model provides a good explanation for how phased nucleosome arrays can be established throughout the genome by a combination of DNA binding factors and nonspecific chromatin remodeling factors, the fundamental assumptions of the barrier model have not been thoroughly tested.

Unexplained Experimental Observations with ISWI in Yeast

It has been shown through genetic and recent biochemical experiments that members of the ISWI family of ChRPs functionally interact with transcription factors *in vivo* (Krietenstein et al., 2016; Gelbart et al., 2005; Goldmark et al., 2000; Fazzio et al., 2001; Yadon et al., 2013). One of the most well-defined interacting partners of ISWI proteins is the meiotic repressor unscheduled meiotic gene expression (Ume6), which is found in yeasts. It has been previously demonstrated that Ume6 and Isw2, an ISWI-containing ChRP complex in *Saccharomyces cerevisiae* (homologous to the ATP-dependent chromatin assembly factor [ACF] complex in humans and flies), share genetic targets of repression and likely interact physically (Goldmark et al., 2000).

While interactions with sequence-specific DNA binding proteins can potentially determine precise nucleosome targeting and final nucleosome positions (Donovan et al., 2019; Bowman and McKnight, 2017; McKnight et al., 2016), the mechanisms through which physical interactions between Isw2 and any genomic recruitment factor like Ume6 influence nucleosome positioning activity in cells have not been defined. For example, it

is not known how these physical interactions occur or what role they play in the biochemical outcomes of chromatin remodeling reactions and the resulting downstream biological outputs.

Isw2 Complex Activity is Inconsistent with the Current Model

We wished to understand how the conserved Isw2 protein complex in yeast behaves genome-wide and at specific promoter nucleosomes at target sites. Yeast Isw2 has been characterized extensively in biochemical assays, which all suggest that it has nonspecific DNA binding, ATP hydrolysis, nucleosome sliding, mononucleosome centering, and nucleosome spacing activities (Stockdale et al., 2006; Kagalwala et al., 2004; Lusser et al., 2005; Tsukiyama et al., 1999; Dang and Bartholomew, 2007; Dang et al., 2006; Hota et al., 2013; Kassabov et al., 2002; Zofall et al., 2004; Zofall et al., 2006).

These nonspecific nucleosome mobilizing activities suggest that the Isw2 protein should be able to organize nucleosome arrays against a barrier across the genome in yeast cells since (1) it is estimated that there are enough Isw2 molecules for every 10–20 nucleosomes in the genome (Gelbart et al., 2005), (2) *Drosophila melanogaster* ACF, an Isw2 ortholog, can organize nucleosomes into evenly spaced arrays (Baldi et al., 2018), and (3) other nonspecific and related nucleosome spacing factors can globally space nucleosomes across the genome in yeast and other organisms (Pointner et al., 2012; Wiechens et al., 2016; Gkikopoulos et al., 2011; Zhang et al., 2011).

To first determine how Isw2 positions nucleosomes in *S. cerevisiae*, we examined nucleosome positioning activity in an *isw1/chd1* deletion background to remove known

and potentially overlapping global spacing factors and highlight 'isolated positioning activity' by Isw2. When examining the positioning of nucleosomes with and without Isw2 at all yeast pre-initiation complex sites (PICs), it is evident that Isw2 activity is specialized at only a subset of target sites (Figure 1A). As seen previously (Gkikopoulos et al., 2011; Ocampo et al., 2016), no global nucleosome spacing or organizing activity is detected by Isw2 alone (Figure S1, see Appendix A for all supplemental material). Close inspection of Isw2-targeted PICs suggests that Isw2 can only organize a single PIC-proximal nucleosome, while subsequent nucleosomes become more poorly phased as the distance from the initially positioned nucleosome increases (Figure 1A, Figure S2). Importantly, the PICs that display specific Isw2-directed activity are bound by Isw2, while those lacking any detectable nucleosome organization by Isw2 are unbound (Figure 1A, middle panel).

Figure 1 (next page): Isw2 is a Specialist Remodeler that Positions Single Nucleosomes at Target Sites.

(**A**) (Left) Clustered heatmap showing differences in nucleosome dyad signal between *isw2*/*isw1*/*chd1* and *ISW2*/*isw1*/*chd1* strains at 5942 pre-initiation complex sites (PICs). Black indicates positions where Isw2 preferentially positions nucleosomes compared to the strain lacking Isw2. (Middle) Heatmap of ISW2(K215R) ChIP signal, with rows linked to the PIC data on the left, shows that Isw2-dependent nucleosome changes overlap with regions where Isw2 is present. (Right) Average nucleosome dyad signal for wild type (WT) (black), *isw1*/*chd1* (cyan), and *isw2*/*isw1*/*chd1* (red) strains for the 178 PIC sites in cluster 3. Black arrows denote Isw2-driven nucleosome shifts. Green arrows indicate rapid decay of positioning at PIC-distal nucleosomes in the *ISW2*/*isw1*/*chd1* mutant. (**B**) (Left) Genome Browser image showing nucleosome dyad signal at a *u*nscheduled *m*eiotic gene *e*xpression (Ume6) motif (cyan rectangle) for indicated strains. Vertical gray dashed line denotes the motif-proximal WT nucleosome positions while vertical pink dashed line indicates the nucleosome positions in the absence of Ume6 or Isw2. (Center) Clustered heatmap showing the difference in nucleosome dyad signal between *isw2*/*isw1*/*chd1* and *ISW2*/*isw1*/*chd1* strains at 202 intergenic Ume6 motifs. Black indicates positions where Isw2 preferentially positions nucleosomes compared to strains lacking Isw2. (Right) Average nucleosome dyad signal for indicated strains at Ume6 motifs in cluster 1. Black arrows indicate direction of nucleosome positioning by Isw2. Green arrows signify decreased positioning of motif-

distal nucleosomes in the *ISW2*/*isw1*/*chd1* strain (cyan) compared to WT (black). (**C**) (Left) Cartoon depicting the expected activity of Isw2 at barrier elements according to current biochemical data and nucleosome positioning models. Isw2 is thought to move nucleosomes away from bound factors and space nucleosomes with an approximately 200 base pair repeat length. (Right) Cartoon of the observed activity of Isw2 at target sites where only a motif-proximal single nucleosome is precisely positioned but distal nucleosomes are not well-spaced by Isw2.

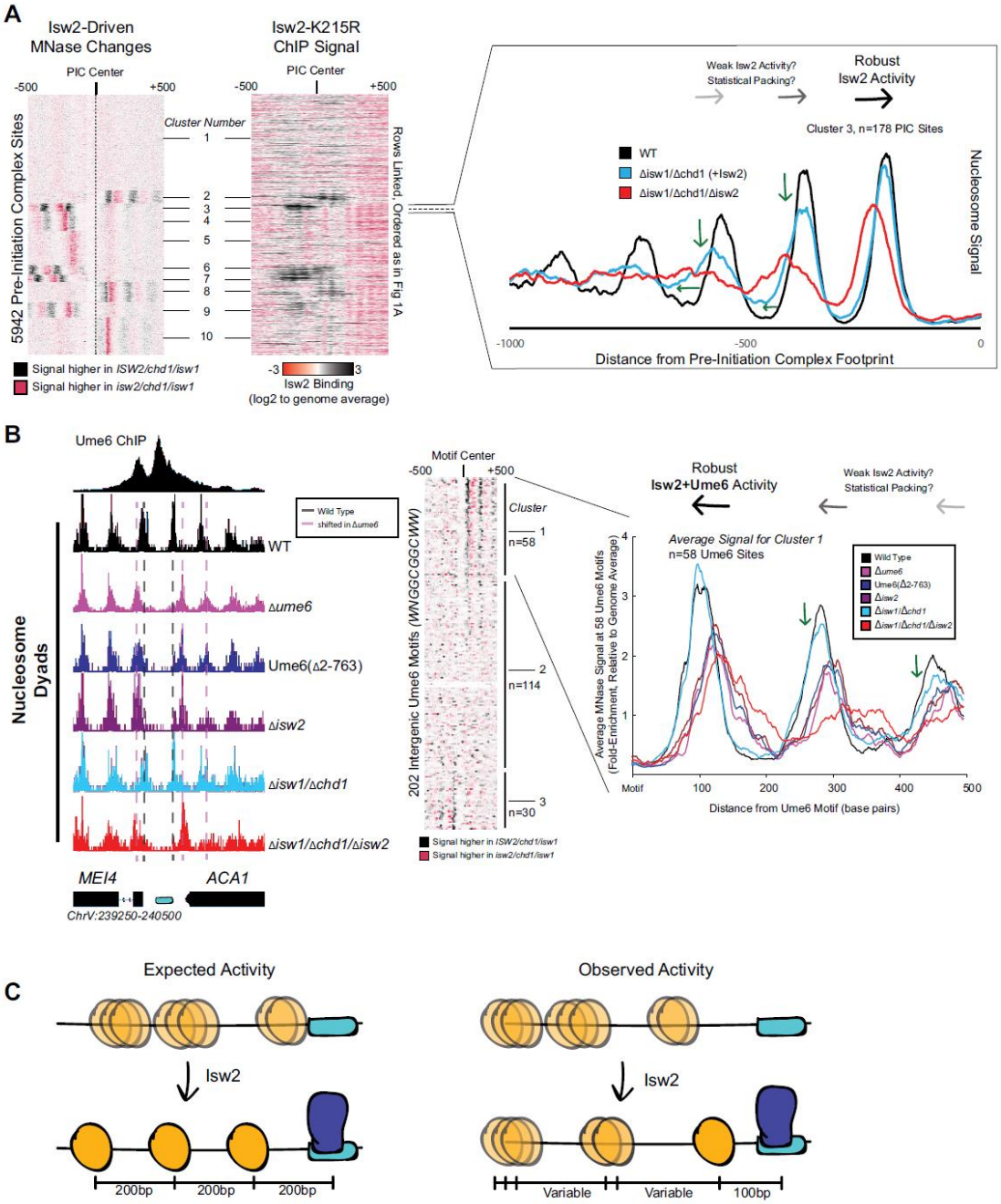

It has been shown that Isw2 associates with sequence-specific DNA binding factors, such as the transcriptional repressor Ume6 (Goldmark et al., 2000; Fazzio et al., 2001). Isw2 activity at Ume6- bound loci has been previously characterized as precise, with Isw2 reproducibly moving nucleosomes until the predicted edge of the nucleosome core particle is 30 base pairs from the center of the Ume6 binding motif (McKnight et al., 2016). Because of the connection to Ume6, we examined nucleosome positions in an *isw1/chd1* background in the presence and absence of Isw2 to determine whether Isw2 is similarly restricted at known target sites. Again, we determined that Isw2 is efficient at positioning the Ume6-proximal nucleosome but positioning of nucleosomes decays rapidly as the distance from the proximal nucleosome increases, suggesting that Isw2 may only position single nucleosomes at target sites (Figure 1B, clusters 1 and 3). Nucleosomes also appear to always be positioned toward Ume6 motifs as nucleosome positions in the absence of Isw2 are always more distal to the Ume6 motif than when Isw2 is present. Finally, these nucleosomes are positioned with the dyad only separated from the Ume6 motif by 100 nucleotides rather than the ~200 nucleotides that would be expected between dyads in a nucleosome array based on Isw2 preferentially leaving 60 base pairs of linker DNA between nucleosomes *in vitro* (Kagalwala et al., 2004; Tsukiyama et al., 1999). Of note, a subset of Ume6-bound sites do not display Isw2-dependent nucleosome remodeling (Figure 1B, cluster 2). We have observed slightly reduced chromatin immunoprecipitation (ChIP) signal for Ume6 at these sites (Figure S3). We speculate that for cluster 2 sites where Ume6 is bound, the Isw2 complex might in fact be recruited but that the nearest nucleosome is too distant from the recruitment

site, making it out of reach of the remodeler and thus resulting in no change in nucleosome position at these sites.

The observations that (1) Isw2 is solely required to move single nucleosomes at target sites, (2) Isw2 does not have global nucleosome spacing/organizing activity, and (3) Isw2 moves nucleosomes within 100 nucleotides of bound Ume6 suggest that Isw2 behavior in cells is distinct from our understanding of Isw2 activity from decades of biochemical characterization. Similarly, these specific movements toward Ume6 (a barrier) are inconsistent with previous biophysical studies, where ISWI proteins were shown to move nucleosomes away from inert DNA-bound factors (Li et al., 2015).

Because of these inconsistencies, we wished to know if Isw2 followed the 'barrier model' for positioning nucleosomes at Ume6-bound targets. To initially test this, we created a variant Ume6 construct where all residues were deleted except for the DNA binding domain. This Ume6(Δ2–763) construct binds to the same targets as full-length Ume6 (Figure S3). However, Isw2 does not appear to have any activity on global Ume6-proximal nucleosomes in the presence of the Ume6 DNA binding domain alone as nucleosomes in this strain occupy identical positions when Ume6 or Isw2 are completely absent (Figure 1B). In the presence of full-length Ume6, the Isw2 complex appears to be necessary and sufficient for moving motif-proximal nucleosomes as nucleosome positions in the *ISW2/isw1/chd1* strain could achieve identical motif-proximal nucleosome positions as the wild-type strain. Additionally, the *CHD1/isw1/isw2* and *ISW1/chd1/isw2* strains were unable to move any Ume6-proximal nucleosomes (Figures S4 and S5), which strongly argues that Ume6 is not acting as a passive barrier against which nucleosome spacing factors can pack nucleosomes.

How Do These Molecular Machines Act with High Fidelity and Plasticity?

If the Isw2 complex does not pack against a barrier as the current model suggests, then how can it function to remodel the chromatin in a reproducible and context-dependent manner? The data here are more consistent with the recent characterization of Isw2 as a 'puller' (Kubik et al., 2019), with Ume6 being a DNA-bound factor that may immobilize Isw2 to create leverage for 'pulling'. Consistent with this immobilized pulling model and consistent with the directional movement of single nucleosomes toward Ume6-bound sites, artificially tethered chromatin remodeling proteins were previously shown to always move nucleosomes toward target sites (Donovan et al., 2019). We suspected that Ume6 and Isw2 likely interact in a specific fashion to faithfully select and precisely move single-target nucleosomes toward a recruitment motif (Figure 1C). The connection of the molecular machine that is the Isw2 complex to other transcription factor proteins that localize to the genome in a context and sequence specific manner may explain the fidelity and plasticity exhibited by chromatin remodeling proteins in establishing chromatin structure. Determining if and how this connection occurs will deepen our understanding of the complex actions of chromatin remodeling proteins.

Bridge to Chapter II

In this chapter I have introduced the concept of chromatin as well as the molecular machines known as chromatin remodeling proteins. I have further discussed the current "barrier" model of chromatin remodeling protein function in genetic

regulation and highlighted some unexplained data and observed inconsistencies with this model. Finally, I have introduced the concept of an alternative model of chromatin remodeling protein function whereby the Isw2 complex interacts with a transcription factor protein to be targeted to genetic loci in a specific manner. In the following chapter I will present our research that further supports this alternative model and demonstrate how the Isw2 complex physically interacts with these specific targeting proteins. Additionally, I will offer a potential explanation of where the “barrier” model originated and why it has persisted.

CHAPTER II

THE EFFECTS OF GENOMIC DNA SEQUENCES ON CHROMATIN REMODELER LOCALIZATION

*****This chapter contains previously published co-authored material.

Donovan, D.A., Crandall, J.G., Truong, V.N., Vaaler, A.L., Bailey, T.B., Dinwiddie, D., Banks, O.G.B., McKnight, L.E., McKnight, J.N. (2021). Basis of Specificity for a Conserved and Promiscuous Chromatin Remodeling Protein. eLife 10:e64061

Author Contributions: Conceptualization, D.A.D. and J.N.M.; Methodology, D.A.D., J.G.C., V.N.T., A.L.V., T.B.B., L.E.M., and J.N.M.; Investigation, D.A.D., J.G.C., V.N.T., A.L.V., T.B.B., L.E.M., and J.N.M.; Writing – Original Draft, D.A.D. and J.N.M.; Writing – Review & Editing, D.A.D., J.G.C., A.L.V., O.G.B.B., L.E.M., and J.N.M.; Visualization, D.D., O.G.B.B, and J.N.M.; Supervision, L.E.M. and J.N.M.; Project Administration, J.N.M.; Funding Acquisition, J.N.M.

A Previously Uncharacterized Motif on the Transcription Factor Ume6 is Responsible for Interaction with ISW2

To determine which region(s) on Ume6 are required for specific nucleosome positioning by Isw2, we initially created a panel of N-terminal Ume6 truncations to determine when nucleosome positioning by Isw2 is lost (Figure S6). This initial

truncation panel was necessary due to the poor overall conservation of the Ume6 protein even within related yeasts, as well as the disordered structure predicted by Phyre2 (Kelley et al., 2015). Our truncation panel indicated that Isw2 activity was retained if the N-terminus was deleted to residue 322 but lost when deleted to residue 508. Closer inspection of the residues between 322 and 508 revealed a conserved region with a proline-rich segment followed by a predicted alpha helix, altogether spanning Ume6 residues 479–508 (Figure 2A). Deletion of residues 2–479 preserved Isw2-positioned nucleosomes at Ume6 sites, while an internal deletion of 480–507 in the context of an otherwise full-length Ume6 abrogated nucleosome positioning by Isw2 (Figure 2A, Figure S7). Importantly, Ume6 Δ2–479 and Ume6 Δ2–508 showed identical binding as measured by ChIP (Figure S8), indicating that the loss of nucleosome positioning is not due to the loss of Ume6 binding.

Figure 2 (next page): A Small Predicted Helix is the Isw2 Recruitment Epitope in Ume6.

(**A**) (Top left) Schematic diagram of Ume6 truncation and deletion constructs used to identify the Isw2-recruitment epitope, with the known Sin3-interacting domain depicted as a green square, the DNA binding domain as a dark blue rectangle, and the putative Isw2-recruitment helix as a light blue rectangle. (Bottom left) Modeled helical peptide (by Phyre2) and sequence conservation of the identified Isw2-recruitment motif in Ume6 constructs from other yeasts. Asterisks denote invariant residues. (Right) Nucleosome dyad signal for Ume6 truncation and deletion strains indicates deletion of the region from residues 480 to 507 completely abrogates nucleosome positioning by Isw2 at Ume6 target sites. Vertical dashed gray lines denote wild-type (WT) positions of nucleosomes while vertical dashed pink lines indicate *isw2* or *ume6*-deficient positions of nucleosomes. (**B**) Genome Browser image showing transcript abundance at three Ume6 target sites for yeast strains lacking Rpd3 with WT Ume6 (gray), Ume6(Δ2–479) (blue), and Ume6(Δ2–508) (orange). Grossly increased transcription is seen when residues 480–507 are deleted, consistent with expected transcriptional increase associated with loss of Isw2 and Rpd3. Upstream repression sequence (URS) sites are indicated as cyan rectangles. No significant increase in transcription is detected when Ume6 residues 2–479 are deleted. Biological replicates are shown to highlight reproducibility. (**C**) (Top) Cartoon schematic for ectopic display of the Isw2-recruiting helix (residues 480–507) to the C-terminus of a truncated Ume6 construct lacking Isw2-directed nucleosome positioning. A short SpyTag

is appended to the C-terminus of the Ume6 construct and residues 480–507 are fused to the SpyCatcher domain and introduced on a yeast expression vector. (Bottom) Nucleosome dyad signal demonstrating recovery of Isw2-directed nucleosome positions at a subset of Ume6 target genes by the ectopically displayed helical element. Vertical dashed gray lines denote WT positions of nucleosomes while vertical dashed pink lines indicate *isw2* or *ume6*-deficient positions of nucleosomes. URS sites are indicated as cyan rectangles.

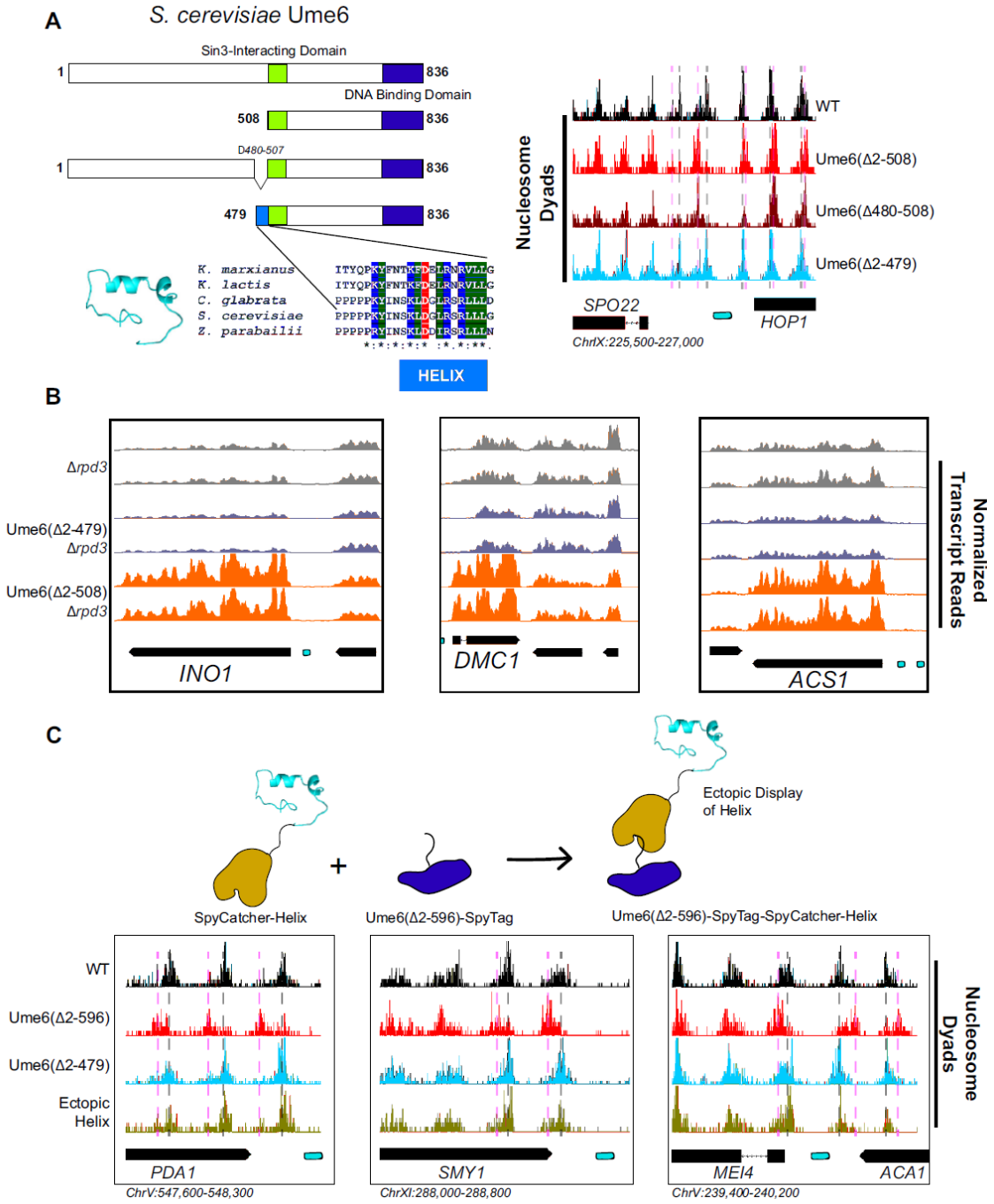

Since this region is proximal to the characterized Sin3-binding domain in Ume6 (Washburn and Esposito, 2001), we wished to validate that the newly determined Isw2-recruitment helix is independent from the Sin3-binding domain. Ume6 recruits both Isw2 and Sin3-Rpd3 for full repression of target genes (Goldmark et al., 2000; Fazzio et al., 2001). If either Isw2 or Sin3-Rpd3 is present, there is partial repression at Ume6-regulated genes. However, if Sin3-Rpd3 and Isw2 are both lost, Ume6 targets are fully de-repressed. We examined transcriptional output at Ume6 genes in Ume6(Δ2–479) +/– Rpd3 and Ume6(Δ2–508) +/– Rpd3. Transcription was modestly increased at Ume6 targets in Ume6(Δ2–508)/*RPD3+* compared to Ume6(Δ2–479)/*RPD3+* (Figure S9), which would be expected if only Isw2 is lost when residues 479–508 are deleted. More convincingly, only a modest increase in transcription was seen at Ume6 targets in the Ume6(Δ2–479)/ Δ*rpd3* strain, suggesting that Isw2 is still present, while the Ume6(Δ2–508)/ Δ*rpd3* strain displayed extreme induction of Ume6-regulated genes, suggesting that both Isw2 and Rpd3 activity are absent (Figure 2B, Figure S10).

Finally, we wanted to know if the predicted helix consisting of Ume6 residues 479–508 was sufficient to bring Isw2 nucleosome positioning activity to Ume6 target sites. To test this, we employed the SpyCatcher/SpyTag system (Zakeri et al., 2012), which creates a spontaneous covalent bond between a short SpyTag peptide and a SpyCatcher domain. We fused the SpyTag peptide to the C-terminus of Ume6(Δ2–596), a construct that is incapable of positioning motif-proximal nucleosomes (Figure S6). We then appended Ume6 residues 479–508 to the C-terminus of the SpyCatcher domain and introduced this fusion on a yeast expression plasmid driven by the ADH1 promoter. In yeast cells, this would create a fusion protein where the helical element is ectopically

displayed on the C-terminus of a DNA binding competent but nucleosome-positioning deficient construct, connected via a SpyTag-SpyCatcher linker. This fusion protein was capable of fully recapitulating Isw2-positioned nucleosomes at a subset of Ume6 sites (Figure 2C, Figures S11 and S12). Perhaps not surprisingly, considering the non-native positioning of the recruitment helix in this fusion construct, not all Ume6 sites were able to gain proper nucleosome positioning with this chimeric system (Figure S11). We conclude that the region spanning residues 479–508 in Ume6 is a yeast-conserved Isw2-recruitment domain and is required and sufficient for recruiting Isw2 nucleosome positioning activity to Ume6 targets.

This Motif is Found in Other ISW2-Interacting Transcription Factors

While dissecting the Isw2-recruitment domain in Ume6, we discovered that deleting the MBP1 gene resulted in ectopic nucleosome positioning at a subset of Mbp1 target loci, which was identical to mispositioned nucleosomes in a ∆isw2 strain. Mbp1 is a conserved cell cycle regulator that complexes with Swi6 to form the MBF complex (Koch et al., 1993). This complex activates the transition from G1 to S and includes the conserved function of regulating Start-specific transcription (Koch et al., 1993; Breeden, 1996).

To determine how Mbp1 recruits Isw2, we similarly made truncations of Mbp1 to determine at which point nucleosome positioning no longer resembles wild-type positioning and reflects ∆isw2 positioning instead. The DNA binding element in Mbp1 resides in the extreme N-terminus (Figure 3A) spanning residues 2–124 (Nair et al.,

2003), so a panel of C-terminal truncations was created. However, before examining the full panel of truncations, we observed that nucleosome positioning was already identical to Δisw2 positioning in Mbp1 Δ562–833, the first C-terminal truncation examined (Figure S13). This extreme C-terminal region interacts with Swi6 (Figure 3A), so we speculated that Swi6 may be responsible for recruiting Isw2. As predicted, deletion of the SWI6 gene led to ectopic nucleosome positions identical to Δmbp1 and Δisw2 strains at the small subset of Mbp1 targets.

Figure 3 (next page): The Cell Cycle Regulator Swi6 Contains a Similar Helical Element and Recruits Isw2 to MBF and SBF Target Genes.

(**A**) (Top left) Schematic representation of the Swi6-Mbp1 MBF complex. Swi6 interacts with Mbp1 through the C-terminal domain (black rectangle). Mbp1 has an N-terminal DNA binding domain (dark blue rectangle). The putative Isw2-recruitment helix is in the Swi6 N-terminus (light blue rectangle). (Center left) Conserved residues in the putative Isw2-recruitment helix in Swi6 for three yeast species compared to the Isw2-recruitment helix in Ume6 for *S. cerevisiae*. (Bottom left) Crystal structure (Protein Data Bank [PDB] ID 1sw6) showing the location of the surface-exposed, conserved helical element from Swi6 in red. (Top right) Schematic representation of the Swi6-Swi4 SBF complex. Swi6 interacts with Swi4 through the C-terminal domain (black rectangle). Swi4 has an N-terminal DNA binding domain (green rectangle). Putative Isw2-recruitment helix is shown (small blue rectangle). (Bottom center) Genome Browser image showing nucleosome dyad signal for indicated strains at the *RAD51* locus, an MBF target gene with an indicated Mbp1 binding motif (blue rectangle). Wild-type (WT) nucleosome positions are indicated by vertical dashed gray lines while ectopic positions associated with *isw2*, *mbp1*, and *swi6* deletion strains are indicated by vertical dashed pink lines. (Bottom right) Genome Browser image showing nucleosome dyad signal for indicated strains at the *HSP12* locus, an SBF target gene with an indicated Swi4 binding motif (green rectangle). WT positions are denoted by vertical gray dashed lines while ectopic nucleosome positions associated with *isw2*, *swi6*, and *swi4* deletion strains are indicated with vertical pink dashed lines. (**B**) (Top) Schematic representation of constructs used to determine if ectopic display of an Isw2-recruitment helix on the Mbp1 N-terminus could recover Isw2-positioned nucleosomes at Mbp1 target genes. Either WT Mbp1, a C-terminal deletion of Mbp1 leaving only the DNA binding domain and an appended SpyTag, or a C-terminal deletion of Mbp1 leaving the DNA binding domain and SpyTag with constitutively expressed SpyCatcher fused to the Isw2-recruitment helix from Ume6 was examined. (Bottom) Genome Browser image showing nucleosome dyad signal for indicated strains at the *ESC8* (left) or *RAD51* (right) loci. Gray vertical dashed lines indicate WT nucleosome positions while vertical dashed pink lines indicate ectopic nucleosome positions associated with inactive Isw2 or Mbp1/Swi6. Biological replicates

for ectopic display of the recruitment helix are provided as two separate tracks (gold) to emphasize reproducibility.

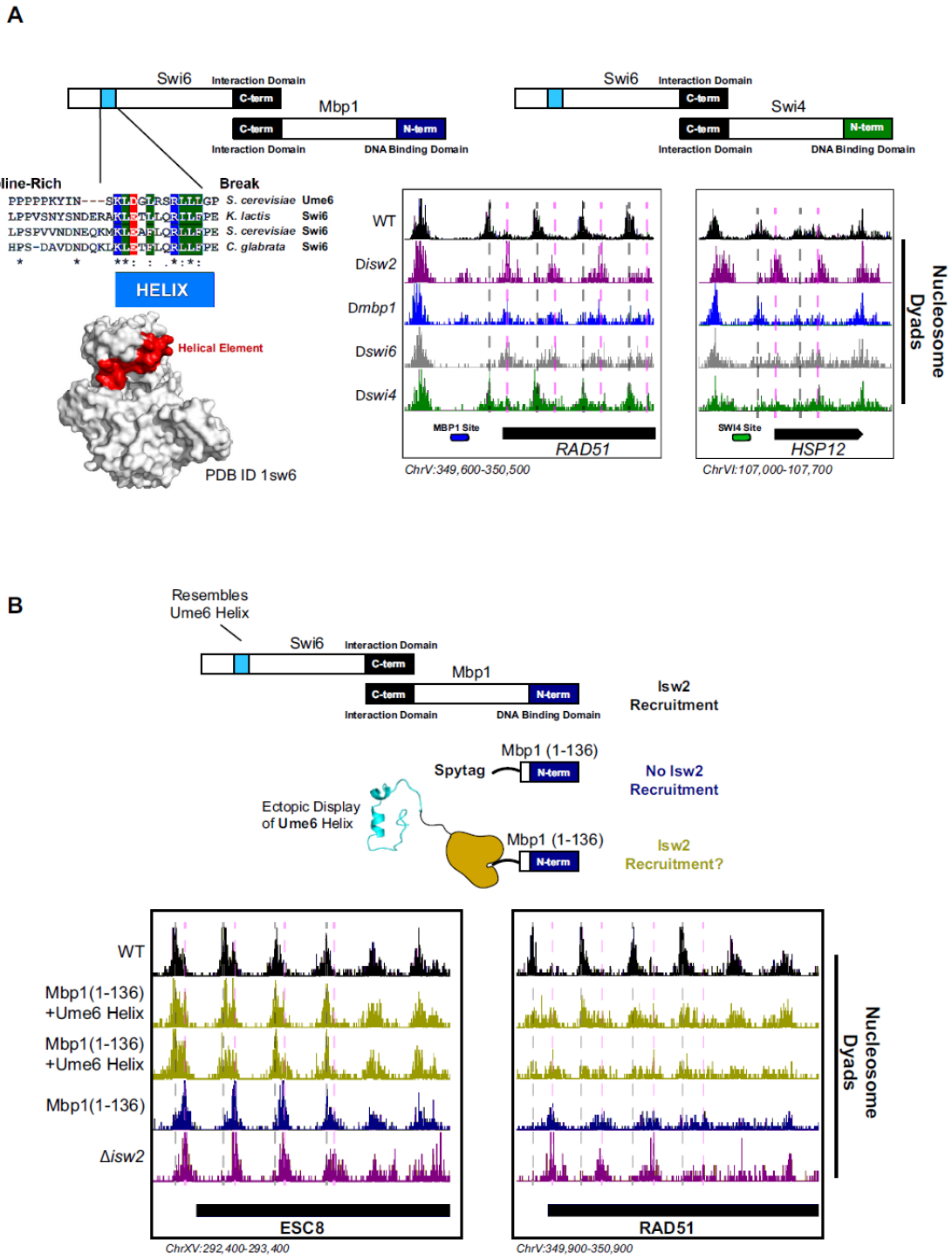

We conducted sequence alignment and conservation analyses between the helical element in Ume6 and full-length Swi6 from multiple yeast species (Figure 3A). We noticed a similarly conserved surface-exposed helix (Foord et al., 1999) in the cell cycle regulating protein Swi6 (Figure 3A). Intriguingly, the function of this helical element has not been determined despite its sequence conservation. Because Swi6 also interacts with Swi4 to form the highly conserved SBF complex (Koch et al., 1993), we speculated that deletion of either Swi6, Swi4, or Isw2 could potentially lead to ectopic nucleosome positions at a subset of SBF targets. Indeed, we observed ectopic nucleosome positioning at the HSP12 locus (an SBF target) when either Isw2, Swi6, or Swi4 was absent (Figure 3A). Wild-type nucleosome positions were observed in the absence of Mbp1, indicating that this is specific to SBF. Similarly, wild-type nucleosome positions were observed at Mbp1 targets when Swi4 was missing (Figure 3A), again suggesting that MBF and SBF have individual Isw2-targeting capacity at their respective binding sites. Swi6 appears to be an adapter protein responsible for recruiting Isw2 to Mbp1 and Swi4 sites since Swi6 has no intrinsic DNA binding domain.

These Transcription Factors Localize ISW2 in a DNA-Sequence and Cellular Context Dependent Manner

To determine if Isw2 recruitment to Mbp1 sites was sufficient to recapitulate proper nucleosome positioning, we again used a SpyTag-SpyCatcher approach (Figure 3B). Mbp1 was truncated to the DNA binding domain alone (Mbp1 1–136), which abolishes its interaction with Swi6 but still allows for proper genomic localization. This truncation construct was appended with SpyTag, and nucleosome positions were

examined in the absence of any SpyCatcher partner present. As expected, we observed aberrant chromatin structure identical to the Δisw2 strain near the Isw2-dependent Mbp1 targets, adjacent to Mbp1 consensus motifs (Figure 3B). We then introduced SpyCatcher fused to the helical element from Ume6, which was characterized above for bringing Isw2 to Ume6-bound loci. Introduction of the SpyCatcher-Ume6 fusion to the Mbp1(1–136)-SpyTag background resulted in the rescue of proper Isw2-directed nucleosome positioning at Mbp1 sites (Figure 3B).

Altogether, these data strongly support our model that these conserved, putatively helical sequences are important for recruiting Isw2 to establish proper chromatin structure at multiple sequence-specific motifs throughout the genome. We also implicate Swi6 as an adapter protein for bringing Isw2 to a small subset of both Swi4 and Mbp1 targets to create Isw2-specific nucleosome positioning at these genes. Finally, the ectopic display of an Isw2-recruitment helix can recapitulate proper Isw2-directed nucleosome positioning, further supporting the notion that a small epitope is necessary and sufficient for communicating specific nucleosome positioning outputs to the Isw2 chromatin remodeling protein.

The WAC Domain of ISW2 is Responsible for its Interaction with Transcription Factors

The Isw2 complex contains two major subunits (Figure 4A). The catalytic subunit Isw2 harbors the energy-producing ATPase domain flanked by biochemically well-defined autoregulatory domains (Clapier and Cairns, 2012; Yan et al., 2016; Ludwigsen

et al., 2017) with a C-terminal HAND-SANT-SLIDE domain, thought to bind linker DNA (Zofall et al., 2004) and interact with the accessory subunit Itc1. Itc1 contains an N-terminal WAC domain, thought to bind to and sense extranucleosomal DNA and help with nucleosome assembly in the *Drosophila* ortholog ACF1 (Fyodorov and Kadonaga, 2002). Itc1 links to Isw2 through a DDT domain (DDT is named for "DNA-binding homeobox-containing proteins and different transcription factors") (Fyodorov and Kadonaga, 2002). The ~350 amino acid N-terminal region of human Acf1 was shown to bind both extranucleosomal linker DNA and the histone H4 tail, suggesting an allosteric mechanism through which ISWI complexes can set proper spacing between nucleosomes (Hwang et al., 2014). Though this work was performed with human ACF complex, Hwang et al. demonstrated that removal of residues 2–374 in *S. cerevisiae* was lethal, suggesting a critical and conserved role of these residues in establishing proper chromatin structure *in vivo* (Hwang et al., 2014).

Figure 4 (next page): The N-terminal WAC Domain in Itc1 Couples Isw2 Biochemical Activity to All Isw2 Genomic Targets.

(**A**) Cartoon representation the Isw2 and Itc1 subunits of the yeast ISW2 complex. Isw2 possesses autoregulatory domains on either side of the catalytic ATPase domain (AutoN and NegC). The HAND-SANT-SLIDE (HSS) domain of Isw2 interacts with the DDT domain of Itc1 for complex formation. Itc1 has an N-terminal region thought to act as a length-sensing domain (gray rectangle) and an N-terminal WAC domain with putative nonspecific linker DNA binding ability. (**B**) Nucleosome sliding assay demonstrating that deletion of the N-terminal domain (Δ9–374) from Itc1 does not impair nucleosome sliding *in vitro* by the Isw2 complex. Higher electrophoretic mobility indicates end-positioned (unslid) nucleosomes while lower electrophoretic mobility indicates centrally positioned (slid) nucleosomes. Isw2-FLAG complexes were purified from exponentially growing yeast cells. Amount of Isw2 added was 1 µl (+) or 1.5 µl (++). Sliding assays were performed three independent times with similar results. (**C**) Genome Browser images showing nucleosome dyad positions for indicated strains at *RAD51* and *ALP1*, two representative Isw2 targets. Only wild-type (WT) cells display the proper nucleosome positions (vertical gray dashed lines) while all Itc1 truncations and *isw2* deletion display similar ectopic nucleosome positions (vertical pink dashed lines). (**D**) Heatmap comparing difference in nucleosome positions at 5942 PIC locations

for *isw2* deletion versus WT strains (left) and Itc1(Δ24–130) versus WT strains (right). Black indicates where nucleosomes are shifted by functional Isw2 while red indicates where nucleosomes shift when Isw2 complex is perturbed. All rows are linked and ordered identically to Figure 1A.

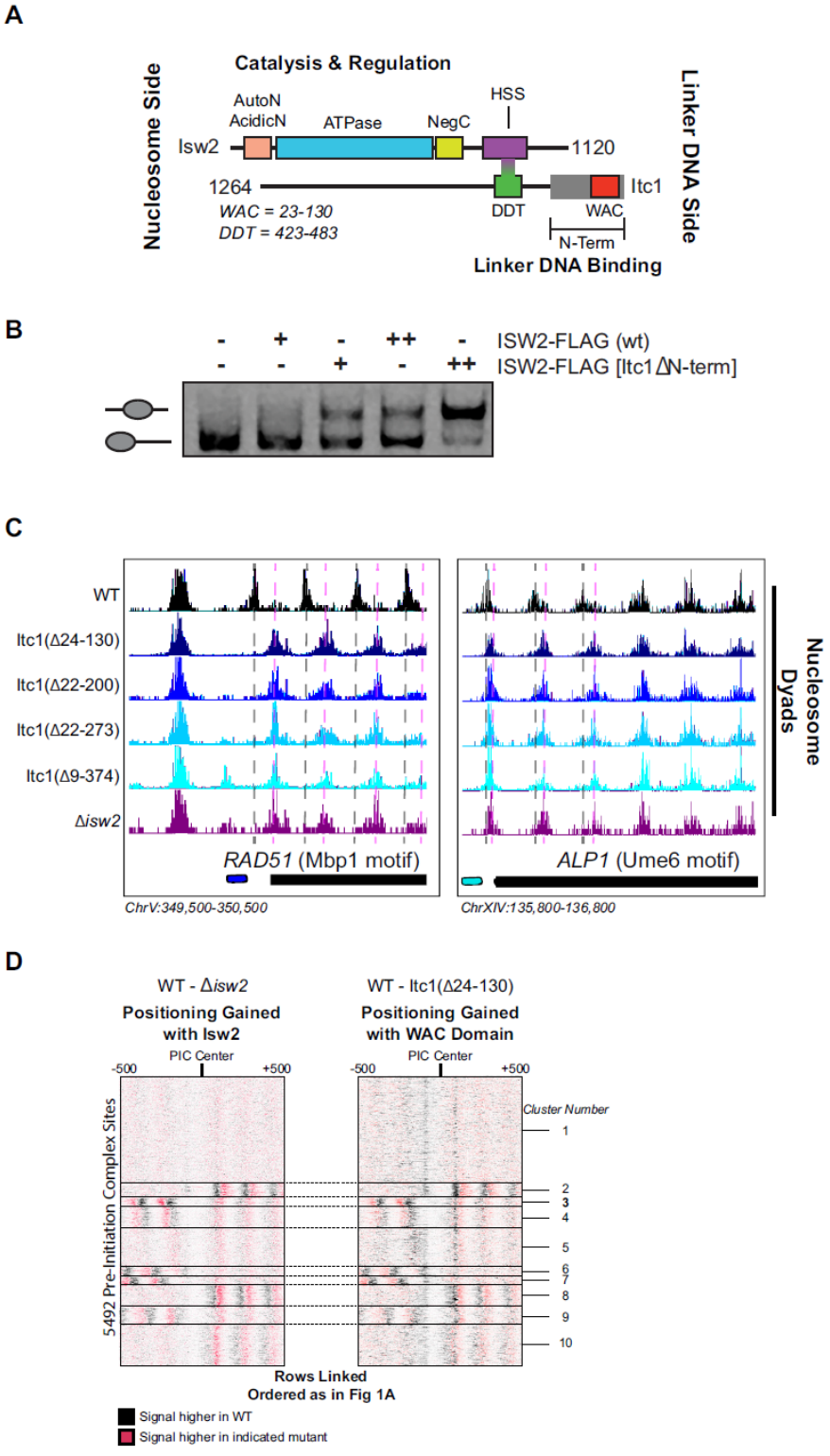

Because of the geometry of the Isw2 complex, with the N-terminus of Itc1 sensing DNA information distal to the nucleosome onto which the catalytic subunit is engaged, we speculated that the N-terminus of Itc1 would be the most likely component of the Isw2 complex for interacting with epitopes in DNA-bound recruitment factors. We first attempted to recapitulate the result from Hwang et al. and made the identical Itc1(Δ2–374) deletion. Isw2 containing Itc1(Δ2–374) did not display any defects in nucleosome sliding using a gel mobility shift assay that detects nucleosome centering by Isw2 (Figure 4B). Surprisingly, this construct was not lethal in our W303 background, but phenocopied a Δisw2 strain by displaying identical ectopic nucleosome positioning at all Isw2 target sites throughout the genome (Figure 4C). Since proper targeted nucleosome positioning was lost when this large N-terminal region was removed, but complex formation and catalytic activity were maintained, we strongly suspected that the Isw2 targeting domain resided in the Itc1 N-terminus.

We created a panel of truncations in this region, guided by sequence conservation through humans, and determined whether wild-type or Δisw2 positions were observed throughout the genome. All truncations tested resulted in loss of positioning at Isw2 targets, and we were able to narrow the targeting region entirely to the highly conserved WAC domain. Deletion of the WAC domain (Itc1 residues 24–130) produced identically ectopic nucleosome positions compared to Δisw2 at target loci (Figure 4C) and genome-wide (Figure 4D). We conclude that the WAC domain of Itc1 is the component of the Isw2 complex responsible for coupling with epitopes on DNA-bound factors such as Ume6, Swi6, and all other Isw2 targeting proteins with yet-to-be-defined recruitment epitopes.

To confirm that the WAC domain can interact with Isw2 targets throughout the genome, we created Itc1(1-73)-FLAG and Itc1(1-132)-FLAG constructs based on two differentially conserved regions within the full WAC domain (Figure 5A). Neither of these constructs contains the DDT domain, so they are incapable of forming a complex with endogenous Isw2. We performed ChIP-Seq to determine if these WAC domain constructs could associate with Isw2 targets without complexing with the Isw2 catalytic domain (Figure 5B, Figure S14). Genome-wide binding demonstrates large, but not complete overlap of Isw2(K215R)-FLAG ChIP peaks with both Itc1(1–73)-FLAG and Itc1(1–132)-FLAG, strongly suggesting that the Itc1 region from 1 to 73 alone can interact with Isw2 targets.

Figure 5 (next page): The Itc1 WAC Domain Associates with Genomic Isw2 Targets and Orients Isw2 on the Proper Nucleosomes.

(**A**) Sequence conservation for regions of Itc1 examined by ChIP. Itc1(1–73)-FLAG incorporates the pink highlighted region while Itc1(1–132)-FLAG incorporates the pink and green highlighted regions. Sequence conservation is shown relative to human BAZ1A and *Drosophila melanogaster* Acf1, two widely studied Itc1 orthologs. (**B**) (Left) Full view of yeast chromosome IX showing Isw2(K215R)-FLAG ChIP (red), Itc1(1–73)-FLAG ChIP (pink), Itc1(1–132)-FLAG ChIP (green), nucleosome dyad signal from wild-type (WT) yeast (black), and nucleosome dyad signal from Itc1(Δ24–130) yeast (blue). Regions indicated by black rectangles are shown with higher resolution on the right. (Right) Zoomed-in view of a locus where Isw2-ChIP and Itc1 truncation ChIP overlap (*RGI2*) or where only Isw2 binding is detected (*PDR11*). Black circles indicate center of ChIP peaks and are connected by a dashed black line to highlight offset of indicated peaks. (**C**) (Left) Heatmap showing 273 detected Isw2 ChIP peaks (red) clustered by associated Itc1(1–73)-FLAG ChIP (pink). The two clusters (right-side Itc1 and left-side Itc1) are shown on the right. (Right) Meta-analysis of Isw2(K215R)-FLAG ChIP signal at 62 cluster 1 peaks or 57 cluster 2 peaks (from left) with associated Itc1(1–73)-FLAG signal. The offset between Isw2 and Itc1 is indicated by two circles connected by a dashed line. Associated nucleosome positions for WT and *isw2* deletion strains for each cluster are shown below in black and blue, respectively. All data are centered at called Isw2 peaks. (**D**) Cartoon representation for how the N-terminal WAC domain of Itc1 interacts with a helical element in a sequence-specific DNA-associated transcription factor to orient Isw2 on the proper motif-proximal nucleosome for directional movement toward the recruitment site.

A

```
Sc  Itc1   23 VQVWHIEETGEWFSSYEEFLERFDFYTRHHFTCEITGTSCLTFFQALDSEE 73
Hs  BAZ1A  22 EEVFYCKVTNEIFRHYDDFFERTILCNSLVWSCAVTGRPGLTYQEALESEK 72
Dm  ACF1   25 DQVFCCYITKRIFRDYEHYFRHVMVINSTVWQCEATGKENLTYEEAVKSER 75
              :*:    * . *  *:.::.:  . .   : *  **   **: :*:.**.

           74 TQFKYVEDRFPLKLREPVARFLHFNGIRRLDALVEKVYARFKNDFFPGEVVYLRKQK 130
           73 KARQN-LQSFPEPLIIPVLYLTSLTHRSRLHEICDDIFAYVKDRYFVEETVEVIRNN 128
           76 AARKK-MEQFKQSLRAPVLLVVEHAQQSAVNTLNMIVAKFLRKRYFIGEEVSVQAKK 131
                 :   : *   *  **  .       :. :   :   .:. :*  * * :  ::
```

B

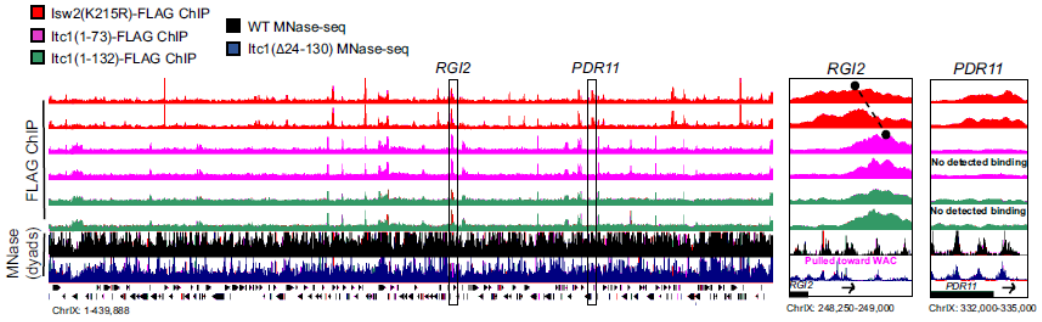

C

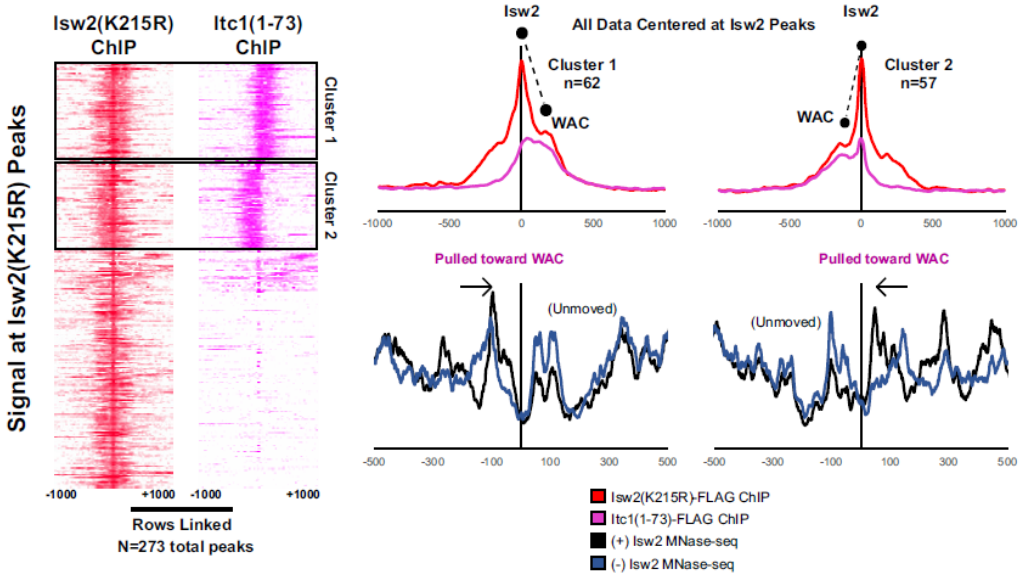

D

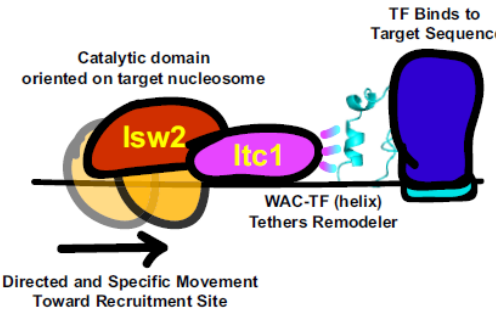

We noticed that the Itc1 signal and Isw2 signal were offset at target genes such that Itc1(1–73) or Itc1(1–132) was upstream and Isw2 was closer to the nucleosome that was selected for repositioning (Figure 5B, Figure S14). Genome-wide analysis showed that Itc1(1–73) was associated with approximately half of Isw2-bound loci and was offset from the catalytic subunit at all co-bound sites (Figure 5C). In all cases, Itc1(1–73) was found upstream of the nucleosome that was repositioned, and Isw2 was located on top of the selected nucleosome. Nucleosomes were always shifted toward the Itc1 subunit (Figure 5C). This geometry matches what was seen by ChIP-Exo mapping with Isw2 subunits at Reb1 target sites (Yen et al., 2012).

We propose a mechanism where the Itc1 WAC domain interacts with a DNA-bound factor, which constrains the Isw2 catalytic subunit to select the proper proximal nucleosome and reposition it toward the immobilized Itc1 (Figure 5D). This is again consistent with the recently proposed 'pulling' model (Kubik et al., 2019), but we postulate that Itc1 is anchored to a DNA-bound factor such as Ume6 to allow Isw2 to pull nucleosomes toward the proper location.

An Anomalous Evolutionary Loss of this Interaction in Drosophila

There is an abundance of literature suggesting that *Drosophila* ACF complex, the Isw2 ortholog, is a nonspecific nucleosome spacing and assembly factor that evenly spaces phased nucleosome arrays against defined genomic barriers (Lusser et al., 2005; Baldi et al., 2018; Fyodorov and Kadonaga, 2002). We wondered if the WAC domain of *Drosophila* Acf1 was different from that of Itc1, so we performed sequence alignment of

WAC domains and compared to Acf1 from the *Drosophila* genus. While sequence alignment demonstrated widespread conservation of the WAC domain, one striking feature was exposed: the *Drosophila* genus underwent reversal or loss of negative charge at multiple residues that are strictly or mostly acidic in other representative organisms (Figure 6A).

Two of these residues are strictly acidic in all organisms except members of the *Drosophila* genus (E33 and E40 in Itc1). The other two (E43 and D70 in Itc1) are more loosely conserved, though they are strictly positive charge in *Drosophila*. We made charge-reversal mutations in *S. cerevisiae* Itc1 to recapitulate the *D. melanogaster* residues at each of these positions either pairwise (a, b and c, d to separate the strictly conserved acidic versus loosely conserved acidic nature) or simultaneously (a, b, c, d) to reverse all charges to the *D. melanogaster* sequence. We assessed whether charge reversal was sufficient to abrogate targeted nucleosome positioning at Isw2 targets across the yeast genome (Figure 6B). Strikingly, the E33R/E40H double mutation (a, b) was enough to completely abolish Isw2 activity at specific and known Isw2 targets (Figure 6B) and at all genomic loci where Isw2 activity is observed (Figure 6C). Mutation of the less-conserved acidic residues E43R/D70K (c, d) retained Isw2-directed nucleosome positioning. As expected, mutation of all four acidic residues (a, b, c, d) E33R/E40H/E43R/D70K resulted in complete loss of Isw2-targeted activity across the genome (Figure 6B, C).

Figure 6 (next page) Essential Targeting-Specific Charged Residues in the Conserved WAC domain are Lost in *Drosophila*.

(**A**) Sequence conservation of the N-terminal region (22–73) of Itc1 across various organisms with key charged residues highlighted in blue or red for positive and negative

charge, respectively. Horizontal dashed line indicates separation of all other species from members of the *Drosophila* genus. (**B**) Genome Browser image showing nucleosome dyad signal at two representative Isw2 target loci. Wild-type (WT) nucleosome positions are indicated by gray vertical dashed lines while ectopic nucleosome positions associated with *isw2* deletion or indicated charge reversal mutations are denoted by vertical pink dashed lines. (**C**) Meta-analysis of nucleosome dyad signal at 178 PIC sites associated with cluster 3 (from Figure 1A). Only WT and charge reversal c, d display proper nucleosome positions while charge reversal a, b or a, b, c, and d display ectopic positions identical to deletion of *ISW2* completely.

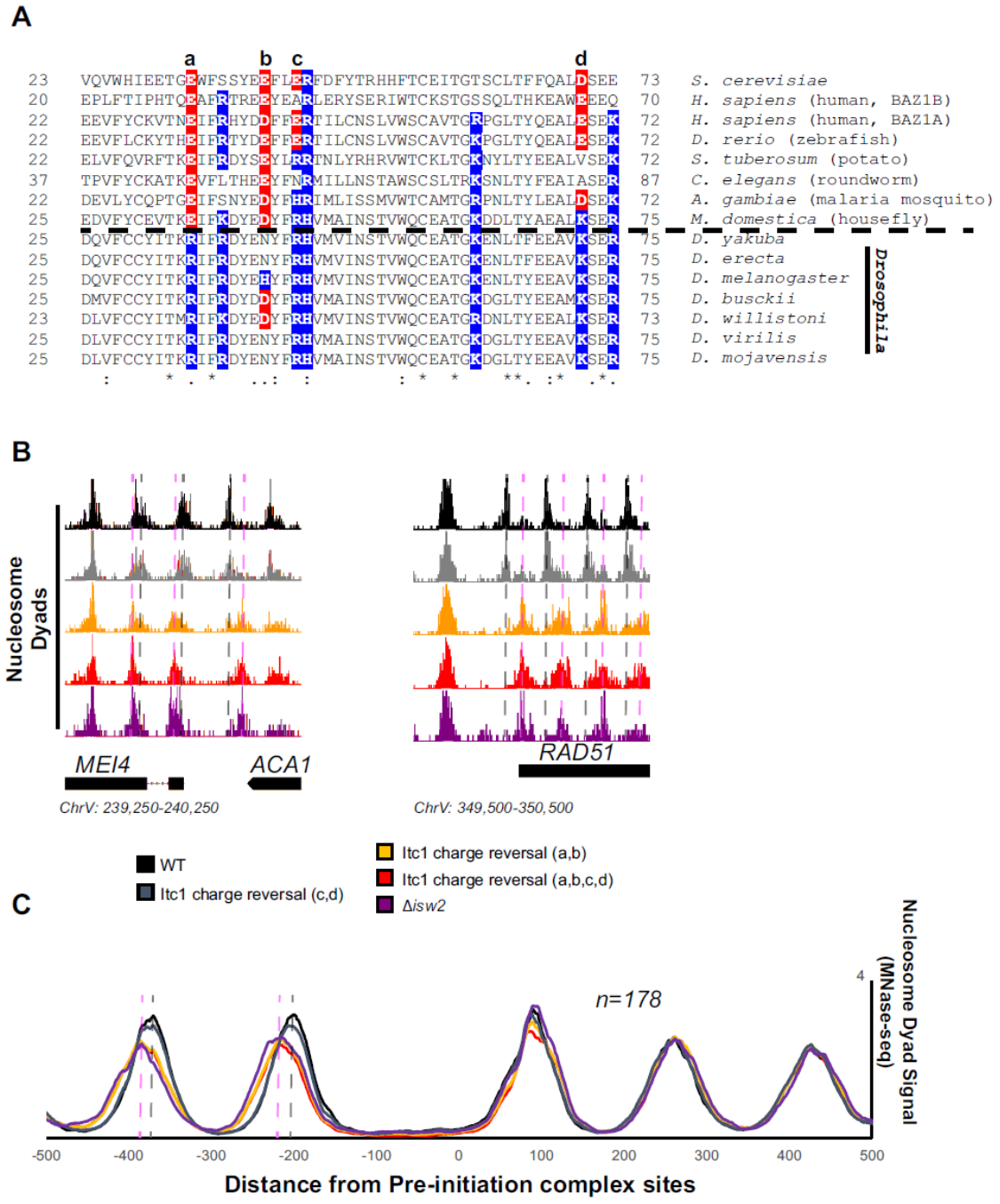

We conclude that the *Drosophila* genus lost critical acidic residues that are essential for targeted nucleosome positioning by *S. cerevisiae* Isw2, potentially explaining the disconnect between the *Drosophila* ACF literature and what we have characterized herein. It is possible that the increase in positive charge simultaneously increases nonspecific binding of *Drosophila* Acf1 to extranucleosomal DNA, and these charge reversals may help explain the nonspecific spacing behavior of Acf1 observed in *Drosophila*. We also believe that there is strong potential that humans and most other organisms have retained targeting potential as they retain mechanistically important acidic residues present in yeast Itc1. In support of conservation, targeted nucleosome array formation has previously been observed in humans at specific transcription factor sites including CTCF, JUN, and RFX5 (Wiechens et al., 2016).

Bridge to Chapter III

In this chapter I have shown that the Isw2 complex is indeed localized to sequence-specific locations in the genome through interactions with the transcription factors Ume6 and Swi6. Importantly, I have revealed the previously unappreciated motifs on the Isw2 complex subunit Itc1 as well as on the transcription factor protein partners that enable this targeted mechanism of chromatin remodeling to occur. I also discuss the evolutionary loss of this function in the *Drosophila* genus and how it may have led to the universal adoption of the barrier model. In the next chapter I will consider how we can engineer the specific targeting of chromatin remodeling proteins to effect synthetic changes on chromatin structure and thereby cellular function. The ability to impose control upon chromatin structure, when taken with the data presented above, serves to

highlight the power and importance of this new mechanism of sequence-specific chromatin remodeling protein function.

CHAPTER III

ENGINEERING CHROMATIN REMODELING PROTEINS TO IMPOSE TARGETED GENETIC CONTROL

*****This chapter contains previously published co-authored material.

Donovan, D.A., Crandall, J.G., Banks, O.G.B., Jensvold, Z.D., Truong, V., Dinwiddie, D., McKnight, L.E., McKnight, J.N. (2019). Engineered chromatin remodeling proteins for precise nucleosome positioning. Cell Reports 29:2520–2535.

Conceptualization, D.A.D., L.E.M., and J.N.M.; Methodology, D.A.D., J.G.C., O.G.B.B., Z.D.J., V.T., L.E.M., and J.N.M.; Investigation, D.A.D., J.G.C., O.G.B.B., Z.D.J., V.T., L.E.M., and J.N.M.; Writing – Original Draft, D.A.D., J.G.C., and J.N.M.; Writing – Review & Editing, D.A.D., J.G.C., Z.D.J., L.E.M., and J.N.M.; Visualization, D.D. and J.N.M.; Supervision, L.E.M. and J.N.M.; Project Administration, J.N.M.; Funding Acquisition, J.N.M.

Developing an Engineered Chromatin Remodeling Protein Core

The core E-ChRP design was inspired by previous work (McKnight et al., 2011, 2016) where individual sequence-specific DBDs replaced the C-terminal nonspecific DBD of a functional *S. cerevisiae* Chd1 chromatin remodeler fragment (Figure 7A). Yeast Chd1 is an ideal enzyme for engineered chromatin remodeling because it is monomeric, displays robust nucleosome positioning activity on nucleosome substrates

derived from multiple organisms, and is less influenced by histone modifications than other chromatin remodelers (Ferreira et al., 2007; Hauk et al., 2010). Following the Chd1 catalytic module, we incorporated restriction sites flanking the targeting domain in vectors allowing recombinant expression in *E. coli*, constitutive expression from ADH1 or GPD promoters in *S. cerevisiae* (Mumberg et al., 1995), or galactose-inducible expression after integration at the HO locus in *S. cerevisiae* (Voth et al., 2001). This scaffold allows easy swapping of the C-terminal targeting domain, resulting in a simple method to design chromatin remodelers that can be localized to desired nucleosomes.

Figure 7 (next page): Strategies for Optimizing Targeted Nucleosome Positioning by E-ChRPs

(A) Architecture of the E-ChRP core where the yeast Chd1 catalytic domain is linked to a targeting domain with a flexible linker. **(B)** Summary of targeting methods used in this work, including sequence-specific DBD targeting to a recognition motif (top), SpyCatcher domain covalently attaching to a SpyTag-containing chromatin-bound protein (middle), and dCas9-bound gRNA interacting with a complementary sequence (bottom). **(C)** Predicted outcome from targeted E-ChRPs, indicating that select nucleosomes are positioned by the E-ChRP onto the recruitment site. **(D)** Nucleosome repositioning *in vitro* by Chd1-Ume6 with and without 11 repeats of glycine-glycine-serine between the Chd1 catalytic domain and Ume6 DBD. Nucleosomes with the Ume6 recognition motif (URS1) located 20 or 40 bp from the nucleosome edge were incubated with Chd1-Ume6(DBD) or Chd1-GGSx11-Ume6(DBD), and nucleosomes were resolved using native PAGE (top). Nucleosome positions before and after remodeling were resolved using 6% native PAGE. Summary of repositioning of each substrate by Chd1 fusions (bottom). **(E)** Genome Browser image showing nucleosome dyad positions at a representative Ume6 binding site (URS1) for a parental strain lacking endogenous Ume6 (black), after introduction of Chd1-Ume6 without (yellow) or with (red) a flexible linker. Dashed line indicates the location of the Ume6 binding motif. Arrow indicates nucleosome that is more efficiently positioned with a Chd1-GGSx11-Ume6(DBD) fusion. **(F)** Average nucleosome positioning (dyad signal) at genomic Ume6 binding sites showing Chd1-GGSx11-Ume6(DBD) more readily positions nucleosomes distal to the recognition element than Chd1-Ume6(DBD) lacking a flexible linker.

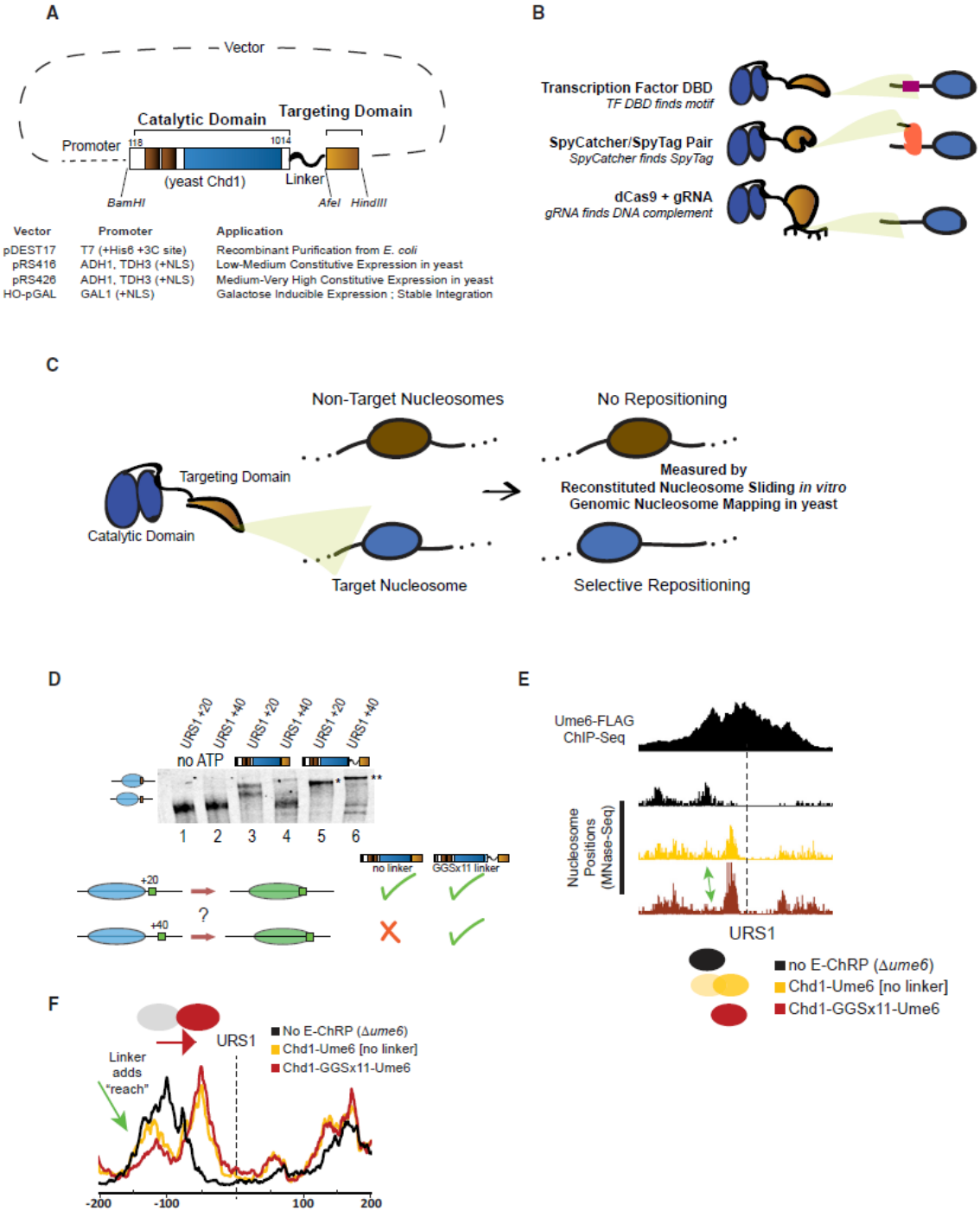

Vector	Promoter	Application
pDEST17	T7 (+His6 +3C site)	Recombinant Purification from *E. coli*
pRS416	ADH1, TDH3 (+NLS)	Low-Medium Constitutive Expression in yeast
pRS426	ADH1, TDH3 (+NLS)	Medium-Very High Constitutive Expression in yeast
HO-pGAL	GAL1 (+NLS)	Galactose Inducible Expression ; Stable Integration

To demonstrate the versatility of the approach, we incorporated and assessed engineered chromatin remodeling through multiple TF DBDs, through SpyCatcher/SpyTag pairs, and through dCas9 targeting (Figure 7B). We first assessed the ability of different E-ChRPs to reposition target-containing mononucleosomes in a purified biochemical assay (Eberharter et al., 2004). To validate *in vivo* function, we introduced E-ChRPs into *S. cerevisiae* and measured global nucleosome positions using MNase sequencing (MNase-Seq). Functional E-ChRPs can position targeted nucleosomes onto recruitment motifs as measured using mononucleosome sliding toward recruitment sequences *in vitro* or target motif occlusion by nucleosomes *in vivo* (Figures 7C–7F).

We previously demonstrated that fusion of a foreign DBD to the Chd1 catalytic core leads to occlusion of a recruitment motif by targeted and directional repositioning of nucleosomes (McKnight et al., 2011, 2016). Although functional both *in vitro* and *in vivo*, remodeler fusions in which the DBD was directly fused to the Chd1 core resulted in a limited ‘‘reach,’’ and nucleosomes residing further than 20 bp from the DNA recognition element were not efficiently moved. In addition, the creation of new remodeler fusion proteins was previously cumbersome and lacked versatility. To address these limitations, we first created the E-ChRP scaffold (Figure 7A), which consists of the catalytic core of the yeast Chd1 protein followed by a flexible linker including 11 repeats of the glycine-glycine-serine sequence, which was previously shown to extend the Chd1 reach *in vitro* (Nodelman and Bowman, 2013). We next created an array of plasmids for recombinant bacterial expression or yeast constitutive or inducible expression, allowing one-step cloning of a desired fusion domain (Figure 7A).

We examined whether the addition of a flexible linker between the Chd1 remodeler core and DBD increased the reach of these E-ChRPs. We tested the ability of an E-ChRP with a DBD from the *S. cerevisiae* meiotic repressor Ume6 to move mononucleosomes containing a recognition motif, URS1 (Park et al., 1992), 20 or 40 bp from the nucleosome edge (Figure 7D). Without a flexible linker, the Chd1-Ume6 E-ChRP was strongly stimulated only when the motif was 20 bp away (compare lane 1 with lane 3 and lane 2 with lane 4). In contrast, the addition of 11 repeats of glycine-glycine-serine (GGSx11) allowed the remodeler to efficiently mobilize both nucleosome substrates (compare lane 1 with lane 5 and lane 2 with lane 6). Additionally, the final location of the positioned nucleosomes was dependent on the location of the recognition motif (Figure 7D, compare lanes 5 and 6). Consistent with this increased reach *in vitro*, the Ume6 E-ChRP containing a GGSx11 linker positioned a larger fraction of distal nucleosomes onto target sequences across the *S. cerevisiae* genome as measured using paired-end MNase-Seq (Figures 7E and 7F). Because the flexible linker led to more robust E-ChRP activity and our design was compatible *in vitro* and *in vivo*, we used this scaffold in all subsequent experiments.

A Diverse Array of Engineered Chromatin Remodeling Proteins Can Specifically Position Nucleosomes *In Vitro* and *In Vivo*

We next tested mononucleosome targeting of multiple E-ChRPs with various DBDs. We fused the DBD from *E. coli* AraC, *S. pombe* Res1, *D. melanogaster* engrailed, or *R. norvegicus* glucocorticoid receptor to the E-ChRP scaffold. To determine if these E-ChRPs were functional on target nucleosomes *in vitro*, we generated end-positioned

mononucleosomes assembled on the 601-positioning sequence (Lowary and Widom, 1998) with 125 bp of flanking DNA. The extranucleosomal DNA either contained or lacked a consensus binding motif corresponding to each different fusion tested. E-ChRPs were able to mobilize nucleosomes possessing well-defined recruitment motifs for each distinct E-ChRP DBD (Ades and Sauer, 1994; Alroy and Freedman, 1992; Ayté et al., 1995; Niland et al., 1996) as measured using a native PAGE nucleosome sliding assay (Figure 8A). These E-ChRPs were inactive on nucleosomes lacking their respective motifs (Figure 8A, lanes 22–27), demonstrating specificity for target substrates *in vitro.* Fusion of the native, sequence-nonspecific DBD from Chd1 to our E-ChRP scaffold showed no apparent discrimination against DNA sequences and was capable of fully mobilizing the nonspecific mononucleosome control (Figure 8A, lanes 28–30).

Figure 8 (next page): E-ChRPs with Distinct TF DBDs Specifically Position Target Nucleosomes *In Vitro* and *In Vivo*

(A) Nucleosome sliding assay demonstrating functionality of increasing concentrations of E-ChRPs containing AraC DBD (lanes 1–5 and 22–24), Res1 DBD (lanes 6–10 and 25–27), engrailed DBD (lanes 11–15), glucocorticoid receptor DBD (lanes 16–20), or Chd1 endogenous DBD (lanes 28–30) *in vitro*. Nucleosomes in lanes 1–20 possess recognition motifs in extranucleosomal DNA for the respective E-ChRP (Ades and Sauer, 1994; Alroy and Freedman, 1992; Anderson et al., 1995; Ayté et al., 1995; Khan et al., 2018; Niland et al., 1996), while lanes 21–30 have no recognition motif. Lower electrophoretic mobility indicates repositioning of nucleosomes away from their end positions.**(B)** Yeast genomic nucleosome dyad positions are shown at representative Ume6 targets (URS1, top) or engrailed targets (TAAT, bottom) in the presence or absence of Ume6 E-ChRP or engrailed E-ChRP. Motif-proximal nucleosomes are highlighted next to indicated motifs, with blue arrows showing direction of nucleosome movement. Cartoon representations of nucleosome positions are provided for each locus. **(C)** Nucleosome dyad signal at a representative locus in yeast demonstrating positioning of nucleosomes toward recruitment motif (dashed line) by galactose inducible Ume6 E-ChRP or a constitutively expressed E-ChRP under the ADH1 promoter.

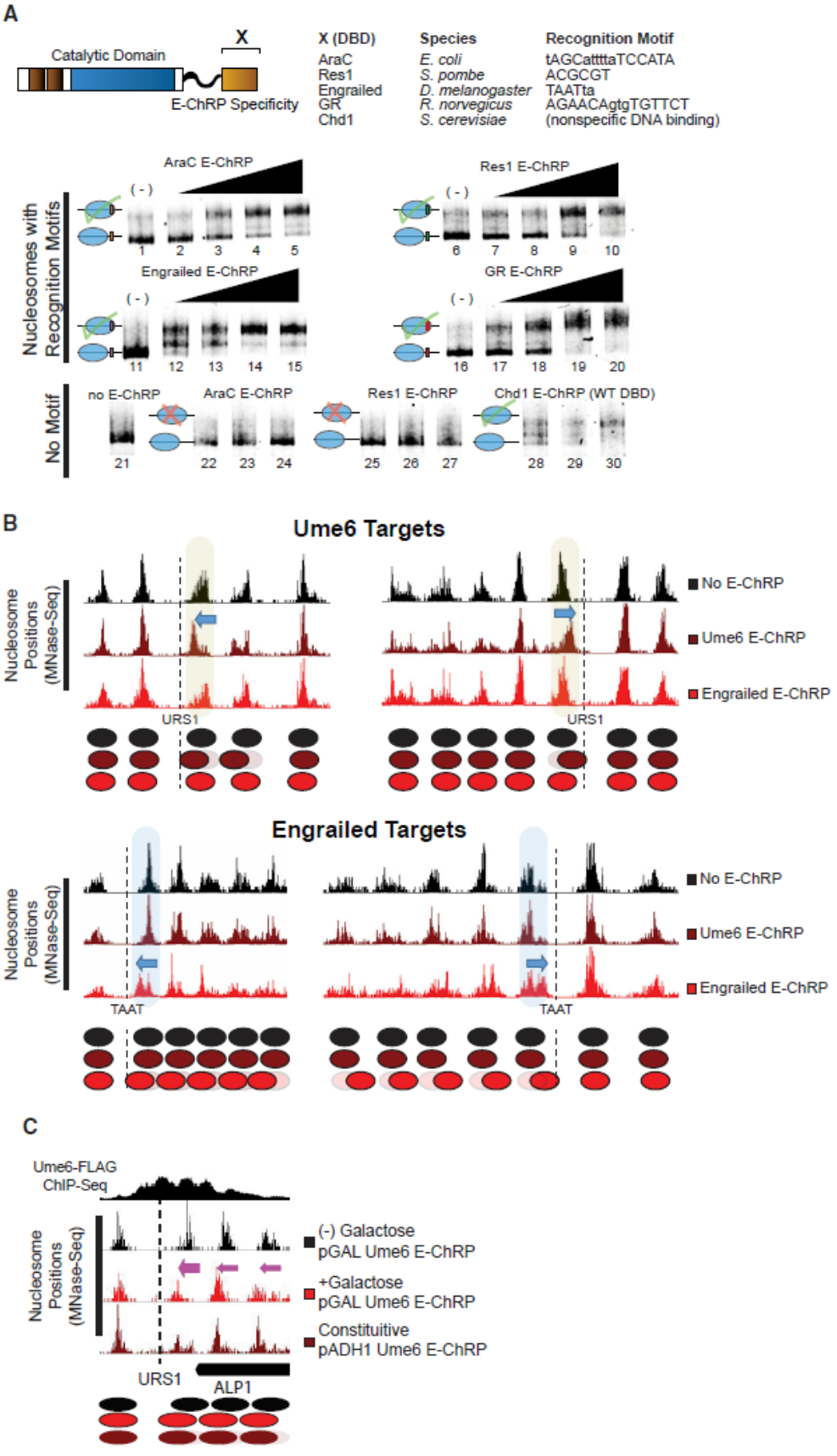
A
Catalytic Domain
X
E-ChRP Specificity
X (DBD)
AraC
Res1
Engrailed
GR
Chd1
Species
E. coli
S. pombe
D. melanogaster
R. norvegicus
S. cerevisiae
Recognition Motif
tAGCattttaTCCATA
ACGCGT
TAATta
AGAACAgtgTGTTCT
(nonspecific DNA binding)
Nucleosomes with Recognition Motifs
AraC E-ChRP
Res1 E-ChRP
Engrailed E-ChRP
GR E-ChRP
No Motif
no E-ChRP
AraC E-ChRP
Res1 E-ChRP
Chd1 E-ChRP (WT DBD)
B
Ume6 Targets
Nucleosome Positions (MNase-Seq)
No E-ChRP
Ume6 E-ChRP
Engrailed E-ChRP
URS1
Engrailed Targets
TAAT
C
Ume6-FLAG ChIP-Seq
(-) Galactose pGAL Ume6 E-ChRP
+Galactose pGAL Ume6 E-ChRP
Constituitive pADH1 Ume6 E-ChRP
ALP1

To determine whether E-ChRPs can be differentially targeted to specific subsets of nucleosomes *in vivo,* we introduced E-ChRPs into *S. cerevisiae* on a constitutive, ADH1-driven expression plasmid. When the E-ChRP possessed a Ume6 DBD, nucleosomes were repositioned toward Ume6 binding motifs across the genome (Figure 8B). Although no nucleosome changes were detected at other genomic loci, we cannot rule out the possibility that these E-ChRPs possessed low-level nonspecific nucleosome positioning activity throughout the genome, as MNase-Seq detects population-average nucleosome positions. Similarly, an E-ChRP containing the engrailed DBD moved nucleosomes onto engrailed motifs in the yeast genome without altering nucleosome positions at Ume6 binding motifs (Figure 8B).

We also introduced Ume6 and engrailed E-ChRPs into yeast under the high-expression GPD (TDH3) promoter on a 2 μm plasmid (Mumberg et al., 1995). Expression of the Ume6 E-ChRP from this construct resulted in positioned nucleosomes at target sites without detected off-target activity, similar to an ADH1-driven E-ChRP (Figure S15A). Again, we cannot rule out the possibility of low-level, global off-target activity that does not give rise to reproducibly shifted nucleosomes at specific sites. However, introduction of this higher expression plasmid containing an engrailed E-ChRP only produced viable transformants in which the E-ChRP construct was deleted, truncated, or mutated. This obligate inactivation of the engrailed E-ChRP at high expression levels may result from promiscuous action of the engrailed E-ChRP at tens of thousands of potential target sequences, which would presumably disrupt global nucleosome positioning in a pleiotropic manner. Importantly, even when driven from the GPD (TDH3) promoter, neither the Ume6 E-ChRP nor the engrailed E-ChRP was active

at target sites when the Chd1 remodeler core contained a catalytically inactive Walker B (D513N) substitution (Hauk et al., 2010; Walker et al., 1982) (Figures S15A and S15B).

To gain temporal control of E-ChRPs *in vivo,* we introduced the Ume6 E-ChRP under a galactose-inducible promoter integrated at the HO locus in yeast (Voth et al., 2001). Prior to addition of galactose, endogenous Ume6 associates with its consensus sequence across the genome and cooperates with the ISW2 complex to position motif-proximal nucleosomes, leaving 30 bp between the nucleosome edge and URS1 motif (Goldmark et al., 2000; McKnight et al., 2016). After galactose-driven transcriptional induction of the Ume6 E-ChRP, a majority of nucleosomes nearest the URS1 site are efficiently repositioned to occlude the URS1 motif within 2 hours (Figure 8C). This galactose inducible approach allows a larger fraction of nucleosomes to be repositioned in a population compared with the same E-ChRP under the control of a constitutively active ADH1 promoter, potentially commensurate with differing expression levels under these distinct promoters (Figure 8C).

Taken together, these results suggest that E-ChRPs can be specifically targeted with temporal regulation using multiple distinct DBDs that recognize sequence motifs with high or low complexity both *in vitro* and *in vivo*.

Engineered Chromatin Remodeling Proteins Can Occlude the Binding of Native Genomic Proteins and Inhibit Their Function

After E-ChRP activity, the population average of positioned nucleosomes displays a maximum nucleosome dyad signal 49 nt from the recruitment motif center (distribution

from 73 to 15 nt), which corresponds to the motif being buried within the 145 bp nucleosomal footprint by approximately 25 bp. This matches what we have mapped previously *in vitro* (McKnight et al., 2011), where we see occlusion of motifs by 20–30 bp in the presence of E-ChRPs. We reasoned that because the post-induction nucleosome position results in the Ume6 recruitment motif becoming buried within nucleosomal DNA, remodeling by the Ume6 E-ChRP should interfere with binding of endogenous Ume6 (Figure 9A). To test this possibility, we tagged endogenous Ume6 with a FLAG epitope and measured Ume6-FLAG binding by chromatin immunoprecipitation sequencing (ChIP-Seq) before and after induction of the Ume6 E-ChRP. Prior to induction, reproducible Ume6-FLAG binding was observed at URS1 sites across the genome (Figure S16A). After induction of the Ume6 E-ChRP, which shifted nucleosomes over URS1 sites, Ume6 binding (as measured by Ume6-FLAG ChIP signal) was strongly reduced or eliminated at many genomic locations (Figures 9B and S16A).

Figure 9 (next page). E-ChRPs Can Inducibly Remove Endogenous Ume6 from Chromatin

(A) Cartoon depiction of Ume6 E-ChRP activity blocking association of endogenous Ume6 at target sites. **(B)** Representative examples of E-ChRP targets where endogenous Ume6 is removed (top) or not removed (bottom) after galactose induction of Ume6 E-ChRP. The catalytic null E-ChRP retains a Ume6 DBD but has a Walker B (D513N) substitution in the Chd1 catalytic core. **(C and D)** Representative Genome Browser images showing E-ChRP-dependent nucleosome dyad movement (within black rectangles) onto Ume6 sites (dashed line) with associated reduction of Ume6-FLAG ChIP, increase in acetylation, and transcriptional induction for the SRT1 locus (C) and MEI5 locus (D).

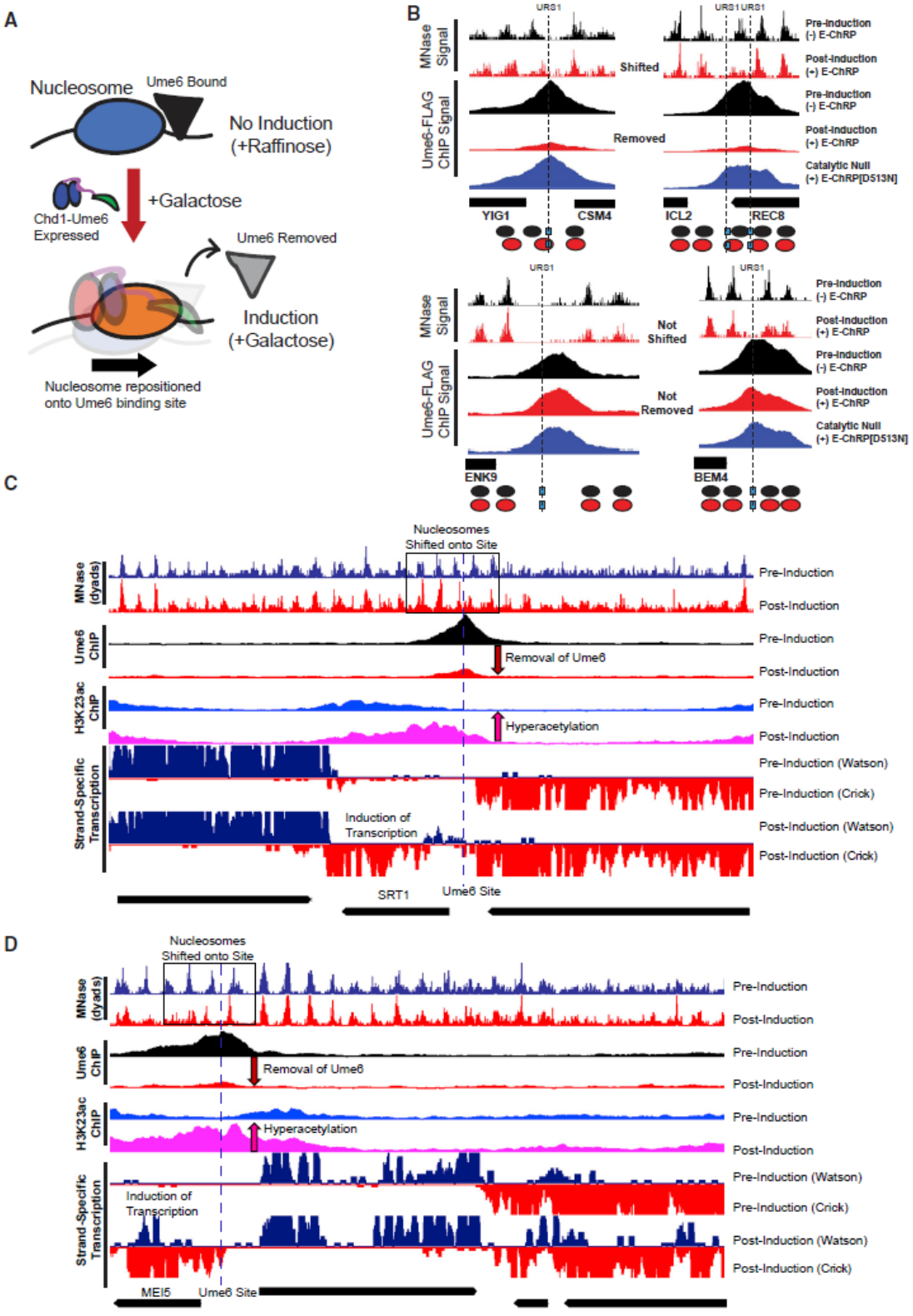
A
Nucleosome
Ume6 Bound
No Induction
(+Raffinose)
+Galactose
Chd1-Ume6
Expressed
Ume6 Removed
Induction
(+Galactose)
Nucleosome repositioned
onto Ume6 binding site
B
MNase Signal
Ume6-FLAG ChIP Signal
URS1
Shifted
Removed
Not Shifted
Not Removed
Pre-Induction (-) E-ChRP
Post-Induction (+) E-ChRP
Catalytic Null (+) E-ChRP[D513N]
YIG1
CSM4
ICL2
REC8
ENK9
BEM4
C
Nucleosomes Shifted onto Site
MNase (dyads)
Ume6 ChIP
H3K23ac ChIP
Strand-Specific Transcription
Pre-Induction
Post-Induction
Removal of Ume6
Hyperacetylation
Pre-Induction (Watson)
Pre-Induction (Crick)
Post-Induction (Watson)
Post-Induction (Crick)
Induction of Transcription
SRT1
Ume6 Site
D
Nucleosomes Shifted onto Site
MEI5
Ume6 Site

When we sorted Ume6 binding sites on the basis of whether proximal nucleosome positions were shifted after Ume6 E-ChRP induction, we noticed that loss of Ume6-FLAG signal was strikingly reduced where nucleosomes were shifted but minimally reduced where nucleosomes were not shifted (Figures 9B and S16B). To verify that this reduction in Ume6-FLAG signal was not due to direct binding competition between endogenous Ume6-FLAG and the E-ChRP Ume6 DBD, we measured Ume6-FLAG ChIP signal in the presence of a catalytically inactive Ume6 E-ChRP. This construct, which cannot move nucleosomes but retains the Ume6 DBD, did not similarly reduce Ume6-FLAG signal (Figures 9B and S16A). Together with the observation that Ume6 was removed only where nucleosome shifts were observed (Figures 9B and S16B) but not where nucleosomes remained, we therefore believe the detected loss of Ume6 is due to site occlusion by E-ChRP activity rather than direct competition for DNA binding by the E-ChRP DBD. Thus, E-ChRPs can inducibly move nucleosomes over target sequences to restrict access of the underlying DNA to endogenous DNA binding factors.

We next assessed the functional consequences of endogenous Ume6 removal by E-ChRP induction. Because Ume6 recruits the Rpd3 histone deacetylase to strongly repress target genes (Goldmark et al., 2000; Kadosh and Struhl, 1997), we tested whether Ume6 displacement could lead to increased histone acetylation (as measured using H3K23ac ChIP) and transcriptional induction (as measured using strand-specific RNA sequencing [RNA-Seq]). Strikingly, at sites where E-ChRP induction led to loss of Ume6-FLAG signal, we detected strong increases in histone acetylation and associated increases in transcription (Figures 9C, 9D, S16B, and S16C). Importantly, the increased histone acetylation was observed only at targets where nucleosome positions were altered

and Ume6-FLAG was removed, indicating that these effects were likely not due to simple competition between the E-ChRP and endogenous Ume6. These highly correlated results, where temporally regulated nucleosome positioning onto Ume6 target sites led to Ume6 removal and loss of Ume6 mediated repression, demonstrate that E-ChRPs can be used for disrupting the binding and activity of transcriptional regulators at target sites.

Using the SpyCatcher/SpyTag System to Target and Identify Tightly Bound Native Genomic Proteins

One limitation of the above-described E-ChRPs is their need to compete with endogenous factors for binding sites. To circumvent this problem, we created an E-ChRP in which the SpyCatcher protein is fused in place of a DBD in the Chd1 E-ChRP scaffold. SpyCatcher specifically recognizes a short (1 kDa) SpyTag epitope, forming an isopeptide linkage that allows covalent protein fusions to be created *in vitro* and *in vivo* (Zakeri et al., 2012). This fusion provides two major improvements to the E-ChRP system. First, by simply appending SpyTag to different chromatin-binding factors of interest, nucleosome positioning can be achieved by a single SpyCatcher E-ChRP without the need to design new DBD fusions (Figure 10). Second, by tagging a TF at its endogenous locus, nucleosomes can only become targetable for the SpyCatcher E-ChRP when the TF is bound to chromatin (Figure 10A). This bypasses the requirement of a vacant DNA binding site to target a DBD-containing E-ChRP, allowing access to sequences in the genome that could otherwise be blocked by a stably bound TF. In sum, this strategy produces a single SpyCatcher E-ChRP that can be targeted to any chromatin-bound protein of interest in the genome by simple attachment of a short SpyTag.

To validate the function of the SpyCatcher E-ChRP design, we purified recombinantly expressed Chd1-SpyCatcher and two SpyTag-containing DBDs. Mononucleosomes harboring recognition sequences for each DBD were incubated with the SpyCatcher E-ChRP with and without addition of SpyTag-engrailed(DBD) or SpyTag-AraC(DBD). The SpyCatcher E-ChRP has no activity on nucleosome substrates in the absence of a SpyTag-DBD pair (Figure 10B, lanes 2–4), because SpyCatcher has no intrinsic DNA binding affinity. However, addition of either SpyTag-AraC(DBD) (Figure 10B, lanes 5–7) or SpyTag-engrailed(DBD) (Figure 10B, lanes 8–10) resulted in robust repositioning of mononucleosomes *in vitro*, demonstrating the versatility of this system. We next introduced the SpyCatcher E-ChRP under a constitutive ADH1 promoter into *S. cerevisiae* cells in which a C-terminal SpyTag was added to full-length Ume6 at the endogenous locus. As expected, we observed repositioned nucleosomes at URS1 sites across the genome, indicating chromatin remodeling at Ume6-bound loci (Figure 10C).

Figure 10 (next page). Development and Validation of E-ChRPs Containing SpyCatcher/SpyTag Pairs

(A) Cartoon representation for introducing a Chd1-SpyCatcher E-ChRP into cells containing SpyTagged, chromatin-bound proteins. The SpyCatcher domain forms a covalent isopeptide bond with SpyTag, allowing localization of E-ChRP activity to endogenously bound chromatin proteins. **(B)** Nucleosome sliding assay demonstrating that a single SpyCatcher E-ChRP cannot position nucleosomes without a SpyTag-containing DBD (lanes 2–4) but can use a SpyTagged AraC DBD (lanes 5–7) or engrailed DBD (lanes 8–10) to reposition nucleosomes containing respective DBD recognition motifs. The AraC and engrailed recognition elements are located 7 and 11 nt from the nucleosome edge, respectively. **(C)** Representative motif in yeast where ADH1-driven SpyCatcher E-ChRP can reposition nucleosomes (dyads) at a Ume6 binding site in the presence of Ume6-SpyTag (left) and genomic analysis of nucleosome dyad positioning by SpyCatcher E-ChRP at 202 intergenic instances of the Ume6 recognition sequence in cells containing SpyTagged Ume6 (right). **(D)** Genomic analysis of nucleosome dyad positions in Reb1-SpyTagged cells (left) or Ume6-SpyTagged cells (right) before and after 2 h induction of galactose inducible SpyCatcher E-ChRP.

Heatmaps show change in nucleosome dyad signal after induction of SpyCatcher E-ChRP, and individual traces show average positions of nucleosomes in each cluster before and after SpyCatcher E-ChRP induction for each SpyTag-DBD strain.

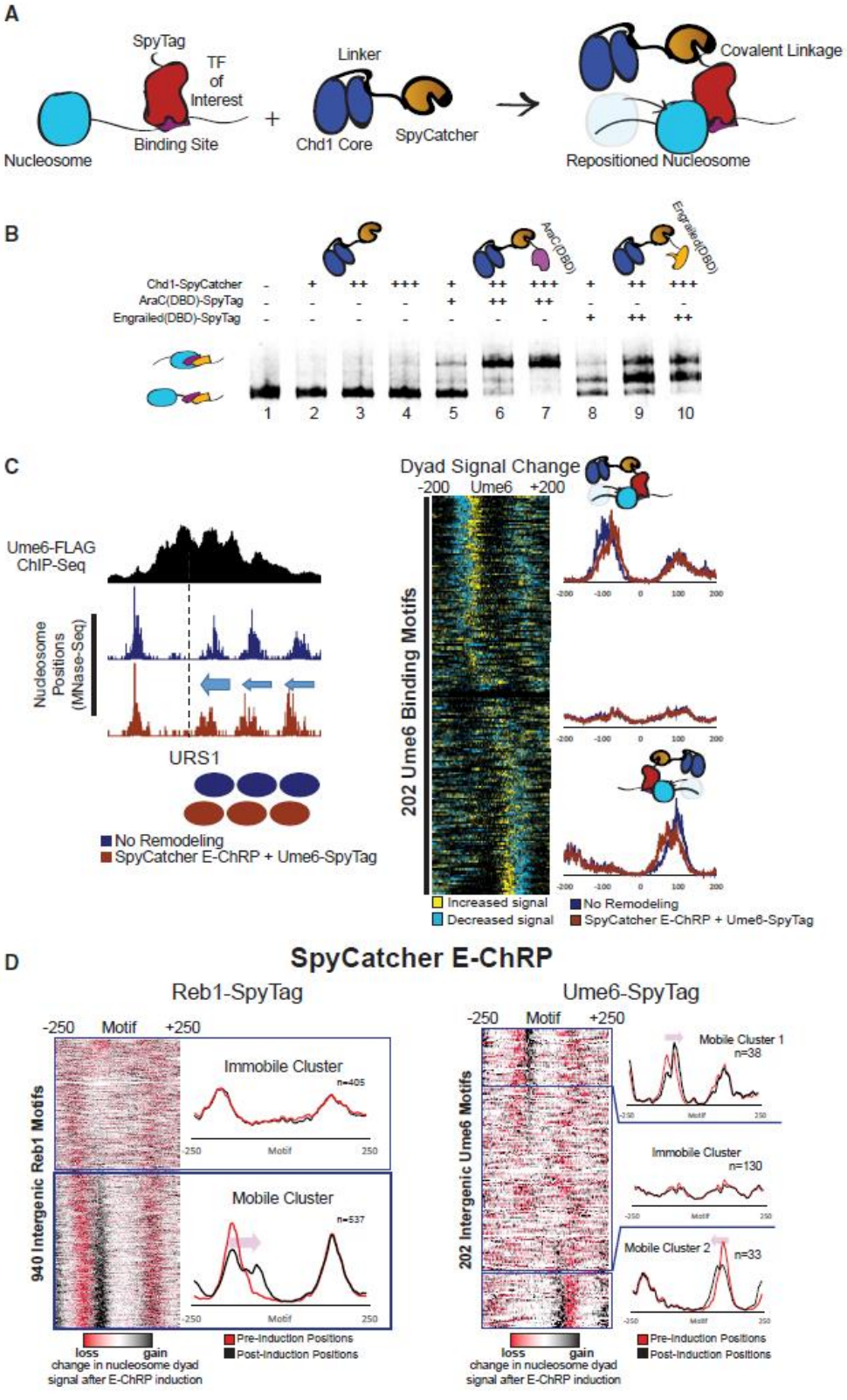

To achieve temporal control of this modular system *in vivo*, we appended SpyTag to the C terminus of either Ume6 or Reb1, a yeast general regulatory factor, in a strain harboring a galactose-inducible SpyCatcher E-ChRP at the HO locus. After induction of SpyCatcher E-ChRP expression, nucleosomes were shifted toward Ume6 binding sites in cells containing Ume6-SpyTag or toward Reb1 binding sites in cells containing Reb1-SpyTag (Figures 10D, S17A, and S17B). Interestingly, the fraction of shifted nucleosomes was generally low at Ume6 binding sites in Ume6-SpyTag cells but comparatively higher at Reb1 binding sites in Reb1-SpyTag strains (Figure 10D). This difference could be explained by higher occupancy or stability of Reb1 than Ume6 binding at target sites, which would allow a greater fraction of Reb1-tethered SpyCatcher to mobilize motif-proximal nucleosomes. Consistent with this possibility, the cellular abundance of Ume6 is significantly lower than that of Reb1 (Kulak et al., 2014). For Reb1-SpyTag strains, the positioning of a single motif-proximal nucleosome by the SpyCatcher E-ChRP initiated the shift of an entire array of nucleosomes toward the target motif (Figure S17C), consistent with previous observations that the positioning of a ‘‘barrier nucleosome’’ influences and constrains positions of an entire array of nucleosomes (Mavrich et al., 2008; McKnight et al., 2016).

Interestingly, the positioning of nucleosomes appeared to occur on only the 5’ side of the Reb1 recognition sequence, suggesting the orientation of Reb1 binding affects the ability of Chd1 to reach nucleosomes near binding sites (Figures 10D and S17C). This restriction could be explained by a constrained C terminus of Reb1 when bound to chromatin, which is consistent with similarly constrained Reb1-MNase cleavage patterns seen in previous chromatin endogenous cleavage sequencing (ChEC-Seq) experiments

(Zentner et al., 2015). Importantly, the nucleosome shifts observed are not due to the inability of Reb1 to associate with target sites, because the changes in nucleosome positions are distinct from bidirectional nucleosome repositioning observed when Reb1 is depleted from the nucleus using the anchor-away method (Kubik et al., 2015) (Figure S18A). In aggregate, induction of the SpyCatcher E-ChRP in a Reb1-SpyTag strain leads to nucleosome depleted region (NDR) occlusion at roughly 650 TSSs (Figure S18B). Unexpectedly, the fraction of nucleosomes shifted at individual Reb1 binding sites varied greatly in our dataset, with some sites exhibiting repositioning of nearly 100% of motif-proximal nucleosomes in the population and others having much smaller fractions moved (Figures 11A–11C). These differences are not explained by initial nucleosome occupancy or location differences (Figure 11B) but are possibly related to relative Reb1 occupancy at different genomic locations.

Figure 11 (next page). E-ChRP Targeting to Chromatin-Bound Reb1 Provides Differential Occupancy Information at Reb1 Motifs

(A) Nucleosome dyad signal at 943 intergenic Reb1 binding motifs in Reb1-SpyTag strains before (left) and after (right) 2 h induction of SpyCatcher E-ChRP. Rows are ordered by change in nucleosome positioning after galactose induction. Purple shading highlights the region to which nucleosomes are moved by SpyCatcher E-ChRP in the Reb1-SpyTag strain. **(B)** The purple mobile fraction from (A) was split into deciles (~50 motifs per decile) showing average positioning by SpyCatcher E-ChRP for each decile. Dashed lines indicate the pre-induction, unremodeled position (red) or post-induction, remodeled position (black). Ume6-SpyTag control traces are provided for the top and bottom deciles demonstrating that SpyCatcher E-ChRP cannot function at Reb1 sites in the presence of Ume6-SpyTag instead of Reb1-SpyTag. **(C)** Genome Browser images for representative loci showing nucleosome dyad positioning by SpyCatcher E-ChRP in a Reb1-SpyTag strain for the top, middle, and bottom deciles. Purple shading indicates the motif-proximal, repositioned nucleosomes. Dashed lines indicate the location of Reb1 motif.

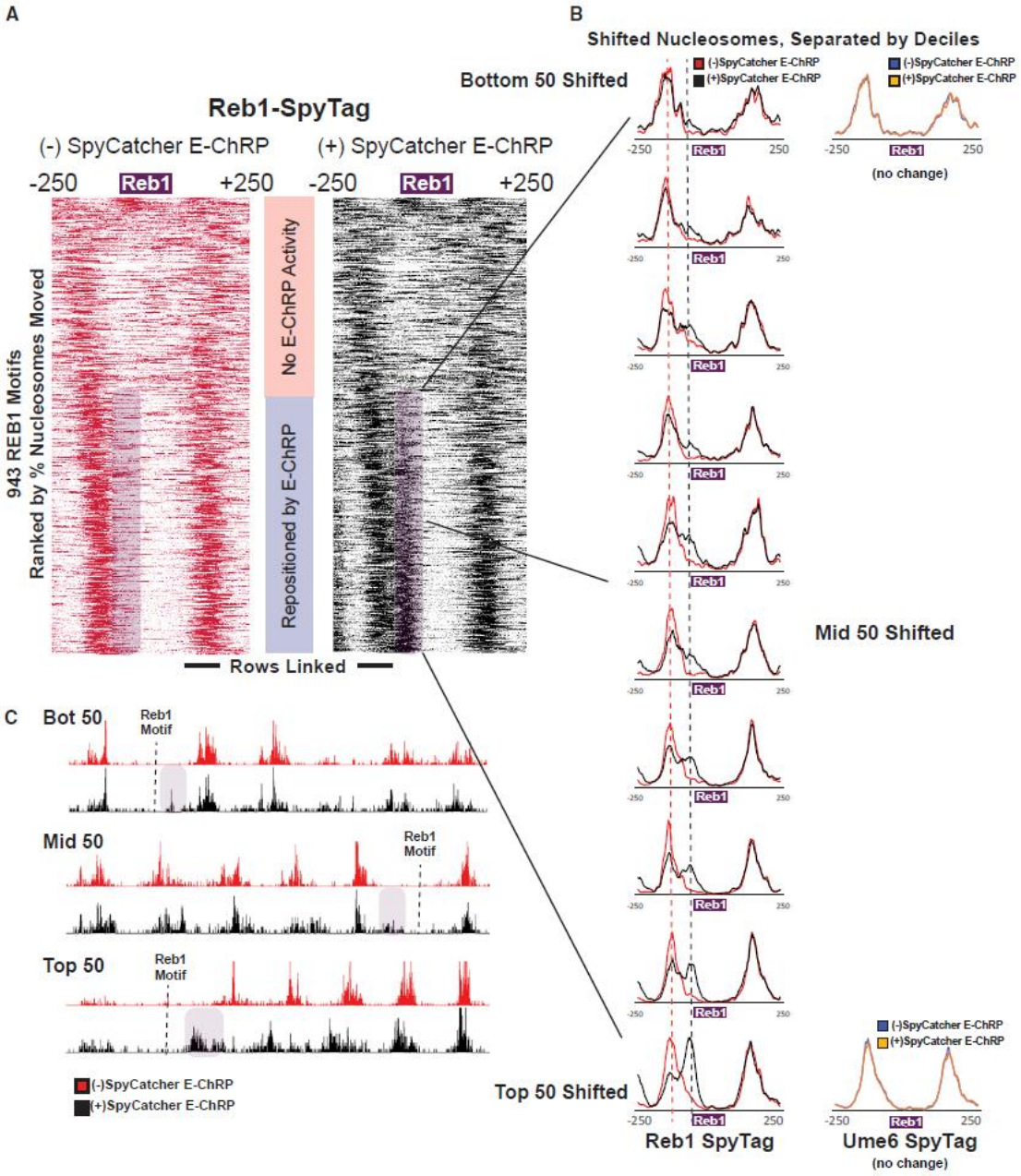
A
Reb1-SpyTag
(-) SpyCatcher E-ChRP
(+) SpyCatcher E-ChRP
-250
Reb1
+250
-250
Reb1
+250
943 REB1 Motifs
Ranked by % Nucleosomes Moved
No E-ChRP Activity
Repositioned by E-ChRP
Rows Linked
B
Shifted Nucleosomes, Separated by Deciles
Bottom 50 Shifted
(-)SpyCatcher E-ChRP
(+)SpyCatcher E-ChRP
(no change)
Mid 50 Shifted
Top 50 Shifted
Reb1 SpyTag
Ume6 SpyTag
(no change)
C
Bot 50
Reb1
Motif
Mid 50
Top 50
(-)SpyCatcher E-ChRP
(+)SpyCatcher E-ChRP

To further characterize the ability of SpyCatcher E-ChRP to identify fractional Reb1 occupancy at Reb1 binding sites, we compared our dataset with crosslinking ChIP-Seq, CUT&RUN (Skene and Henikoff, 2017), ORGANIC (Kasinathan et al., 2014), and ChEC-Seq (Zentner et al., 2015) datasets. There was striking correlation among our data, ORGANIC, and ChEC-Seq, with some motifs exclusively showing Reb1 occupancy when measured using these three methods (Figure S19). Minimally, the observation that all nucleosomes are shifted at some Reb1 binding sites in a population of cells argues that some Reb1 sites are nearly 100% occupied, as E-ChRP-derived nucleosome movement cannot be observed without Reb1 binding (Figure 11C). Although these Reb1 occupancy estimates are conflated with presence, accessibility and relative occupancy of motif-proximal nucleosomes, our data suggest that SpyCatcher E-ChRPs can serve as a relative measure of protein localization in cells that is orthogonal to ChIP, allowing a lower limit estimate of SpyTagged protein occupancy at individual binding motifs in the genome.

Custom DNA Sequence Targeting of Engineered Chromatin Remodeling Proteins with dCas9

Although the E-ChRPs described above show robust nucleosome positioning activity when targeted through various DBDs or through SpyCatcher/SpyTag pairs, their ability to alter nucleosome positions depends on the interaction between pre-existing DBDs with defined DNA motifs. To overcome this limitation and allow targeted positioning of single nucleosomes by design, we created a dCas9 (Gilbert et al., 2013; Qi et al., 2013) E-ChRP (Figure 12). This construct allows versatile targeting to specific

nucleosomes by designing proximal guide RNAs (gRNAs). We recombinantly expressed the dCas9 E-ChRP in *E. coli* and purified the 300 kDa fusion protein.

To test its ability to move gRNA-targeted nucleosomes, we reconstituted end-positioned mononucleosomes and designed gRNAs with or without complementarity to the extranucleosomal DNA. Successful gRNA-stimulated chromatin remodeling would result in movement of the nucleosome toward the target sequence, producing a slower migrating, centrally positioned nucleosome (Figure 12A). Although nucleosomes were

---

Figure 12 (next page). Remodeling Can Be Targeted Using a dCas9 E-ChRP with Canonical and Noncanonical gRNA Substrates

(A) Cartoon depiction of dCas9-targeted chromatin remodeling and predicted repositioning of target nucleosome. **(B)** Nucleosome sliding assay showing irreversible association of the dCas9 E-ChRP with target nucleosomes and free DNA. The ‘‘slid ctrl’’ includes ATP and a control Chd1 protein capable of positioning nucleosomes toward the center of the DNA fragment. Excess unlabeled competitor DNA was added 3 days prior to loading. Nucleosome concentration was 25 nM, and E-ChRP concentration was 75 nM. **(C)** Cartoon depiction of canonical and nonstandard gRNA protospacers. **(D)** Nucleosome sliding assay demonstrating robust positioning of nucleosomes by a dCas9 E-ChRP targeted with nonstandard gRNAs in single-turnover (top) or multi-turnover (bottom) conditions. The slid ctrl (lanes 2 and 12) includes ATP and a control Chd1 protein. The ‘‘no gRNA’’ lanes (3 and 13) contain a dCas9 E-ChRP, ATP, and no gRNA. No-target gRNA samples (lanes 4 and 14) contain a dCas9 E-ChRP and a gRNA without any sequence complementarity to the substrate nucleosome. Note that the order of lanes between the upper and lower panels is similar except for loading of hp-gRNA (lanes 5, 6, 17, and 18) and mmgRNA (lanes 7, 8, 15, 16). **(E)** Nucleosome sliding assay demonstrating lack of stable association of dCas9 E-ChRPs with target nucleosomes or DNA in the presence of nonstandard gRNAs. For the upper gel, competitor DNA was added prior to loading. The bottom gel contains the identical reactions in the same order as the upper gel, but no competitor DNA was added before loading. **(F)** Genome Browser image showing both canonical and mismatched gRNAs allow repositioning of nucleosome dyads (note appearance of dyad signal in blue rectangle regions) by a dCas9 E-ChRP at the ALP1 locus when the gRNA sequence is exposed but not when gRNA sequence is occluded in the absence of dCas9 E-ChRP.

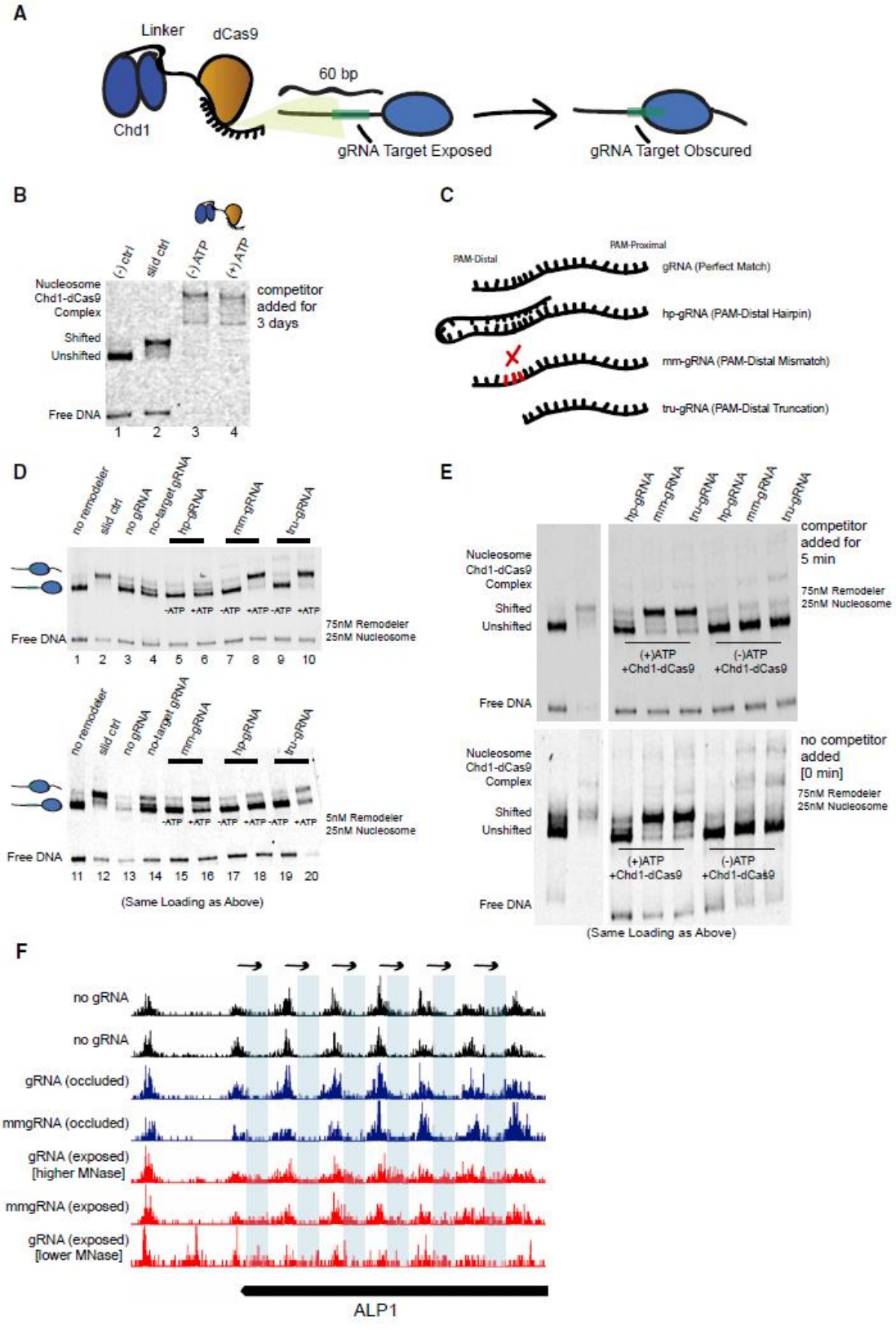
A
Linker
dCas9
Chd1
60 bp
gRNA Target Exposed
gRNA Target Obscured
B
(-) ctrl
slid ctrl
(-) ATP
(+) ATP
Nucleosome
Chd1-dCas9
Complex
Shifted
Unshifted
Free DNA
competitor
added for
3 days
1 2 3 4
C
PAM-Distal
PAM-Proximal
gRNA (Perfect Match)
hp-gRNA (PAM-Distal Hairpin)
mm-gRNA (PAM-Distal Mismatch)
tru-gRNA (PAM-Distal Truncation)
D
no remodeler
slid ctrl
no gRNA
no-target gRNA
hp-gRNA
mm-gRNA
tru-gRNA
-ATP +ATP -ATP +ATP -ATP +ATP
75nM Remodeler
25nM Nucleosome
Free DNA
1 2 3 4 5 6 7 8 9 10
5nM Remodeler
25nM Nucleosome
11 12 13 14 15 16 17 18 19 20
(Same Loading as Above)
E
competitor
added for
5 min
75nM Remodeler
25nM Nucleosome
(+)ATP
+Chd1-dCas9
(-)ATP
+Chd1-dCas9
no competitor
added
[0 min]
(Same Loading as Above)
F
no gRNA
no gRNA
gRNA (occluded)
mmgRNA (occluded)
gRNA (exposed)
[higher MNase]
mmgRNA (exposed)
gRNA (exposed)
[lower MNase]
ALP1

efficiently moved toward the center of DNA fragments with control Chd1 protein, introduction of Chd1-dCas9 and complementary gRNA resulted in supershifted complexes with unresolved nucleosome positions. Even in the presence of 1,000-fold competitor DNA for 3 days, the Chd1- dCas9 fusion protein would not release from gRNA-targeted nucleosomes (Figure 12B). This inability of dCas9 to release from target sequences is consistent with the ability of dCas9 to specifically bind and interfere with transcription in cells because of stable R-loop formation (Jinek et al., 2012; Laughery et al., 2019; Qi et al., 2013). Importantly, the inability of the dCas9 EChRP to release from substrate prevents its utility *in vitro* and could possibly limit use for precise, gRNA-targeted nucleosome positioning in cells.

To promote release of the dCas9 E-ChRP from nucleosome substrates, we used gRNAs with noncanonical structures (Figure 12C), including a truncated gRNA (tru-gRNA) (Fu et al., 2014) containing only 14 nt of complementarity to target sequences, a gRNA with a PAM-distal hairpin (Josephs et al., 2015) that has predicted self-annealing capacity and reduced affinity for target sequences, and a 20 nt gRNA with a PAM-distal 3 nt mismatch (mm-gRNA) that would result in an R-loop with a frayed end. Both the tru-gRNA and the mmgRNA allowed efficient targeted repositioning of nucleosomes toward the gRNA binding site either through direct Chd1-dCas9 fusion or introduction of Chd1-SpyCatcher and dCas9-SpyTag pairs (Figure 12D, lanes 1–10; Figure S20). These noncanonical gRNAs promoted multi-turnover catalysis by the dCas9 E-ChRP, demonstrating that the weakened dCas9/gRNA complexes were stable enough to promote specific enzymatic activity but weak enough to readily and repeatedly disengage from its substrate (Figure 12D, lanes 11–20). Strikingly, dCas9-Chd1 targeted through weakened

gRNAs did not require any competitor DNA to disengage from nucleosome substrates (Figure 12E). We believe this ability to readily dissociate from DNA targets while providing enough dwell time and specificity for targeted nucleosome positioning could provide a facile method to alter nucleosome positions by design.

To test whether the dCas9 E-ChRP is functional in cells, we targeted the ALP1 locus with either perfect match or 3 nt mismatched gRNAs targeting a region that was either nucleosome occluded or within the nucleosome linker region. Both the perfect-match and mismatched gRNA allowed repositioning of a nucleosome array in the targeted region (Figure 12F), though only a fraction of nucleosomes in the population were moved in both cases. Nucleosome repositioning was observed only with a gRNA targeted within the nucleosome linker region but not when targeted to nucleosome-occluded DNA. These results suggest that dCas9-targeted nucleosome positioning can be achieved in cells but may require additional optimization; gRNA success is likely dependent on initial nucleosome positioning, and unlike what was observed *in vitro,* mm-gRNAs behave similarly to perfect match gRNAs in a cellular context.

Bridge to Chapter IV

In this chapter I have highlighted our ability to engineer chromatin remodeling proteins to have the desired effects on chromatin structure *in vitro* and *in vivo* using a combination of biochemistry and genomic techniques. This is a newly appreciated means of targeting chromatin remodeling proteins to sequence-specific locations in the genome, employed both by organisms natively and by researchers synthetically. The work herein

has challenged the accepted notion of the “barrier” model and has called attention to the potentials of DNA sequence-specific chromatin remodeling. In the next chapter, I will succinctly summarize all of the data presented above and I will discuss some of the future potential of this knowledge in biology, research, and medicine.

CHAPTER IV

FUTURE APPLICATIONS AND CONCLUSIONS

Summary of This Work

The ability to modulate the structure of chromatin appropriately to regulate downstream genetic processes is critical to the survival of all cells. One of the major ways that this ability is achieved is through the use of chromatin remodeling proteins. Although chromatin remodeling proteins from the ISWI and CHD families have been thought to be non-specific spacing enzymes for the past two decades, this activity does not inherently allow cells to regulate genetic processes in a specific and reproducible manner. Furthermore, this activity is inconsistent with the data observed both in the literature and in the experiments conducted in our lab.

The work presented here sheds light on a new sequence-specific model of chromatin remodeling protein function that exists natively in many organisms and can be co-opted synthetically by biological researchers. The first part of this work focused on the relationship between sequence-specific transcription factor proteins and the chromatin remodeling complex Isw2. Contrary to the prevailing model of non-specific packing against a barrier, we demonstrate instead that Isw2 is a highly specifically targeted enzyme through physical interactions of motifs conserved throughout evolution. Additionally, we show that the notion of non-specific packing against a barrier likely came from work done on these proteins in the *Drosophila* genus, which has an anomalous Isw2 complex when compared to other eukaryotes.

The second part of this work focused on how we as researchers may benefit from the sequence-specific repositioning of nucleosomes through engineered chromatin remodeling proteins. By appending the catalytically active core of Chd1 with a variety of DNA-binding modalities, we have created a suite of tools that can establish a researcher-directed chromatin structure *in vitro* and *in vivo.* Moreover, we demonstrate that downstream biological outputs, such as transcription, can be altered through the use of these engineered chromatin remodeling proteins. Taken together, this work has advanced the study of the field of chromatin on two distinct and complementary fronts.

Remaining Questions and Future Directions

Although we have uncovered a new sequence-specific model of chromatin remodeling protein function in organisms, many questions about this system remain unanswered. Additionally, the creation of these engineered tools to alter chromatin structure in cells may potentially lend itself to many diverse applications in the future. In this section I will ponder a few of the outstanding questions and conceive of some of the applications that this work may inspire.

How Widespread are these Newly Appreciated Functions of Chromatin Remodeling Proteins?

This work revealed two transcription factors, Ume6 and Swi6, that are responsible for targeting the Isw2 complex. The identification of these two proteins in yeast begs the questions: How widespread is this phenomenon? In yeast, are there other transcription

factors that recruit the Isw2 complex (or another chromatin remodeling protein)? And does this recruitment of chromatin remodeling proteins occur in humans? We believe that the answer to both questions is yes for the following reasons.

First, the very nature of regulating chromatin structure by appending a small epitope on a genome binding protein creates the opportunity for diversity with limited evolutionary constraints. Second, we were able to identify the unrelated cell cycle regulator Swi6 as a new Isw2-recruitment adapter for Swi4 and Mbp1 based on the primary sequence of the Ume6 recruitment motif. Third, we know that the two critical acidic residues of Itc1 that allow these interactions to occur are conserved in humans. Finally, it has been observed that Isw2 orthologs can precisely position nucleosomes adjacent to specific factors in the human genome (Wiechens et al., 2016).

For these reasons, we find it likely that more transcription factors that interact with chromatin remodeling proteins will be discovered from a variety of organisms. Importantly, the identification of such interaction interfaces in human cells could lead to the development of targeted drugs to specifically disrupt these defined chromatin remodeling protein-transcription factor interactions.

What Keeps Isw2 from Having Off-Target Effects?

In this work we show that Isw2 acts on particular genomic loci through sequence-specific transcription factor interactions, rather than acting on all nucleosomes genome-wide. This lack of generalized activity is not consistent with previous work done *in vitro* and we speculate that it may be caused by a regulatory interaction that is not recapitulated

in biochemical systems. For example, there may be an unknown inhibitory factor that interacts with Isw2 or the nucleosome *in vivo* that is lost during protein purification, allowing for the more general Isw2 chromatin remodeling activity observed *in vitro.* Additionally, it is possible that Isw2 is unable to bind to extranucleosomal DNA the same way in a genomic context as it can bind *in vitro*, potentially due to the presence of unknown chromatin interacting components, chromatin folding, or other physiological differences not recapitulated biochemically.

Maintaining Isw2 in an inactive state may allow organisms to conserve energy by controlling errant ATP hydrolysis while being primed for rapid changes in chromatin structure in differing contexts. It will be of interest to the field to determine which factors alter the activity of Isw2 *in vivo* to elicit such precise nucleosome positioning outcomes.

What are the Biophysical Mechanisms of Final Nucleosome Positioning in These Contexts?

While this work shows how the Isw2 complex is localized to the genome through transcription factors, it does not inform the biophysical means by which nucleosomes reach their "correct" position. The data indicate that the N-terminus of Itc1 does not have the function of evenly spacing nucleosomes *in vivo* as has been reported *in vitro*, however, the Itc1 N-terminus may be able to bind H4 tail and transcription factor epitopes *in vivo* similarly to how it binds extranucleosomal DNA and H4 tail *in vitro.* If that were true, the Hwang et al. model (Hwang et al., 2014) could mechanistically explain the precise nucleosome positioning seen at targeted sites in cells.

Speculatively, Itc1 would bind a targeting transcription factor at a genomic locus when the upstream nucleosome is far away. This would orient the Isw2 subunit on the appropriate nucleosome, which would then be remodeled toward the recruitment site. When the length between the nucleosome and the recruitment site reaches some threshold, the Itc1 N-terminus may switch to binding the H4 tail to inactivate Isw2 through a known autoinhibition mechanism. Determining whether this toggling between the binding of Itc1 to a transcription factor and to the H4 tail can result in precise distance measurements in cells will be important in future characterizations of chromatin remodeling protein function.

The Future Potential of Engineered Chromatin Remodeling Proteins

We believe that engineered chromatin remodeling proteins are versatile and powerful tools for studying the direct consequences of chromatin changes without alteration of the underlying DNA. We have shown that these engineered proteins can induce precise aberrant positioning of nucleosomes in cells that can establish ectopic nucleosomal arrays, occlude transcription factor binding motifs across the genome which can inhibit their regulatory function, and report on relative protein occupancy at target motif sites.

We envision that future research can use engineered chromatin remodeling proteins to probe questions directly relating to the position of nucleosomes. For example: what effects do nucleosomes positioned over heat shock elements have on downstream biological processes such as heat stress response? What effects do mispositioned

nucleosomes have on higher order chromatin structure? These interrogations may lead to insight into how cells can tolerate or correct ectopic nucleosome positioning and improper chromatin structure. Finally, the ability to position nucleosomes directly onto target sequences may potentially lead to the development of engineered chromatin remodeling proteins that can block oncogenic or other disease-related transcription factors from accessing their binding sites genome wide, leading to new therapeutic approaches.

APPENDIX

SUPPLEMENTAL MATERIALS

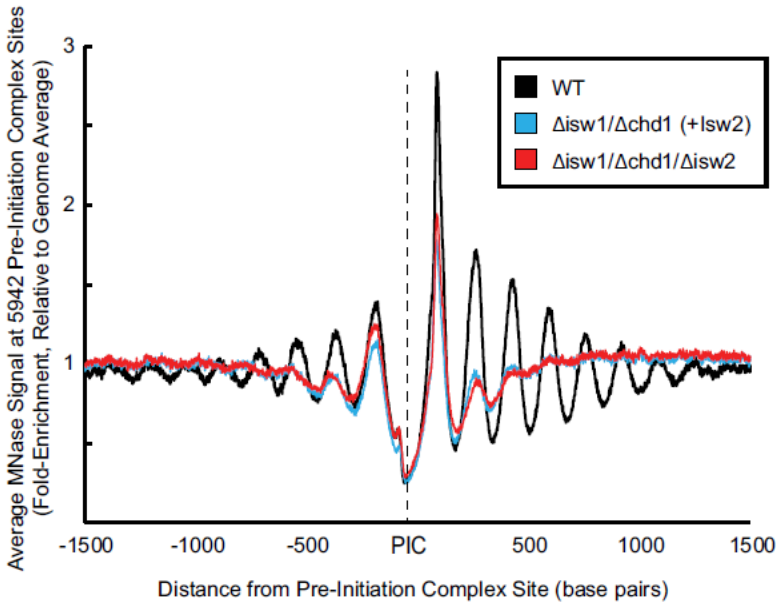

Figure S1, Related to Figure 1. Isw2 is a Precise Specialist at Target Nucleosomes.

Meta-analysis nucleosome dyad signal at all 5942 pre-initiation complex sites (PICs) shows that Isw2 confers no global nucleosome organizing activity throughout yeast cells. WT: wild type.

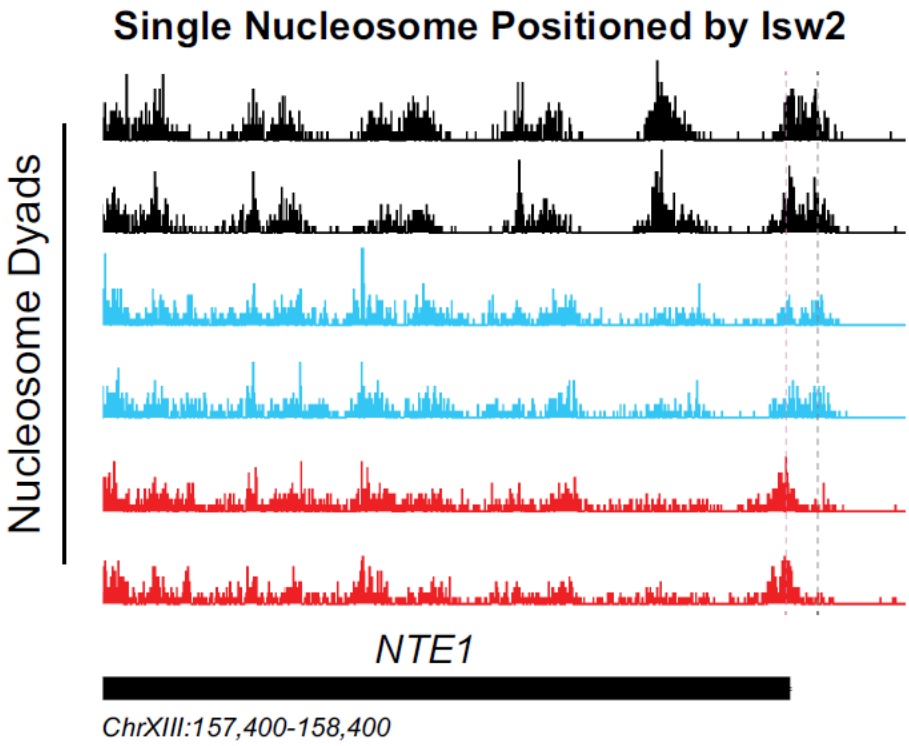

Figure S2, Related to Figure 1. Isw2 is a Precise Specialist at Target Nucleosomes.

Example Isw2 target locus where addition of Isw2 in the absence of Isw1 and Chd1 leads to positioning of a single motif-proximal nucleosome at the NTE1 locus. Vertical gray dashed lines indicate the wild-type nucleosome locations while vertical dashed pink lines indicate an alternate isw2 deletion strain position at the motif-proximal nucleosome. The *ISW2/chd1/isw1* strain can position the motif-proximal nucleosome, but all distal nucleosomes are disorganized much like the *isw2/chd1/isw1* strain.

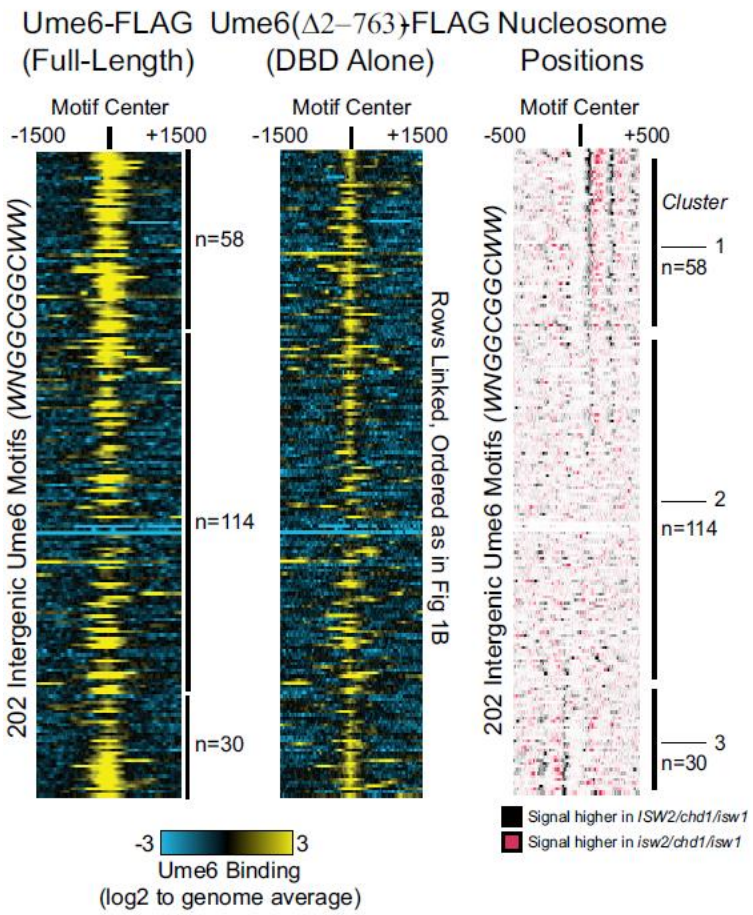

Figure S3, Related to Figure 1. Isw2 is a Precise Specialist at Target Nucleosomes.

Heatmaps showing that full-length unscheduled meiotic gene expression (Ume6)-FLAG (left) and Ume6(Δ2–763)-FLAG (middle) associate with similar targets. (Right) Clustered heatmap from Figure 1B showing the difference in nucleosome dyad signal between *isw2/isw1/chd1* and *ISW2/isw1/chd1* strains at 202 intergenic Ume6 motifs. Black indicates positions where Isw2 preferentially positions nucleosomes compared to strains lacking Isw2. All rows are linked, and all 202 intergenic Ume6 motifs are displayed.

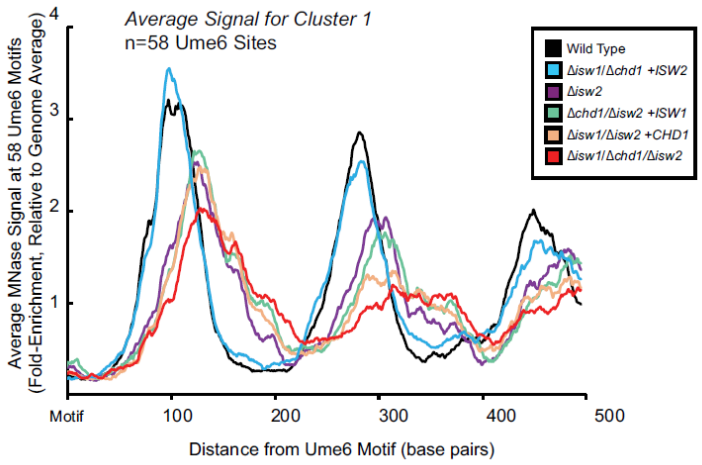

Figure S4, Related to Figure 1. Isw2 is a Precise Specialist at Target Nucleosomes.

Meta-analysis of nucleosome dyad signal for indicated strains at the 58 unscheduled meiotic gene expression (Ume6) target loci associated with cluster 1 in Figure 1B demonstrates that Isw2 but not Chd1 or Isw1 is necessary and sufficient to position nucleosomes at Ume6 target loci.

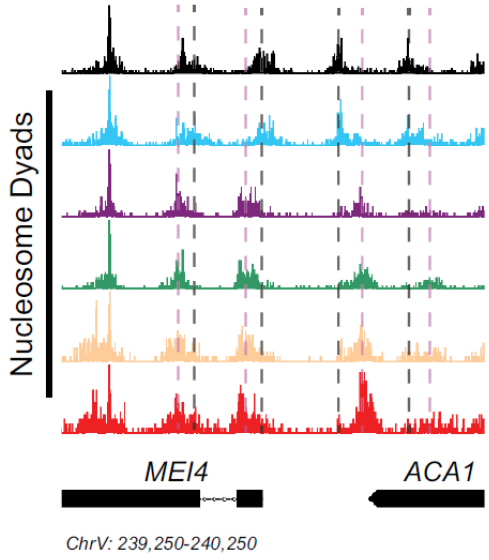

Figure S5, Related to Figure 1. Isw2 is a Precise Specialist at Target Nucleosomes.

Genome Browser image showing nucleosome dyad signal for indicated strains at the MEI4-ACA1 locus, a representative unscheduled meiotic gene expression (Ume6) target locus. The color schemes are shared between Figures S4 and S5 according to the key in Figure S4. Vertical gray lines indicate wild-type nucleosome positions while vertical pink lines indicate ectopic nucleosome positions associated with loss of Isw2 activity.

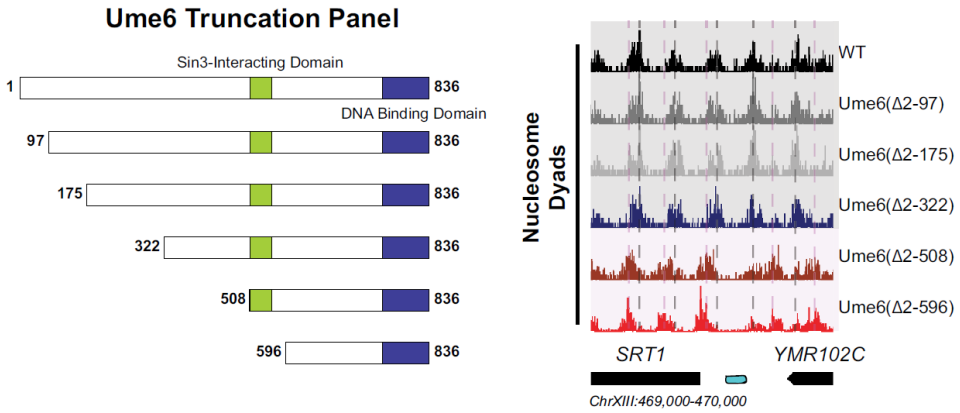

Figure S6, Related to Figure 2. The Ume6 Helix Between Residues 479 and 508 Recruits Isw2 to Ume6 Targets.

(Left) Schematic representation of the truncation panel initially used to identify the region of Ume6 required for Isw2 recruitment. Green square indicates the part of Ume6 known to recruit SIN3 while the blue rectangle indicates the Ume6 DNA binding domain. (Right) Genome Browser image for a representative locus showing nucleosome dyad signal for the indicated strains. Vertical gray lines denote wild-type (WT) nucleosome positions while vertical pink lines indicate ectopic nucleosome positions associated with truncations beyond 322 N-terminal amino acids. The Isw2-recruitment domain was thus determined to be between residues 322 and 508 in Ume6.

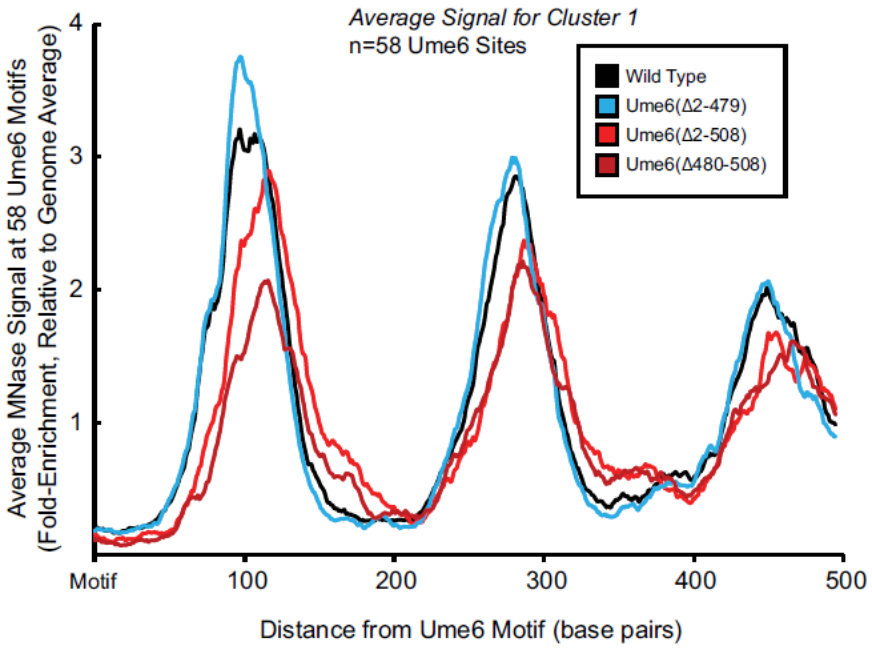

Figure S7, Related to Figure 2. The Ume6 Helix Between Residues 479 and 508 Recruits Isw2 to Ume6 Targets.

Meta-analysis of nucleosome dyad signal at the 58 Ume6 target loci associated with cluster 1 in Figure 1B showing loss of residues 479–508 from Ume6 results in ectopic nucleosome positioning while N-terminal deletion of residues 2–479 preserves wild-type (WT) nucleosome positioning at Ume6 sites.

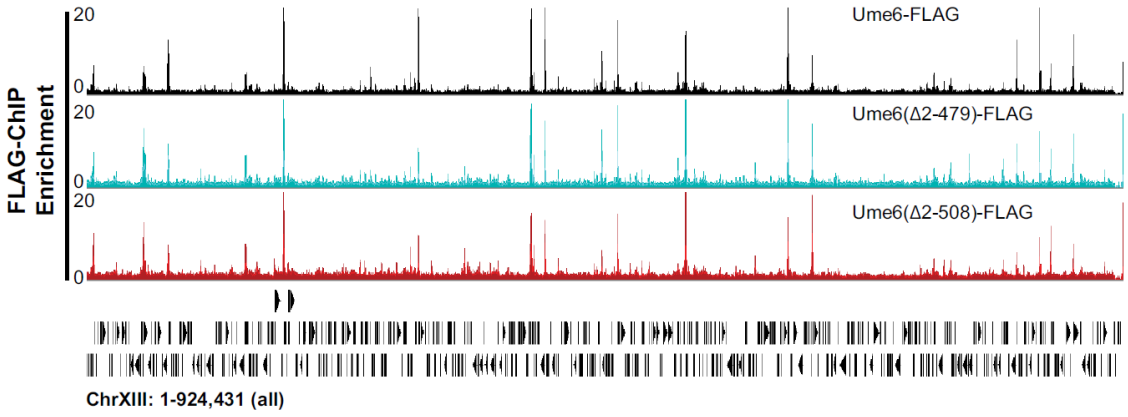

Figure S8, Related to Figure 2. The Ume6 Helix Between Residues 479 and 508 Recruits Isw2 to Ume6 targets.

Genome Browser image demonstrating no loss in Ume6-ChIP signal for relevant Ume6 truncations across all of chromosome XIII. Signal is read-corrected for enrichment, relative to genome average.

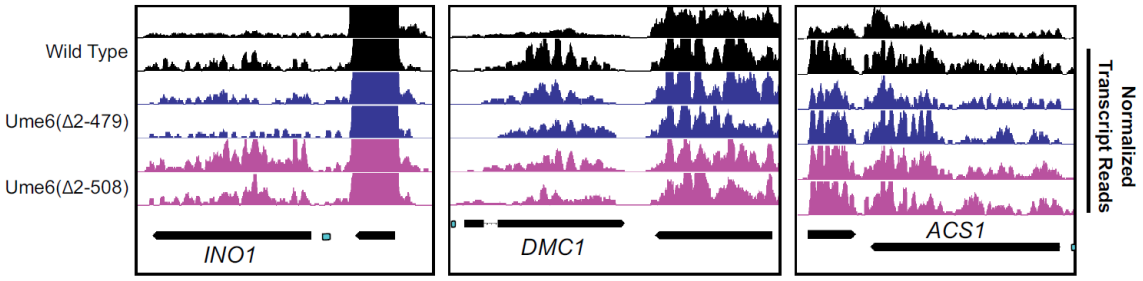

Figure S9, Related to Figure 2. Transcription Data Support a Role of Ume6 Residues 479–508 for Isw2 Recruitment and Not Rpd3 Activity.

Genome Browser images showing transcript abundance for the three representative Ume6 target loci for indicated Ume6 truncation strains in the presence of functional Rpd3, demonstrating the expected very subtle increase in transcription associated with loss of Isw2 at the INO1 locus. URS sites are indicated as cyan rectangles. Biological replicates for each strain are shown.

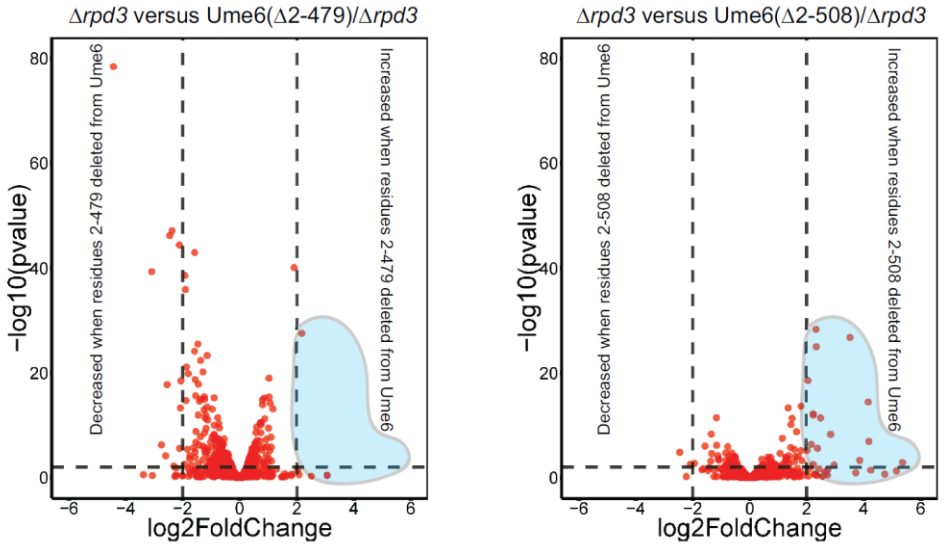

Figure S10, Related to Figure 2. Transcription Data Support a Role of Ume6 Residues 479–508 for Isw2 Recruitment and Not Rpd3 Activity.

Volcano plots for genes containing Ume6 motifs showing log2 change in transcription and associated statistical significance for indicated strains. Horizontal dashed line indicates a p value of 0.01. Vertical dashed lines indicate a change in transcription of ±4-fold. Retention of residues 479–508 prevents large-scale increases in transcription associated with deletion of Rpd3 and Isw2 (see blue shaded region).

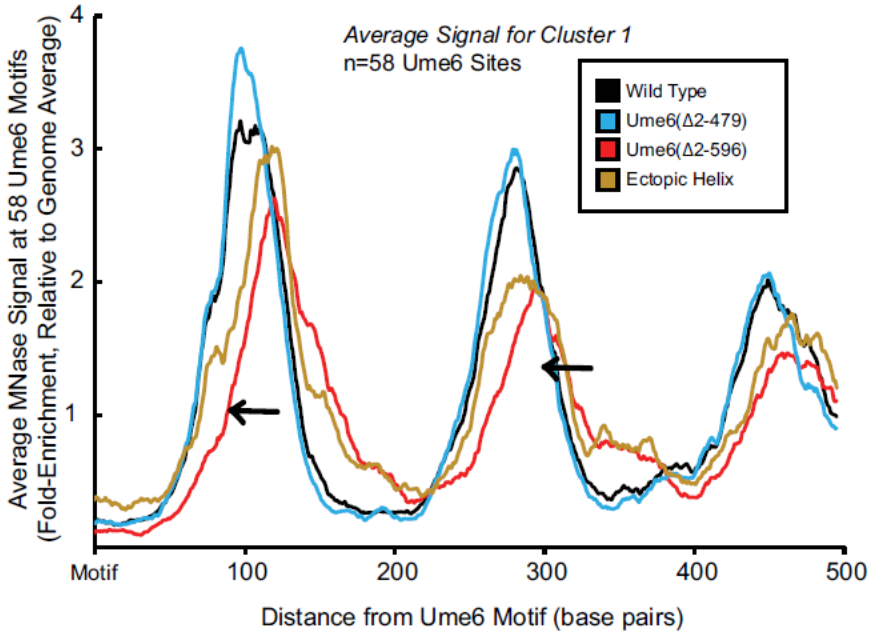

Figure S11, Related to Figure 2. Ectopic Display of the Ume6 Helical Element can Rescue Isw2 Activity at Ume6 Targets.

Meta-analysis of nucleosome dyad signal at the 58 Ume6 target loci associated with cluster 1 in Figure 1B showing partial rescue of nucleosome positioning when residues 479–508 are ectopically displayed on the C-terminus of Ume6 Δ2–596 through SpyTag-SpyCatcher pairs. Black arrows indicate wild-type signal gained by ectopic display of the recruitment helix.

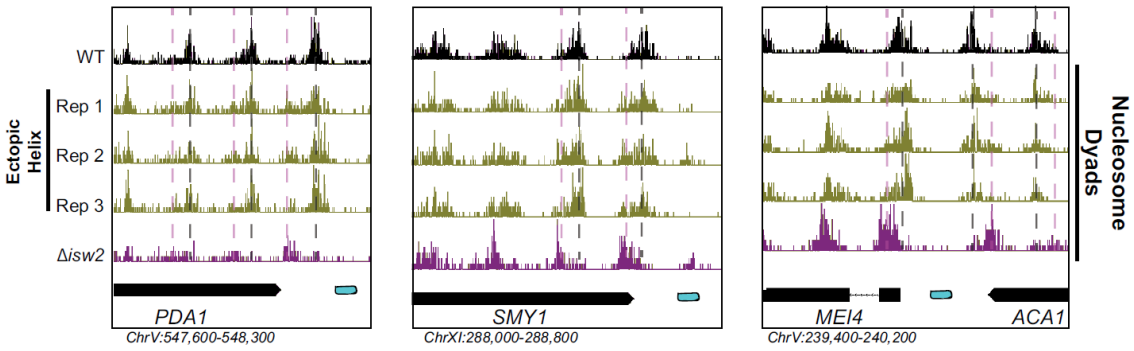

Figure S12, Related to Figure 2. Ectopic Display of the Ume6 Helical Element can Rescue Isw2 Activity at Ume6 Targets.

Genome Browser image showing additional replicates where SpyTag/SpyCatcher-mediated ectopic tethering of Ume6 residues 479–508 recovers wild-type nucleosome positions at Ume6 targets (as in Figure 2C).

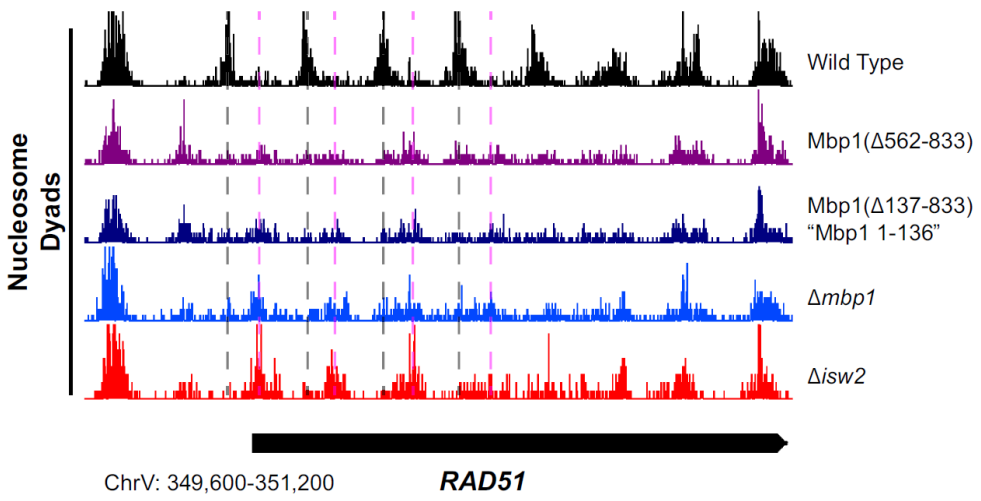

Figure S13, Related to Figure 3. Truncation of the Mbp1 C-terminus Eliminates Isw2-Directed Nucleosome Positioning at Mbp1 Targets.

Genome Browser image showing nucleosome positioning at the RAD51 locus for indicated strains. Dashed vertical gray lines denote positions of nucleosomes in the wild-type strain while dashed vertical pink lines show positions of nucleosomes in the absence of functional Isw2.

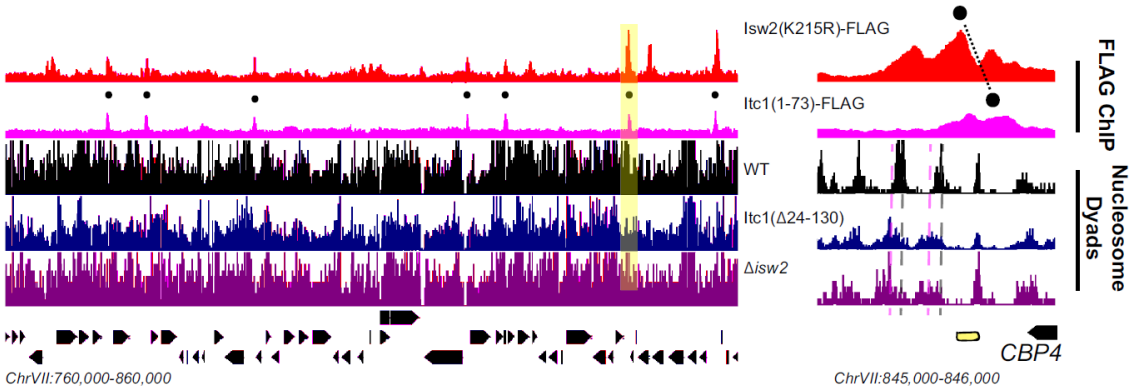

Figure S14, Related to Figure 5. The WAC Domain Orients the Isw2 Catalytic Domain at Nearly Half of Detected Isw2 Targets in Yeast.

(Left) Genome Browser image showing Isw2(K215R)-FLAG and Itc1(1–73)-FLAG ChIP signal and wild type (WT), Itc1(Δ24–130), and Δ*isw2* nucleosome dyad signal for a 100 kb section of chromosome VII. Black circles indicate genomic loci where Isw2(K215R) and Itc1(1–73) ChIP signal overlap. (Right) Zoomed Genome Browser image of the section highlighted in yellow showing offset nature of the Isw2 peak and Itc1 peak. Black circles connected by a black line indicate the offset nature of the Isw2 and Itc1 ChIP peaks. The shifted nucleosome is to the left of the Itc1-Isw2 axis.

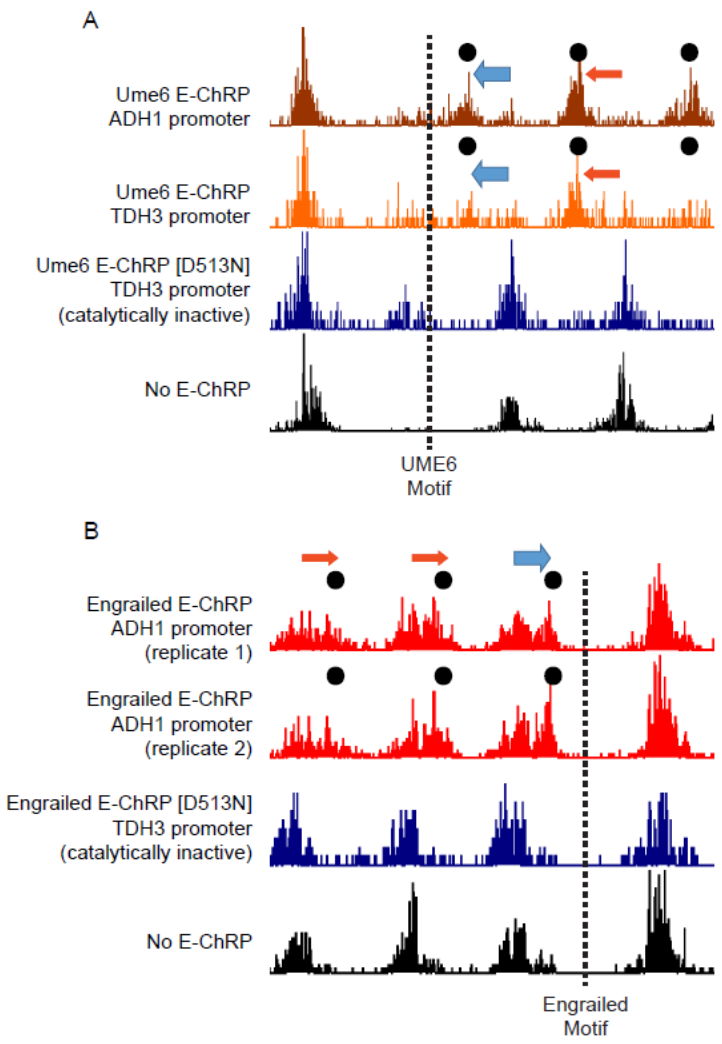

Figure S15, Related to Figure 8. Nucleosome Positioning by E-ChRPs Requires Chd1 Catalytic Activity.

(A) Representative locus showing changes in nucleosome dyad signal after lower (dark red) or higher (orange) expression levels of catalytically active Ume6 E-ChRP. Black circles mark altered nucleosome positions compared to a catalytically inactive E-ChRP with a Walker B D513N mutation in the Chd1 remodeling core (blue) or a parental strain (black). **(B)** Representative locus showing altered nucleosome dyad positions at an Engrailed binding motif by catalytically active (red) but not catalytically inactive (blue) Engrailed E-ChRP compared to a parent strain (black). Respective motif locations are indicated with a dashed line.

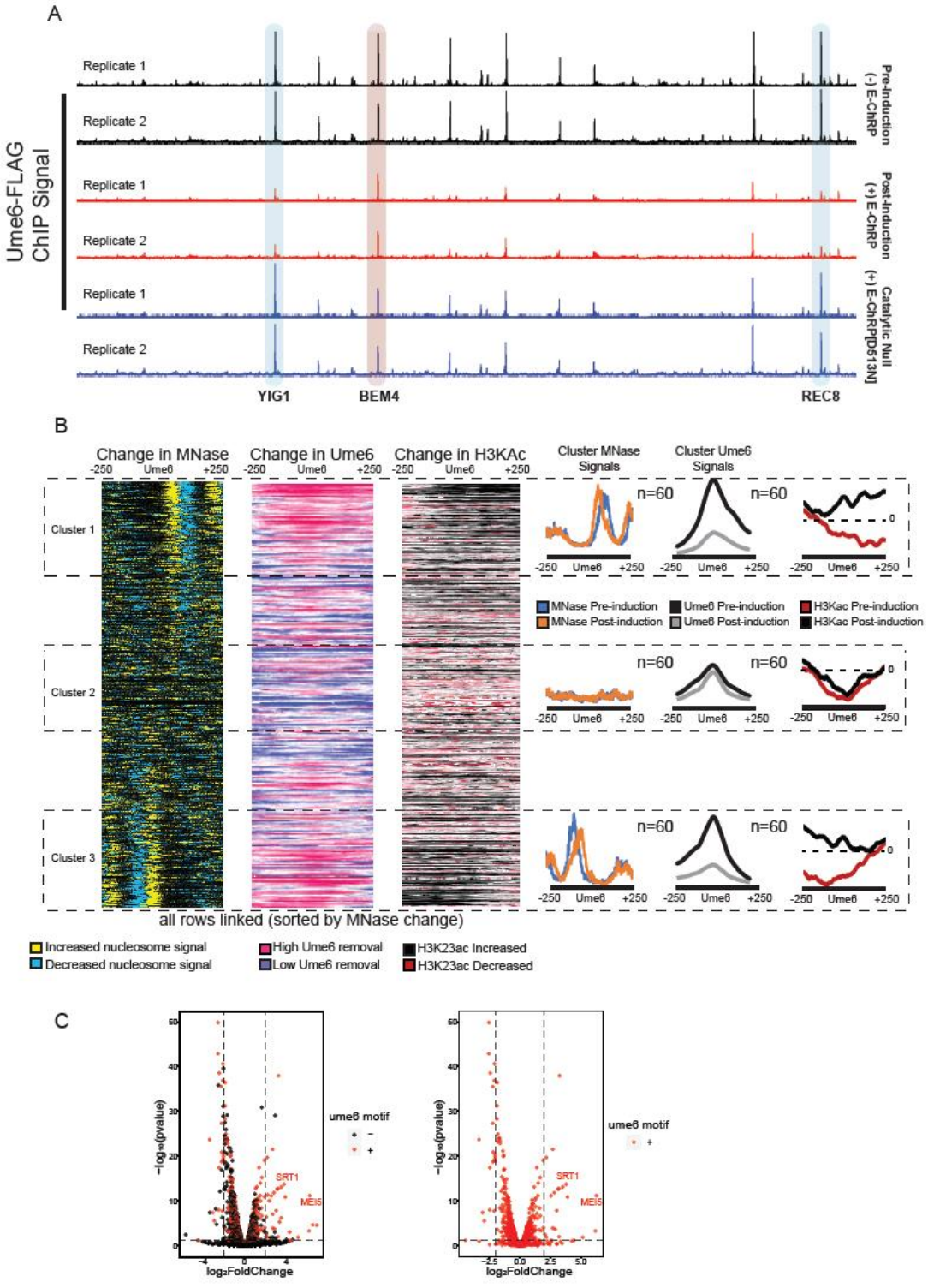
A
Ume6-FLAG ChIP Signal
Replicate 1
Replicate 2
Pre-Induction (-) E-ChRP
Post-Induction (+) E-ChRP
Catalytic Null (+) E-ChRP[D513N]
YIG1
BEM4
REC8
B
Change in MNase
Change in Ume6
Change in H3KAc
Cluster MNase Signals
Cluster Ume6 Signals
Cluster 1
Cluster 2
Cluster 3
n=60
MNase Pre-induction
MNase Post-induction
Ume6 Pre-induction
Ume6 Post-induction
H3Kac Pre-induction
H3Kac Post-induction
all rows linked (sorted by MNase change)
Increased nucleosome signal
Decreased nucleosome signal
High Ume6 removal
Low Ume6 removal
H3K23ac Increased
H3K23ac Decreased
C
ume6 motif
SRT1
MEI5
log2FoldChange

Figure S16, Related to Figure 9. Eviction of Ume6-FLAG by a Catalytically Active E-ChRP.

(A) Genome Browser image showing biological replicates of Ume6-FLAG ChIP signal across ChrXVI before (black) and after (red) 2-hour induction of Ume6 E-ChRP with galactose. Blue peaks correspond to a Ume6-FLAG ChIP signal in the presence of a catalytically-inactive Ume6 E-ChRP containing a Walker B (D513N) substitution in the Chd1 remodeling core. Blue and red highlights correspond to loci in (Fig 3B). **(B)** Global analysis centered on 600 Ume6-FLAG ChIP peaks for change in nucleosome dyad signal (yellow/blue) after Ume6 E-ChRP induction and associated change in endogenous Ume6-FLAG ChIP signal (blue/red) or H3K23ac ChIP (red/black). Clusters represent Ume6 peaks with the highest and lowest change in nucleosome positioning based on ranked changes in MNase signal. Average nucleosome dyad signal for each cluster before and after E-ChRP induction is given in blue and orange, respectively. Change in Ume6-FLAG ChIP signal for each cluster is provided in black and gray traces, respectively. Change in H3K23ac is provided in red and black traces. Note that reduction in Ume6 binding (Ume6-FLAG loss) and increased histone acetylation are only observed for clusters displaying change in nucleosome positions. **(C)** Volcano plots showing Ume6 E-ChRP driven transcription changes (x-axis) and associated statistical significance (y-axis) for all genes (left) or genes containing Ume6 motifs (right). Vertical dashed lines indicate 4-fold transcription change. Horizontal dashed line represents a corrected p value threshold of 0.01. Loci represented in Figure 9C and D are labeled.

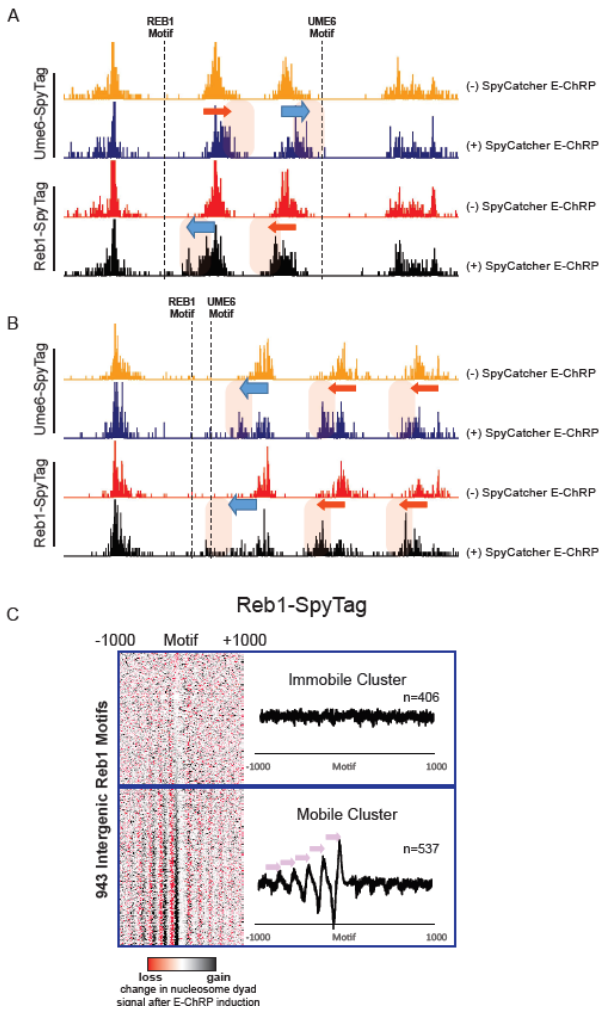

Figure S17, Related to Figure 10. Targeted Chromatin Remodeling with Chd1-SpyCatcher and SpyTagged Chromatin Factors

(A) Genome Browser image showing nucleosome dyad positions before and after induction of SpyCatcher E-ChRP in cells containing Ume6-SpyTag (top) or Reb1-SpyTag (bottom). Location of a proximal Reb1 binding motif or Ume6 binding motif is denoted by a dashed line while directional nucleosome positioning is indicated by blue and red arrows. At this locus, Reb1-SpyTag and Ume6-SpyTag cause different nucleosomes to be selectively moved by SpyCatcher E-ChRP as directed by the location of bound Ume6 or Reb1. **(B)** Same as (A) showing a locus where Reb1 and Ume6 motifs are adjacent to each other. In this case, both Reb1-SpyTag and Ume6-SpyTag allow the SpyCatcher E-ChRP to select the same nucleosome but the nucleosome is moved to different final locations based on the location of the individual bound factors. Reb1-SpyTag leads to further positioning than Ume6-SpyTag because the Reb1 motif is distal to the Ume6 motif. **(C)** Heat map (left) showing the difference in nucleosome dyad signal +/- 1000 bp from 943 Reb1 motifs after SpyCatcher E-ChRP induction in Reb1-SpyTag cells. Average change in nucleosome signal after SpyCatcher E-ChRP induction at Reb1 motifs where nucleosomes are moved (mobile cluster) or not moved (immobile cluster) are provided (right).

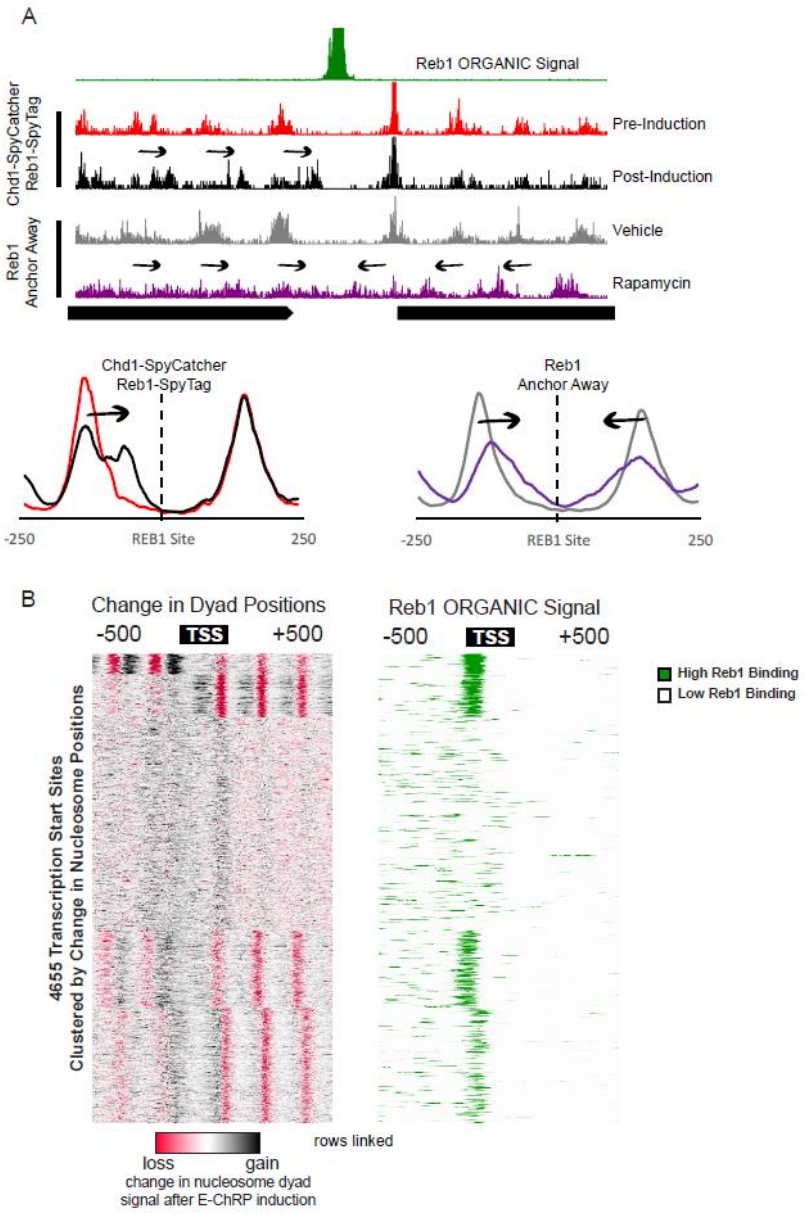

Figure S18, Related to Figure 11. SpyCatcher E-ChRP Induction in a Reb1-SpyTag Strain Reduces NDR Size at Reb1 Target Genes in a Manner Distinct from Reb1 Loss.

(A) Genome Browser image (top) showing Reb1 binding signal from ORGANIC data (Kasinathan et al., 2014), NDR loss by SpyCatcher E-ChRP induction in Reb1-SpyTag strain and NDR loss by Reb1 depletion using anchor away (Kubik et al., 2015). Meta analysis (bottom) of nucleosome dyad movement toward Reb1 motifs for SpyCatcher induction or Reb1 anchor away are also provided for Reb1 sites corresponding to those highlighted in Figure 5A as "Repositioned by E-ChRP". **(B)** Clustered changes in nucleosome dyad positions at 4655 transcription start sites showing migration of nucleosomes into NDRs (left) where Reb1 ORGANIC signal is highest (right).

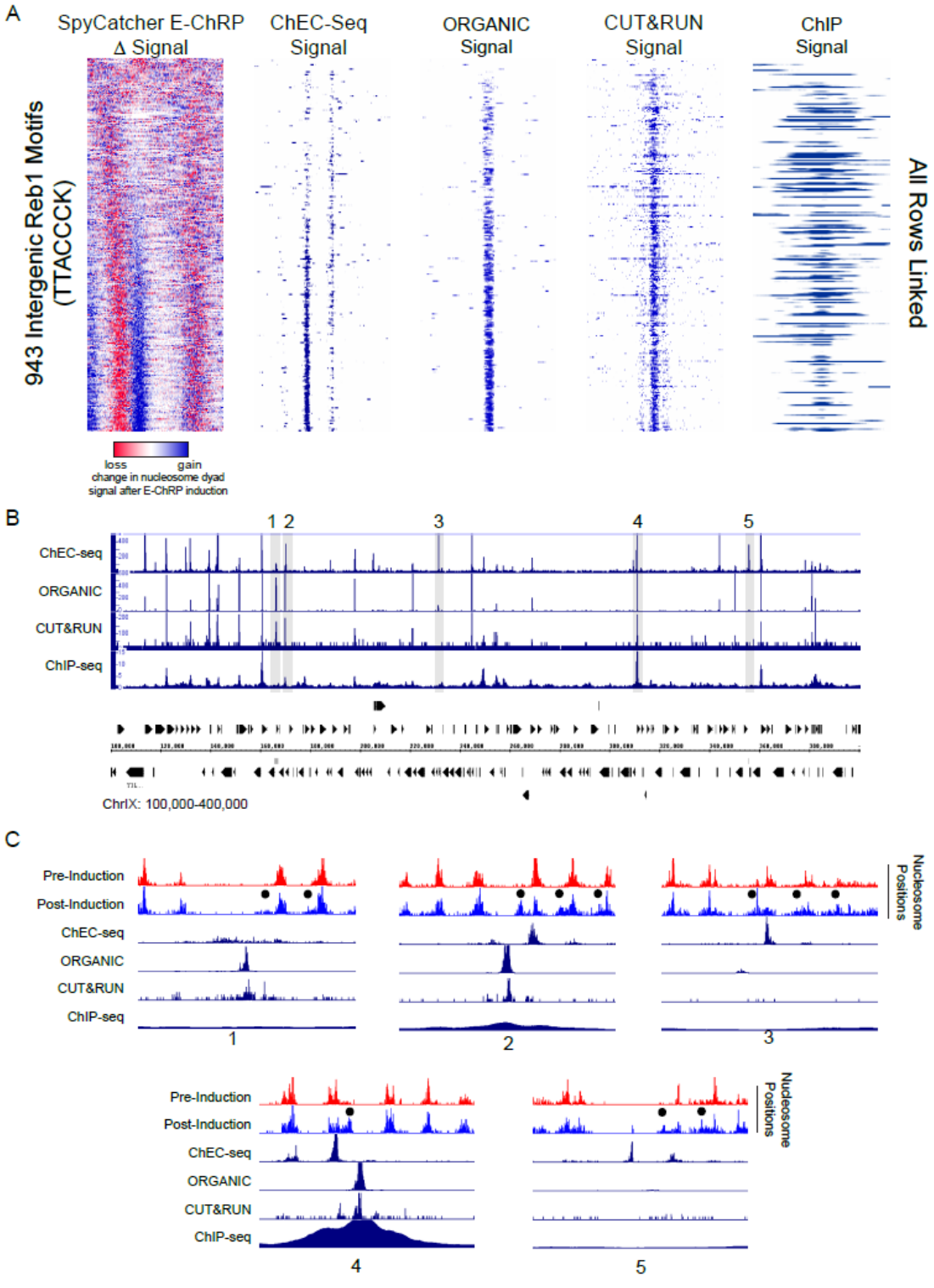
A
SpyCatcher E-ChRP
Δ Signal
ChEC-Seq
Signal
ORGANIC
Signal
CUT&RUN
Signal
ChIP
Signal
943 Intergenic Reb1 Motifs
(TTACCCK)
All Rows Linked
loss
gain
change in nucleosome dyad
signal after E-ChRP induction
B
1 2
3
4
5
ChEC-seq
ORGANIC
CUT&RUN
ChIP-seq
ChrIX: 100,000-400,000
C
Pre-Induction
Post-Induction
ChEC-seq
ORGANIC
CUT&RUN
ChIP-seq
Nucleosome
Positions
1
2
3
4
5

Figure S19, Related to Figure 11. Comparison of SpyCatcher-Induced Chromatin Remodeling at Reb1-SpyTag Sites to Previous Reb1 Mapping Strategies.

(A) Analysis of Reb1 binding at 943 intergenic Reb1 motifs (TTACCCK) using indicated methods for Reb1 mapping. All data are ordered based on the ranked change in nucleosome dyad positioning after SpyCatcher E-ChRP induction in a Reb1-SpyTag strain (left). All data are centered at the Reb1 motif and display +/- 250 base pairs from each motif. **(B)** Genome Browser image showing Reb1 binding across ChrIX for indicated Reb1 mapping strategies. Highlighted regions of interest are displayed in (C). **(C)** Zoomed-in Genome Browser images showing nucleosome repositioning by SpyCatcher E-ChRP at Reb1-SpyTag sites (blue versus red) and relative Reb1 signal from indicated methods. All regions show nucleosome shifts by SpyCatcher E-ChRP (black circles), ChEC-Seq signal and ORGANIC signal. Regions 2 and 4 show Reb1 binding using all methods. Regions 1,3 and 5 lack ChIP signal. Regions 3 and 5 lack CUT&RUN signal. Regions 3 and 5 have very low but detectable ORGANIC signal despite significant nucleosome shifts by SpyCatcher E-ChRP and high ChEC-Seq signal. Numbering corresponds to (B).

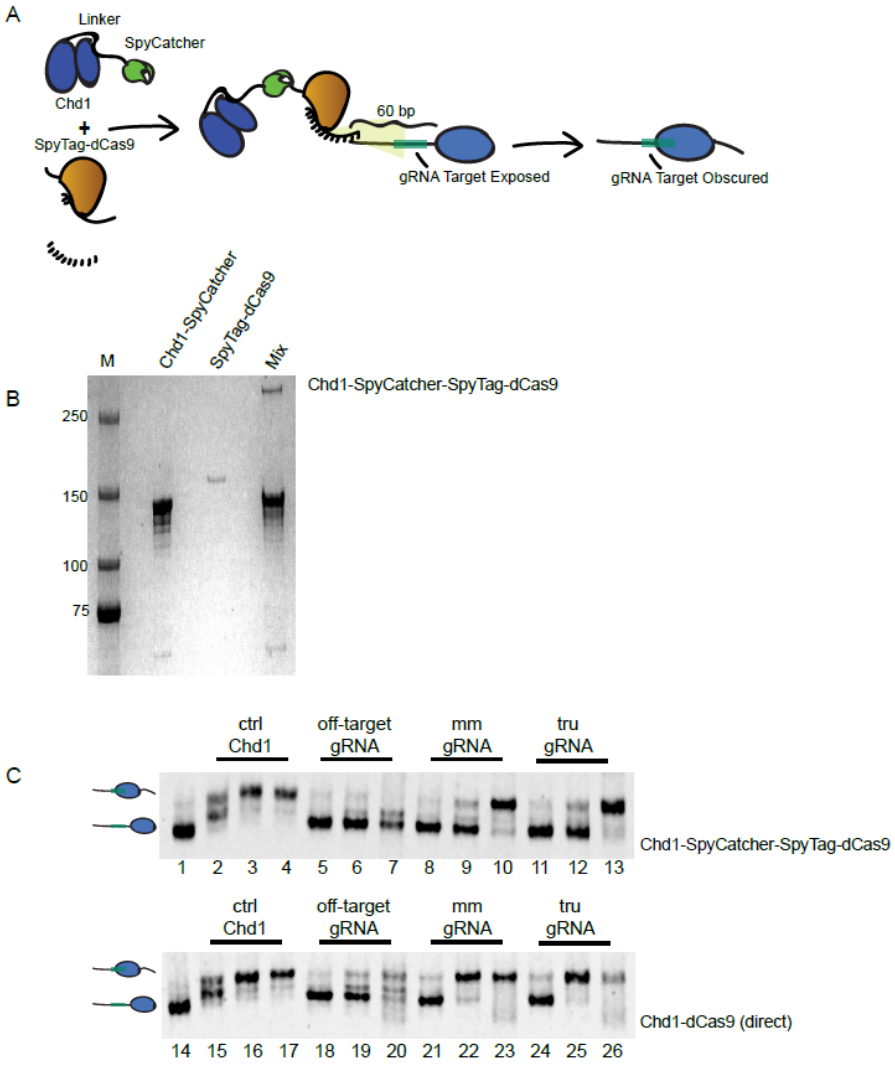

Figure S20, Related to Figure 12. Noncanonical gRNAs Stimulate E-ChRP Activity for a Split Chd1-Spycatcher and SpyTag-dCas9 Pair.

(A) Cartoon representation of Chd1-SpyCatcher combining with SpyTag-dCas9 to form a functional, gRNA-targeted E-ChRP and predicted nucleosome positioning at a target nucleosome. **(B)** SDS-PAGE demonstrating full conversion of SpyTag-dCas9 to Chd1-SpyCatcher-SpyTag-dCas9 in the presence of excess Chd1-SpyCatcher prior to remodeling assays. **(C)** Comparison of Chd1-SpyCatcher-SpyTag-dCas9 remodeling activity (top) on target nucleosomes to Chd1-dCas9 (direct fusion) activity (bottom) using indicated gRNAs. A catalytically active Chd1-Ume6 protein was used as a positive control (ctrl Chd1) for nucleosome positioning. Lanes 1 and 14 contain unremodeled nucleosome (25nM). Lanes 2-4 and 15-17 include 1.5, 15 and 150nM Chd1-Ume6. All other lanes contain the indicated Chd1-dCas9 (either direct fusion or SpyCatcher/SpyTag pair) with 1.5, 15 and 150nM remodeler for each gRNA condition. For “off-target gRNA” conditions, a gRNA with no complementarity to the nucleosome substrate was included in the reaction.

REFERENCES CITED

Ades, S.E., and Sauer, R.T. (1994). Differential DNA-binding specificity of the engrailed homeodomain: the role of residue 50. Biochemistry 33, 9187–9194.

Alroy, I., and Freedman, L.P. (1992). DNA binding analysis of glucocorticoid receptor specificity mutants. Nucleic Acids Res. 20, 1045–1052.

Anders, S., Pyl, P.T., and Huber, W. (2015). HTSeq—a Python framework to work with high-throughput sequencing data. Bioinformatics 31, 166–169.

Anderson, S.F., Steber, C.M., Esposito, R.E., and Coleman, J.E. (1995). UME6, a negative regulator of meiosis in *Saccharomyces cerevisiae*, contains a C-terminal Zn2Cys6 binuclear cluster that binds the URS1 DNA sequence in a zincdependent manner. Protein Sci. 4, 1832–1843.

Ayté, J., Leis, J.F., Herrera, A., Tang, E., Yang, H., and DeCaprio, J.A. (1995). The *Schizosaccharomyces pombe* MBF complex requires heterodimerization for entry into S phase. Mol. Cell. Biol. 15, 2589–2599.

Baldi, S., Jain, D.S., Harpprecht, L., Zabel, A., Scheibe, M., Butter, F., Straub, T., Becker, P.B. (2018). Genome-wide rules of nucleosome phasing in *Drosophila.* Molecular Cell 72:661–672.

Bowman, G.D., McKnight, J.N. (2017). Sequence-specific targeting of chromatin remodelers organizes precisely positioned nucleosomes throughout the genome. BioEssays 39:e201600183.

Breeden L. (1996). Start-specific transcription in yeast. Current Topics in Microbiology and Immunology 208:95– 127

Clapier, C.R., Iwasa, J., Cairns, B.R., Peterson, C.L. (2017). Mechanisms of action and regulation of ATP-dependent chromatin-remodelling complexes. Nature Reviews Molecular Cell Biology 18:407–422.

Clapier, C.R., Cairns, B.R. (2012). Regulation of ISWI involves inhibitory modules antagonized by nucleosomal epitopes. Nature 492:280–284

Dang, W., Kagalwala, M.N., Bartholomew, B. (2006). Regulation of ISW2 by concerted action of histone H4 tail and extranucleosomal DNA. Molecular and Cellular Biology 26:7388–7396.

Dang, W., Bartholomew, B. (2007). Domain architecture of the catalytic subunit in the ISW2-nucleosome complex. Molecular and Cellular Biology 27:8306–8317.

Donovan, D.A., Crandall, J.G., Banks, O.G.B., Jensvold, Z.D., Truong, V., Dinwiddie, D., McKnight, L.E., McKnight, J.N. (2019). Engineered chromatin remodeling proteins for precise nucleosome positioning. Cell Reports 29:2520–2535.

Eberharter, A., Langst, G., and Becker, P.B. (2004). A nucleosome sliding assay for chromatin remodeling factors. Methods Enzymol. 377, 344–353.

Fazzio, T.G., Kooperberg, C., Goldmark, J.P., Neal, C., Basom, R., Delrow, J., Tsukiyama, T. (2001). Widespread collaboration of Isw2 and Sin3-Rpd3 chromatin remodeling complexes in transcriptional repression. Molecular and Cellular Biology 21:6450–6460.

Ferreira, H., Flaus, A., and Owen-Hughes, T. (2007). Histone modifications influence the action of Snf2 family remodelling enzymes by different mechanisms. J. Mol. Biol. 374, 563–579.

Foord, R., Taylor, I.A., Sedgwick, S.G., Smerdon, S.J. (1999). X- ray structural analysis of the yeast cell cycle regulator Swi6 reveals variations of the ankyrin fold and has implications for Swi6 function. Nature Structural Biology 6: 157–165

Fu, Y., Sander, J.D., Reyon, D., Cascio, V.M., and Joung, J.K. (2014). Improving CRISPR-Cas nuclease specificity using truncated guide RNAs. Nat. Biotechnol. 32, 279–284.

Fyodorov, D.V., Kadonaga, J.T. (2002). Binding of Acf1 to DNA involves a WAC motif and is important for ACF mediated chromatin assembly. Molecular and Cellular Biology 22:6344–6353.

Gelbart, M.E., Bachman, N., Delrow, J., Boeke, J.D., Tsukiyama, T. (2005). Genome-wide identification of Isw2 chromatin-remodeling targets by localization of a catalytically inactive mutant. Genes & Development 19:942– 954.

Gilbert, L.A., Larson, M.H., Morsut, L., Liu, Z., Brar, G.A., Torres, S.E., SternGinossar, N., Brandman, O., Whitehead, E.H., Doudna, J.A., et al. (2013). CRISPR-mediated modular RNA-guided regulation of transcription in eukaryotes. Cell 154, 442–451.

Gkikopoulos, T., Schofield, P., Singh, V., Pinskaya, M., Mellor, J., Smolle, M., Workman, J.L., Barton, G.J., Owen-Hughes, T. (2011). A role for Snf2-related nucleosome-spacing enzymes in genome-wide nucleosome organization. Science 333:1758–1760.

Goldmark, J.P., Fazzio, T.G., Estep, P.W., Church, G.M., and Tsukiyama, T. (2000). The Isw2 chromatin remodeling complex represses early meiotic genes upon recruitment by Ume6p. Cell 103, 423–433.

Hauk, G., McKnight, J.N., Nodelman, I.M., and Bowman, G.D. (2010). The chromodomains of the Chd1 chromatin remodeler regulate DNA access to the ATPase motor. Mol. Cell 39, 711–723.

Hota, S.K., Bhardwaj, S.K., Deindl, S., Lin, Y.C., Zhuang, X., and Bartholomew, B. (2013). Nucleosome mobilization by ISW2 requires the concerted action of the ATPase and SLIDE domains. Nat. Struct. Mol. Biol. 20, 222–229.

Hwang, W.L., Deindl, S., Harada, B.T., Zhuang, X. (2014). Histone H4 tail mediates allosteric regulation of nucleosome remodelling by Linker DNA. Nature 512:213–217.

Jinek, M., Chylinski, K., Fonfara, I., Hauer, M., Doudna, J.A., and Charpentier, E. (2012). A programmable dual-RNA-guided DNA endonuclease in adaptive bacterial immunity. Science 337, 816–821.

Josephs, E.A., Kocak, D.D., Fitzgibbon, C.J., McMenemy, J., Gersbach, C.A., and Marszalek, P.E. (2015). Structure and specificity of the RNA-guided endonuclease Cas9 during DNA interrogation, target binding and cleavage. Nucleic Acids Res. 43, 8924–8941.

Kadosh, D., and Struhl, K. (1997). Repression by Ume6 involves recruitment of a complex containing Sin3 corepressor and Rpd3 histone deacetylase to target promoters. Cell 89, 365–371.

Kagalwala, M.N., Glaus, B.J., Dang, W., Zofall, M., Bartholomew, B. (2004). Topography of the ISW2-nucleosome complex: insights into nucleosome spacing and chromatin remodeling. The EMBO Journal 23:2092–2104.

Kasinathan, S., Orsi, G.A., Zentner, G.E., Ahmad, K., and Henikoff, S. (2014). High-resolution mapping of transcription factor binding sites on native chromatin. Nat. Methods 11, 203–209.

Kassabov, S.R., Henry, N.M., Zofall, M., Tsukiyama, T., Bartholomew, B. (2002). High-resolution mapping of changes in histone-DNA contacts of nucleosomes remodeled by ISW2. Molecular and Cellular Biology 22:7524–7534.

Kelley, L.A., Mezulis, S., Yates, C.M., Wass, M.N., Sternberg, M.J. (2015). The Phyre2 web portal for protein modeling, prediction and analysis. Nature Protocols 10:845–858.

Koch, C., Moll, T., Neuberg, M., Ahorn, H., Nasmyth, K. (1993). A role for the transcription factors Mbp1 and Swi4 in progression from G1 to S phase. Science 261:1551–1557.

Kornberg, R.D. (1974). Chromatin structure: a repeating unit of histones and DNA. Science 184:868–871.

Krietenstein, N., Wal, M., Watanabe, S., Park, B., Peterson, C.L., Pugh, B.F., Korber, P. (2016). Genomic nucleosome organization reconstituted with pure proteins. Cell 167:709–721.

Kubik, S., Bruzzone, M.J., Jacquet, P., Falcone, J.L., Rougemont, J., and Shore, D. (2015). Nucleosome stability distinguishes two different promoter types at all protein-coding genes in yeast. Mol. Cell 60, 422–434.

Kubik, S., Bruzzone, M.J., Challal, D., Dreos, R., Mattarocci, S., Bucher, P., Libri, D., Shore, D. (2019). Opposing chromatin remodelers control transcription initiation frequency and start site selection. Nature Structural & Molecular Biology 26:744–754.

Kulak, N.A., Pichler, G., Paron, I., Nagaraj, N., and Mann, M. (2014). Minimal, encapsulated proteomic-sample processing applied to copy-number estimation in eukaryotic cells. Nat. Methods 11, 319–324.

Lai, W.K.M., and Pugh, B.F. (2017). Understanding nucleosome dynamics and their links to gene expression and DNA replication. Nat. Rev. Mol. Cell Biol. 18, 548–562.

Laughery, M.F., Mayes, H.C., Pedroza, I.K., and Wyrick, J.J. (2019). R-loop formation by dCas9 is mutagenic in *Saccharomyces cerevisiae*. Nucleic Acids Res. 47, 2389–2401.

Lee, W., Tillo, D., Bray, N., Morse, R.H., Davis, R.W., Hughes, T.R., Nislow, C. (2007). A high-resolution atlas of nucleosome occupancy in yeast. Nature Genetics 39:1235–1244.

Li, M., Hada, A., Sen, P., Olufemi, L., Hall, M.A., Smith, B.Y., Forth, S., McKnight, J.N., Patel, A., Bowman, G.D., Bartholomew, B., Wang, M.D. (2015). Dynamic regulation of transcription factors by nucleosome remodeling. eLife 4:e06249.

Lowary, P.T., and Widom, J. (1998). New DNA sequence rules for high affinity binding to histone octamer and sequence-directed nucleosome positioning. J. Mol. Biol. 276, 19–42.

Ludwigsen, J., Pfennig, S., Singh, A.K., Schindler, C., Harrer, N., Forne, I., Zacharias, M., Mueller-Planitz, F. (2017). Concerted regulation of ISWI by an autoinhibitory domain and the H4 N-terminal tail. eLife 6:e21477.

Luger, K., Rechsteiner, T.J., and Richmond, T.J. (1999). Expression and purification of recombinant histones and nucleosome reconstitution. Methods Mol. Biol. 119, 1–16.

Lusser, A., Urwin, D.L., Kadonaga, J.T. (2005). Distinct activities of CHD1 and ACF in ATP-dependent chromatin assembly. Nature Structural & Molecular Biology 12:160–166.

Mavrich, T.N., Jiang, C., Ioshikhes, I.P., Li, X., Venters, B.J., Zanton, S.J., Tomsho, L.P., Qi, J., Glaser, R.L., Schuster, S.C., Gilmour, D.S., Albert, I., Pugh, B.F. (2008a). Nucleosome organization in the *Drosophila* genome. Nature 453:358–362.

Mavrich, T.N., Ioshikhes, I.P., Venters, B.J., Jiang, C., Tomsho, L.P., Qi, J., Schuster, S.C., Albert, I., and Pugh, B.F. (2008b). A barrier nucleosome model for statistical positioning of nucleosomes throughout the yeast genome. Genome Res. 18, 1073–1083.

McKnight, J.N., Jenkins, K.R., Nodelman, I.M., Escobar, T., and Bowman, G.D. (2011). Extranucleosomal DNA binding directs nucleosome sliding by Chd1. Mol. Cell. Biol. 31, 4746–4759.

McKnight, J.N., Tsukiyama, T., and Bowman, G.D. (2016). Sequence-targeted nucleosome sliding in vivo by a hybrid Chd1 chromatin remodeler. Genome Res. 26, 693–704.

Mumberg, D., Muller, R., and Funk, M. (1995). Yeast vectors for the controlled € expression of heterologous proteins in different genetic backgrounds. Gene 156, 119–122.

Nair, M., McIntosh, P.B., Frenkiel, T.A., Kelly, G., Taylor, I.A., Smerdon, S.J., Lane, A.N. (2003). NMR structure of the DNA binding domain of the cell cycle protein Mbp1 from *Saccharomyces cerevisiae*. Biochemistry 42:1266–1273.

Niland, P., Huhne, R., and M € uller-Hill, B. (1996). How AraC interacts specif- € ically with its target DNAs. J. Mol. Biol. 264, 667–674.

Nodelman, I.M., and Bowman, G.D. (2013). Nucleosome sliding by Chd1 does not require rigid coupling between DNA-binding and ATPase domains. EMBO Rep. 14, 1098–1103. Park, H.D.,

Ocampo, J., Chereji, R.V., Eriksson, P.R., Clark, D.J. (2016). The ISW1 and CHD1 ATP-dependent chromatin remodelers compete to set nucleosome spacing in vivo. Nucleic Acids Research 44:4625–4635.

Pointner, J., Persson, J., Prasad, P., Norman-Axelsson, U., Stralfors, A., Khorosjutina, O., Krietenstein, N., Svensson, J.P., Ekwall, K., Korber, P. (2012). CHD1 remodelers regulate nucleosome spacing *in vitro* and align nucleosomal arrays over gene coding regions in *S. pombe*. The EMBO Journal 31:4388–4403.

Qi, L.S., Larson, M.H., Gilbert, L.A., Doudna, J.A., Weissman, J.S., Arkin, A.P., and Lim, W.A. (2013). Repurposing CRISPR as an RNA-guided platform for sequence-specific control of gene expression. Cell 152, 1173–1183.

Skene, P.J., and Henikoff, S. (2017). An efficient targeted nuclease strategy for high-resolution mapping of DNA binding sites. eLife 6, e21856.

Stockdale, C., Flaus, A., Ferreira, H., and Owen-Hughes, T. (2006). Analysis of nucleosome repositioning by yeast ISWI and Chd1 chromatin remodeling complexes. J. Biol. Chem. 281, 16279–16288.

Tsukiyama, T., Palmer, J., Landel, C.C., Shiloach, J., Wu, C. (1999). Characterization of the imitation switch subfamily of ATP-dependent chromatin-remodeling factors in *Saccharomyces cerevisiae*. Genes & Development 13:686– 697.

Valouev, A., Johnson, S.M., Boyd, S.D., Smith, C.L., Fire, A.Z., Sidow, A. (2011). Determinants of nucleosome organization in primary human cells. Nature 474:516–520.

Voth, W.P., Richards, J.D., Shaw, J.M., and Stillman, D.J. (2001). Yeast vectors for integration at the HO locus. Nucleic Acids Res. 29, E59.

Walker, J.E., Saraste, M., Runswick, M.J., and Gay, N.J. (1982). Distantly related sequences in the alpha- and beta-subunits of ATP synthase, myosin, kinases and other ATP-requiring enzymes and a common nucleotide binding fold. EMBO J. 1, 945–951.

Washburn, B.K., Esposito, R.E. (2001). Identification of the Sin3-binding site in Ume6 defines a two-step process for conversion of Ume6 from a transcriptional repressor to an activator in yeast. Molecular and Cellular Biology 21: 2057–2069.

Wiechens, N., Singh, V., Gkikopoulos, T., Schofield, P., Rocha, S., Owen-Hughes, T. (2016). The chromatin remodelling enzymes SNF2H and SNF2L position nucleosomes adjacent to CTCF and other transcription factors. PLOS Genetics 12:e1005940.

Yadon, A.N., Singh, B.N., Hampsey, M., Tsukiyama, T. (2013). DNA looping facilitates targeting of a chromatin remodeling enzyme. Molecular Cell 50:93–103.

Yan, L., Wang, L., Tian, Y., Xia, X., Chen, Z. (2016). Structure and regulation of the chromatin remodeller ISWI. Nature 540:466–469.

Yan, C., Chen, H., Bai, L. (2018). Systematic study of Nucleosome-Displacing factors in budding yeast. Molecular Cell 71:294–305.

Yen, K., Vinayachandran, V., Batta, K., Koerber, R.T., Pugh, B.F. (2012). Genome-wide nucleosome specificity and directionality of chromatin remodelers. Cell 149:1461–1473.

Zakeri, B., Fierer, J.O., Celik, E., Chittock, E.C., Schwarz-Linek, U., Moy, V.T., Howarth, M. (2012). Peptide tag forming a rapid covalent bond to a protein, through engineering a bacterial adhesin. PNAS 109:E690–E697.

Zentner, G.E., Kasinathan, S., Xin, B., Rohs, R., and Henikoff, S. (2015). ChECseq kinetics discriminates transcription factor binding sites by DNA sequence and shape in vivo. Nat. Commun. 6, 8733.

Zhang, Z., Wippo, C.J., Wal, M., Ward, E., Korber, P., Pugh, B.F. (2011). A packing mechanism for nucleosome organization reconstituted across a eukaryotic genome. Science 332:977–980.

Zhou, C.Y., Johnson, S.L., Gamarra, N.I., and Narlikar, G.J. (2016). Mechanisms of ATP-dependent chromatin remodeling motors. Annu. Rev. Biophys. 45, 153–181.

Zofall, M., Persinger, J., Bartholomew, B. (2004). Functional role of extranucleosomal DNA and the entry site of the nucleosome in chromatin remodeling by ISW2. Molecular and Cellular Biology 24:10047–10057.

Zofall, M., Persinger, J., Kassabov, S.R., Bartholomew, B. (2006). Chromatin remodeling by ISW2 and SWI/SNF requires DNA translocation inside the nucleosome. Nature Structural & Molecular Biology 13:339–346.